ISSN 2087-2852

The Journal of Experimental Life Science

Discovering Living System Concept through Nano, Molecular and Cellular Biology

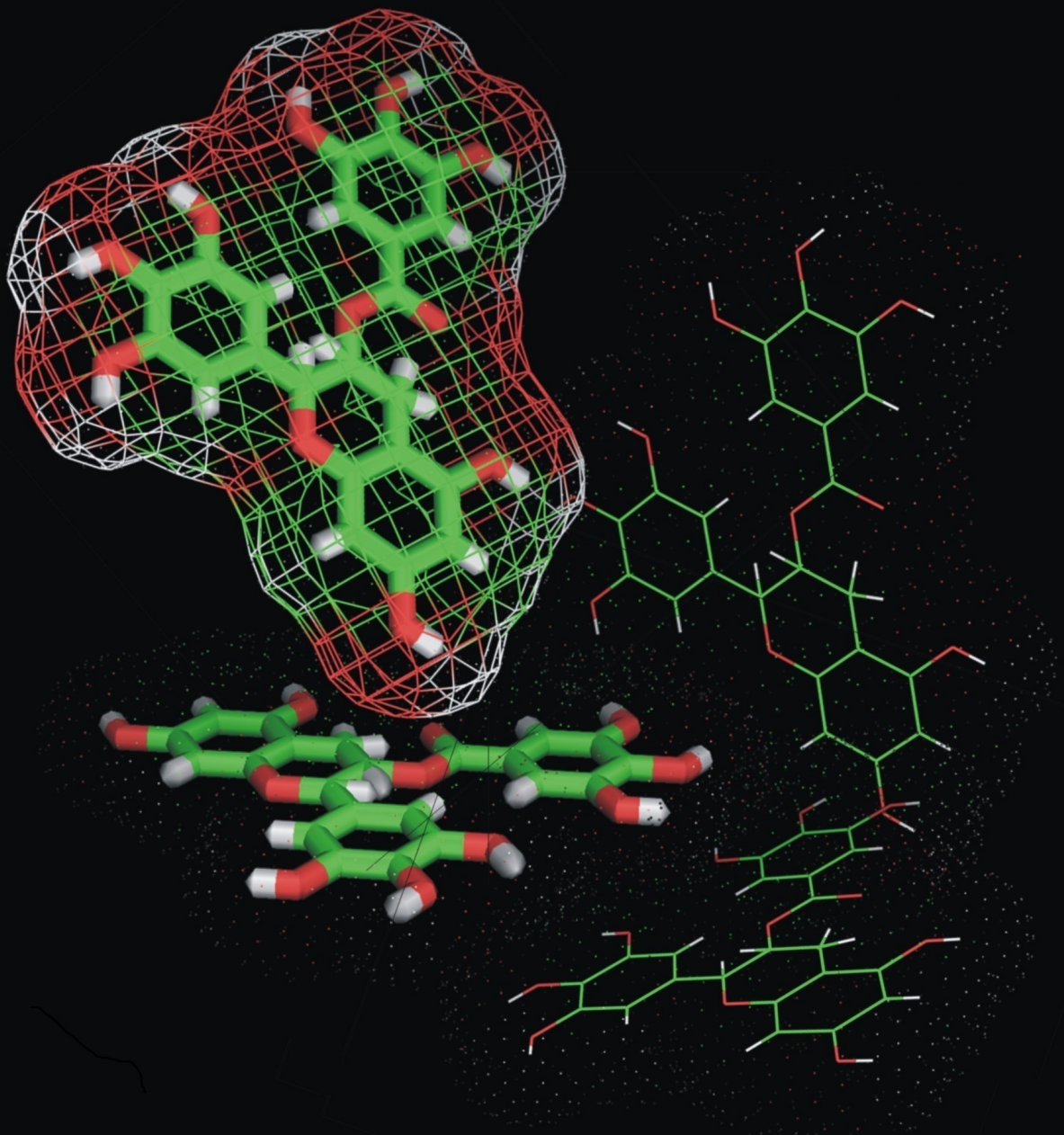

J. Exp. Life. Sci. | Vol. 8 | No. 1 | pages. 1-70 | February 2018

Published by

Graduate Program, University of Brawijaya
in Cooperation With
Masyarakat Nano Indonesia (MNI)

ISSN. 2087-2852
E-ISSN. 2338-1655

The Journal of Experimental Life Science

Discovering Living System Concept through Nano, Molecular and Cellular Biology

Editorial Board

Address
The Journal of Experimental Life Science
Building E, 2nd Floor, Postgraduate School, University of Brawijaya
Jl. Mayor Jenderal Haryono 169, Malang, 65145
Telp: (0341) 571260 ; Fax: (0341) 580801
Email: jels@ub.ac.id
Web: http://www.jels.ub.ac.id

ISSN. 2087-2852
E-ISSN. 2338-1655

Table of Content

Effect of Bulbils Position on Leaf Branches to Plant Growth Responses and Corms Quality of *Amorphophallus muelleri* Blume

Retno Mastuti*, Nunung Harijati, Estri Laras Arumingtyas, Wahyu Widoretno

Department of Biology, Faculty of Mathematics and Natural Sciences, University of Brawijaya, Malang, Indonesia

Abstract

Bulbil (corm leaf) is one material source of vegetative propagation in *Amorphophallus muelleri* Blume. Based on the position in branches there are two types of bulbil, middle and edge bulbils, which are different in shape and size. It has been reported that bulbil size affected not only the growth response of seedlings and plants but also the quality of the produced corms. Therefore, the objectives of this experiment were to study the effect of bulbils origin on *A. muelleri* Blume (Porang) growth and the quality of harvested corms. The quality of corms was assessed based on glucomannan and (CaOx) content. Bulbils from the middle and edge of branches were grown in polybag (ϕ 5 cm) containing compost:fertilizer (1:1) mixed media under 40% shade. Each bulbil origin was repeated 8 times. The results showed that growth responses of plant from middle bulbil were significantly better than that from edge bulbil. However, at the harvesting time, the weight and diameter of corms derived from both types of bulbils were not significantly different. The glucomannan and calcium oxalate (CaOx) content of harvested corms grown from middle bulbil tends to be higher than that from edge bulbil.

Keywords: branching, calcium oxalate (CaOx), germination, glucomannan, Porang.

INTRODUCTION

Porang, *Amorphophallus muelleri* Blume (*A. muelleri*) is one members of the Araceae that produce corms which is actually an underground stem. It is native to Indonesia [1] especially in teak forests in East Java and in undisturbed areas such as riversides and bamboo forests in Central and West Java [2]. It can grow in lowlands areas up to 1000 m above sea level, with temperatures between 25-35°C and rainfall between 300-500 mm per month during the period of growth [3]. The plant will grow better under shade. Environment with shade of 50-60% has high production of corms [1]. *Amorphophallus muelleri* has unique, highly dissected, umbrella-shaped leaf blade which is supported by pesudo-stem or petiole [4,5]. The dissected leaf blade has some branches (leaflets) which are supported by petiolule.

Amorphophallus muelleri can be regenerated through generative and vegetative propagation [1,3]. Bulbils or corms leaf are organ source of vegetative propagation of *A. muelleri* besides corms. The bulbils of *A. muelleri* are classified as epiphyllar bulbil because they were produced on the surface of branching points of the leaf [4]. Based on the position on leaf branches there are two types of bulbils: middle and edge bulbils which are produced on leaf [6] and leaflet branching points, respectively. Spatial distribution of bulbils on leaf contributed to variations in shape, weight and size the bulbils [3]. Middle bulbils have brown color and round shape while edge bulbils have oval shape and smaller than the former. Edge bulbils on the primary leaflet are bigger than that on secondary and tertiary leaflet. Propagation of *A. muelleri* from bulbils is more promising than from seeds. Plants derived from bulbils grew faster than those derived from seeds. At the third stage of growth period plants derived from bulbil were higher (± 180 cm) than those derived from seeds (± 140 cm) [7].

Considerable degree of seed heterogeneity in size, weight and quality has been widely reported [8,9,10]. The effects of bulbil size on the plant growth and corms quality of *A. muelleri* derived from different bulbil size have also been reported [7,11,12]. Different sizes of bulbil showed no difference in the ability to grow but it has effect on plant growth responses [11]. Large bulbils generate higher plants than small bulbils but the diameter of stem and leaves and the number of shoots were not significantly different [12]. It has also been reported that bulbil size determined the amount of the stage of vegetative growth and dormancy [7]. Different sizes of bulbil that were grown in medium containing various doses of lime produced corms with different level of glucomannan content [11].

* Correspondence address:
Retno Mastuti
Email : mastuti7@ub.ac.id
Address : Dept. Biology, Faculty of Mathematics and Natural Sciences, University of Brawijaya, Veteran Malang, Malang 65145.

ISSN. 2087-2852
E-ISSN. 2338-1655

Position-dependent effects have been widely studied on seed or fruit [13,14,15]. The position of a seed or fruit on plant can affect its morphology, mass and dormancy/germination [16,17,18]. However, regarding to corms studies still focused on the placement position on propagation media or planting area [19] rather than the corms position on the maternal plant. The duration of Liatris daughter corms' growth to maturity and their growth rate vary with their position on the mother corm [20].

Currently market demand for the *A. muelleri* chip corms is quite high. *Amorphophallus muelleri* corms have been widely used as raw materials in food, cosmetics and pharmaceutical industry because they contained valuable source of glucomannan, a soluble, non-cellulosic polysaccharide [21]. Chips derived from *A. muelleri* corms are highly exported to Japan, Hongkong and China and other countries. Therefore, today in Indonesia *A. muelleri* has been cultivated in several methods of propagation to produce high quality of corms to meet the increasing market demand.

Considering some previous reports which showed that bulbil size affects the growth response, therefore the spatial distribution of *A. muelleri* bulbil on leaf and leaflet branching is necessary to be examined both in physiological and morphological responses. Therefore, the objectives of the present study were to examine plant growth response and corms quality grown from middle and edge bulbils produced on leaf branches of *A. muelleri*.

MATERIALS AND METHODS

Bulbil Germination

Middle and edge bulbils derived from the second growth period of plants were obtained from Oro-oro Waru Village, Saradan, Madiun District, in East Java, Indonesia. Eight bulbils of each type were germinated in plastic bags (ϕ = 5 cm) containing $\pm$ 500 g fertilizer:compost (1:1) mixed media. The bulbils were planted 5 cm depth in the media and the plastic bag then placed in the experiment field of Biology Department, University of Brawijaya under 40% shading. After bulbil-derived seedling has reached a height of $\pm$ 20 cm then it was grown in larger polybag (ϕ = 40 cm) containing @ 5 kg soil media. Plants were watered to about field capacity twice a week.

Plant Growth and Corms Harvesting

The measurement growths responses were started at three months after the coleoptile sheath merged on the soil surface, once a week for 10 weeks. The parameters of growth responses measured were plant height, stem girth and canopy width. Plant height was measured from petiole base on the soil surface to the top of leaf canopy. To measure canopy width, firstly the two range poles of the extreme edges of the canopy were marked. Subsequently, the distance between the two poles was measured with a measuring tape and recorded as the canopy width. The corms were harvested at $\pm$ 90 days after planting, and prepared for glucomannan and CaOx analysis.

Extraction and Analysis of Glucomannan Content of Fresh Harvested Corms

Fresh harvested corms were rinsed and the skin was peeled. Total 6 g of the rinsed flesh corms were mashed using blender to form pasty. Subsequently, glucomannan extraction and analysis were conducted based on the method of [22] with modification. Pasty of corm was put into beaker glass containing 200 mL of $AlSO_4$ 0.3% and then placed in an incubator at 55°C for 15 min while stirred gently to maximize the process of glucomannan extraction. The extract yield was filtered with cotton cloth, diluted until the final volume reached 600 mL and then centrifuged at 1500 g for 15 min. Supernatant was added by isopropyl alcohol with ratio 1:1. The white precipitate formed was glucomannan. The precipitate glucomannan was oven-dried at 45°C overnight or until dry to obtain glucomannan yield. The weight of dry glucomannan relative to the weight of dried corm used for calculating glucomanan content. The weight of dried corms were obtained from 6 g of flesh corms that was rinsed, chopped and dried by oven at 45°C overnight or until dry. Dried glucomannan sample was weighed and glucomannan content per DW sample was calculated as: (precipitate DW/corms sample DW) x 100%.

Extraction and Analysis of Calcium Oxalate (CaOx) of Fresh Harvested Corms

Extraction and determination of CaOx content of *A. muelleri* corms were conducted by the method of Imouha and Kalu [23] with modification. Determination of CaOx consisted of three phases: digestion, oxalate precipitation and titration of permanganate. Corms were rinsed and then approximately ¼ parts of them was grated. The digestion phase was initiated by dissolving 10 g grated corms into 190 mL aquadest and then added by 10 mL of HCl 6N. The suspension was heated at 100°C for 1 h then allowed to cool.

Aquadest was added into the suspension until reached volume 250 mL and it was filtered by fine cotton cloth. The second phase was initiated by adding six drops of methyl red into filtrate yield. The pH was adjusted by adding some drops of NH_4OH until achieved pH 4-4.5. Subsequently filtrate was heated until 90°C and then allowed to cool. Filtrate was filtered by whattman no. 1 to eliminate Fe. Filtrate was heated at 90 °C, added by 10 mL of $CaCl_2$ 5% and homogenized by magnetic stirrer. Finally, the filtrate was centrifuged at 2500 rpm for 10 min. At the last phase pellet derived from previous centrifugation was put into 10 mL of H_2SO_4 20%. After added with aquadest until reached the volume of 100 mL the solution was heated until almost boiled. Subsequently, titration of this solution was conducted by standardized $KMnO_4$ 0.1 N until produced pink color for 1 min. The content of CaOx (g/FW corms/tubers) was calculated with Eq. 1.

$$\text{CaOx (g)} = \frac{V_{KMnO4} \text{ x } M_{KMnO4} \text{ x } 5 \text{ x ME x DF x } 100}{m_f \text{ x } 1000}$$

Description:
VKM_nO_4 is volume $KMnO_4$ (mL),
M KM_nO_4 is molarity $KMnO_4$,
ME is molar equivalent of $KMnO_4$ in oxalic,
DF is dilution factor, and
m_f is mass of fresh corms

Statistical analysis

Data were subjected to analysis of variance (ANOVA) and means were compared by Tukey test α 0.05 using the SPSS ver. 17.

RESULT AND DISCUSSION

Growth Responses of Plants Derived From Different Types of Bulbils

Middle bulbils have bigger size than edge bulbils (Fig. 1). Both types of bulbils showed significantly different vegetative growth responses. Plants derived from middle bulbils grew faster than that from edge bulbils (Fig. 2A). Plant height derived from different bulbil types showed significantly differentt from the first week until the last week of observation (Fig. 2B). From week to week the plants derived from middle bulbils were taller than those derived from edge bulbils. At the last week observation the plant height derived from middle bulbils reached 60.0 ± 4.7 cm while those from edge bulbils reached only 47.5 ± 4.1 cm. But until the last week the average height of plants derived from each middle and edge bulbils was not significantly different from the first week observation.

Figure 1. Bulbil. (cormes leaf) of *A. muelleri* on leaf branching. * middle bulbil, ♦ edge bulbil

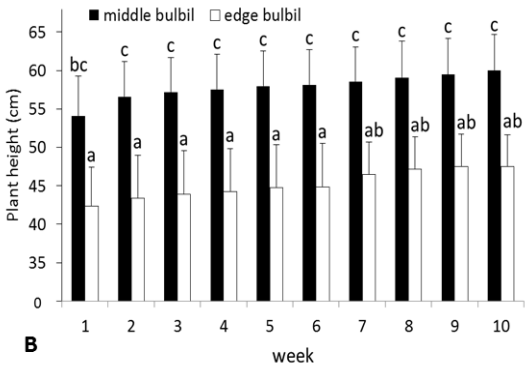

Figure 2. Plant height of *A. muelleri* derived from middle and edge bulbils. (a) *A. muelleri* plants 10 weeks after seedling germination and (b) Plant height at each week observations. Different letters following bars indicate significant differences at the α = 0.05 of Anova test. Means ± SD (n=8).

Stems girth of plants grown from middle bulbils (14 ± 1.39 cm) were also significantly greater than those grown from edge bulbils (10 ± 0.60 cm) (Fig. 3A). Canopy width from both types of bulbils was also significantly different. It derived from middle bulbils had longer diameters than that derived from edge bulbils (Fig. 3B). The de-

ISSN. 2087-2852
E-ISSN. 2338-1655

velopment of storage organ grown from middle and edge bulbils which was represented by weight and diameter of harvested corms were not significantly different. The weight of harvested corms of plant grown from middle and edge bulbils reached 73.3 ± 37 g and 49.6 ± 13.8 g, respectively. Diameter of harvested corms of plant grown from middle and edge bulbils reached 54.4 ± 10.2 mm and 48.2 ± 4.5 mm, respectively (Fig. 4A).

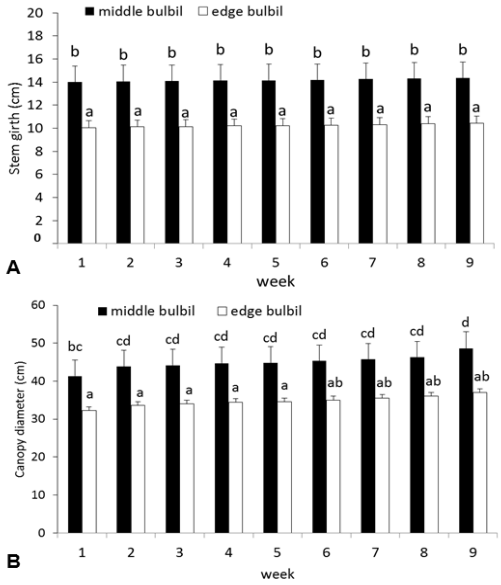

Figure 3. Stem girth and canopy diameter of *A. muelleri* plants. (a) Stem girth and (b) Canopy width. Different letters following bars indicate significant differences at α = 0.05 of Anova test. Means ± SD (n=8).

Bulbil of *A. muelleri* is a small cormes produced on leaf branch. Bulbil is a sink containing storage resources translocated from photosynthetic organs. The size of bulbil indicated the amount of storage resources possessed. In this study the middle bulbils which have bigger size showed better primary and secondary growth responses than edge bulbils based on plant height, stem girth and canopy width. Middle bulbils of *A. muelleri* is apparently to contain greater numbers of photosynthate as food reserves so the process of photosynthesis occurs earlier and the vegetative organs formed faster than edge bulbils. Sumarwoto and Maryana [12] have reported that bigger size of *A. muelleri* bulbil produce higher plant than smaller ones. The same results were shown in other species. Bulb size influenced plant growth and development of Hyacin and Lily [24]. Corms size affected the performance of Gladiolus grandiflorus [25,26] as well as stigma and corm yield of saffron (*Crocus sativus* L.) [19].

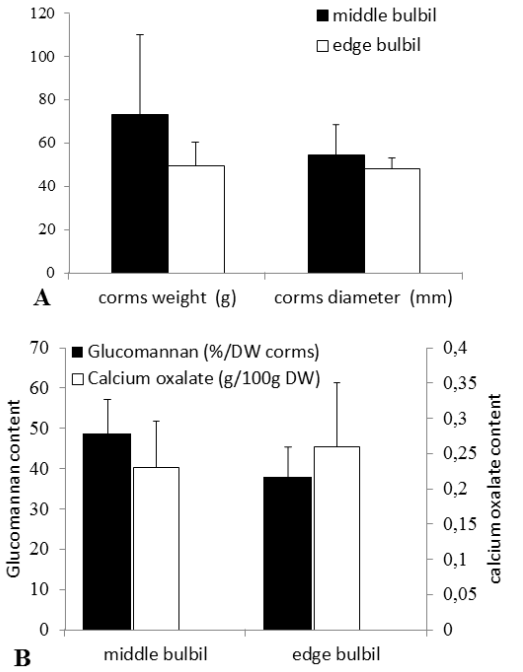

Figure 4. Quality of *A. muelleri* harvested corms planting from different types of bulbils at 90 days after planting: (a) Weight and diameter of harvested cormes and (b) Glucomannan and Calcium oxalate content. Means ± SD (n=8).

Environment is predominant factor which determine size variation of seed produced as a source of generative reproduction [8]. Within-plant variation can be determined by fruit position and seed position within a fruit or inflorescences. Bulbils of *A. muelleri* are vegetative reproduction organ which sized vary as a result of their position on the leaf branch of maternal plants. This maternal position effect of *A. muelleri* bulbils occur in a structurally ordered manner. Bulbils on more periphery branch have smaller size. Within-plant variation arising from position effects is inherited [8]. Effect of seed position resulted in variations in size is always present in every generation. This shows that the inherited character which is more affected by position and the variation in size is due to the distribution of the position.

Corms Quality: Glucomannan and Calcium Oxalate (CaOx) Content

Corms quality both glucomannan or calcium oxalate content of corms harvested from plant grown from middle and edge bulbils were not significantly different. The average of glucomannan content was 48.63 and 37.78% DW corms harvested from plant grown from middle and

ISSN. 2087-2852
E-ISSN. 2338-1655

edge bulbil, respectively (Fig. 4B). In this study it is assumed that corms were not harvested at mature physiological age. Consequently, the content of glucomannan produced by the two plants derived from middle and edge bulbil was not significantly different. Glucomannan content was higher in mature corms than in young corms. Glucomannan within the developing corm changes throughout the growing season and was highest just before the foliage died off, prior to dormancy [27]. Generally foliage died off 5-6 months after planting [3].

Calcium oxalate crystals were also obtained from corms of *A. muelleri* plants derived from bulbils. However there was no significant difference between two plant types in terms of its content. It is suspected that during corms development the formation of calcium oxalate crystals has not been maximized. There is an indirect relationship between the diameter and the density of calcium oxalate in the corms [28].

CONCLUSION

From this result it can be concluded that the position effect of *A. muelleri*'s bulbils on the maternal leaf branch will influence the growth response. The content of glucomannan and CaOx have no significant difference in young corms.

ACKNOWLEDGEMENT

The financial support of this work was provided by DPP-SPP Grant Faculty of Mathematics and Natural Sciences, University of Brawijaya.

REFERENCES

[1] Jansen, P.C.M., C. van der Wilk, W.L.A. Hetterscheid. 1996. *Amorphophallus* Blume ex Decaisne. In: Flach, M., F. Rumawas (Eds). PROSEA: Plant Resources of South-East Asia No. 9. Plant Yielding Non-seed Carbohydrates. Backhuys Publishers,Leiden.

[2] Santoso, E., N. Sugiyama, S. Hikosaka, T. Takano. 2004. Classification of *Amorphophallus variabilis* in West Java, Indonesia based on morphological characteristics of inflorescences. *Jpn J. Trop. Agric.* 48(1). 25-34.

[3] Sumarwoto. 2005. Iles-iles (*Amorphophallus muelleri* Blume); Deskripsi dan sifat-sifat lainnya. *Biodiversitas.* 6. 185-190.

[4] Hetterscheid, W.L.A., S. Ittenbach. 1996. Everything you always wanted to know about Amorphophallus but were afraid to stick your nose into. *Aroideana.* 19. 7-131.

[5] Yuzammi, Y. 2009. The genus of *Amorphophallus* Blume ex Decaisne (Araceae-Thomsonieae) in Java. *Reinwardtia.* 13. 1-12.

[6] McPherson, S., W. Hetterscheid. 2011. *Amorphopallus* in the wild and in cultivation. *The Plantsman.* 10. 91-97.

[7] Serafinah, I. 2011. Pola pertumbuhan Porang (*Amorphophallus muelleri* Blume) dan pengaruh lingkungan terhadap kandungan oksalat dan glukomanan umbi. PhD Thesis. Airlangga University, Surabaya.

[8] Giles, B.E. 1990. The effects of variation in seed size on growth and reproduction in the wild barley Hordeum vulgare ssp. Spontaneum. *Heredity.* 64. 239-250.

[9] Bregtanolle, F., J.D. Thompson, R. Lumaret. 1995. The influence of seed size variation on seed germination and seedling vigor in diploid and tetraploid *Dactylis glomerata* L. *Ann. Bot.* 76(6). 607-615.

[10] Halpern, S.L. 2005. Sources and consequences of seed size variation in *Lupinus perennis* (Fabaceae): adaptive and non-adaptive hypotheses. *Am. J. Bot.* 92(2). 205-213.

[11] Sumarwoto. 2004. Pengaruh pemberian kapur dan ukuran bulbil terhadap pertumbuhan iles-iles (*Amorphophallus muelleri* Blume) pada tanah ber-Al tinggi. *Ilmu Pertanian.* 11. 45-53.

[12] Sumarwoto, Maryana, 2011. Pertumbuhan bulbil iles-iles (*Amorphophallus muelleri* Blume) berbagai ukuran pada beberapa jenis media tanam. *Jurnal Ilmu Kehutanan.* 5. 91-98.

[13] Susko, D.J., L. Lovett-Doust. 2000. Patterns of seed mass variation and their effects on seedling traits in *Alliaria petiolata* (Brassicaceae). *Am. J. Bot.* 87. 56-66.

[14] Pellegrino, G., F. Bellusci, A. Musacchio. 2010. The effects of inflorescence size and flower position on female reproductive success in three deceptive orchids. Bot. Stud. 51. 351-356.

[15] Moussavi Nik, M., M. Babaeian, A. Tavassoli. 2012. Effects of seed position on the parental plant on seed weight and nutrient content of wheat (*Triticum aestivum*) grain in different genotypes. *Ann. Biol. Res.* 3. 534-542.

[16] Gutterman, Y. 2000. Maternal effects on seeds during development. In: Fenner, M. (Ed). Seeds: The Ecology of Regeneration in Plant Communities. CABI, Wallingford.

ISSN. 2087-2852
E-ISSN. 2338-1655

[17] Moravcova, L., I. Perglová, P. Pyšěk, V. Jitěch, J. PergJ. 2005. Effects of fruit position on fruit mass and seed germination in the alien species *Heracleum mantegazzianum* (Apiaceae) and the implications for its invasion. *Acta Oecol.* 28. 1-10.

[18] Wang, A.B., D.Y. Tan, C.C. Baskin, J.M. Baskin. 2010. Effect of seed position in spikelet on life history of *Eremopyrum distans* (Poaceae) from the cold desert of north-west China. *Ann. Bot.* 106(1). 95-105.

[19] Arslan, N., A. Ipek, A. Rahimi, G. Ipke. 2013. The effects of placement position and corm size of saffron (*Crocus sativus* L.) on stigma and corm yields in Ankara conditions. *J. Herbal Drug*. 4(1). 1-6.

[20] Waithaka, K. 1984. Growth and flowering patterns of Liatris corms in Kenya. *Acta Hort.* 158. 249-253.

[21] Widjanarko, S.B., A. Faridah, A. Sutrisno. 2014. Optimation of ultrasound-assisted extraction of Konjac flour from *Amorphophallus muelleri* Blume. In: Williams, P.A., G.O. Phillips (Eds). Gums and The Stabilizer for The Food Industry 17: The Changing Face of Food Manufacture: The Role of Hydrocolloids. Royal Society Chemistry, Cambridge.

[22] Tartirat, O., S. Charoenrein. 2011. Physico-chemical properties of Konjac Glucomannan extracted from Konjac Flour by a simple centrifugation process. *Food Sci. Technol.* 44. 2059-2063.

[23] Imouha, C.I., F.A. Kalu. 1995 Calcium oxalate dan physico-chemical properties of cocoyam (*Colocasia esculenta* and *Xanthosoma sagittifolium*) tuber flour as affected by processing. *Food Chem.* 54. 61-66.

[24] Addai, I.K., P. Scott. 2011. Influence of bulb size at planting on growth and development of the common hyacinth and the lily. *Agric. Biol. J. N. Am.* 2(2). 298-314.

[25] Memon, N.N., M. Qasim, M.J. Jaskani. 2009. Effect of various corm sizes on the vegetative, floral and corm yield attributes of Gladiolus. *Pak. J. Agr. Sci.* 46(1.)13-19.

[26] Kareem, A., M.A. Khan, S.U.R. Rehman, I. Afzal. 2013. Different corm sizes affect performance of Gladiolus grandiflorus cvs. Red Majesty and Early Yellow. *Adv. Zoo Bot.* 1(4). 86-91.

[27] Aroids, B.D. 2000. Plants of the Arum Family. Portland, Oregon: Timber Press.

[28] Indriyani, S., E. Arisoesilaningsih, T. Wardiyati, H. Purnobasuki 2011. A model of relationship between climate and soil factors related to oxalate content in porang (*Amorphophallus muelleri* Blume) corm. *Biodiversitas.* 12(1). 45-51.

An Analysis on Hemocytes Profile in Kijing Taiwan (*Anodonta woodiana*) and Water Quality in Freshwater Aquaculture Ponds

Dyah Ayu Wijayanti[1*], Asus Maizar Suryanto Hertika[2], Bagyo Yanuwiadi[3]

[1]Master Program of Environmental Resource Management and Development, Graduate School, University of Brawijaya, Malang, Indonesia

[2]Faculty of Fisheries and Marine Sciences, University of Brawijaya, Malang, Indonesia

[3]Department of Biology, Faculty of Mathematics and Natural Sciences, University of Brawijaya, Malang, Indonesia

Abstract

Kijing Taiwan (*Anodonta woodiana*) is found in water with muddy substrate. Kijing Taiwan lives in bottom waters and is relatively settled. Kijing Taiwan is a filter feeder organism that can filter water and is able to survive in polluted environment, so it can be used as a bio-indicator of a water body. The study was conducted in the Public Hatchery Unit (UPR) Sumber Mina Lestari. Profile hemocytes in Taiwan Kijing influenced by environment pollution inducer among others. Hemocytes were observed consisting of Total Haemocyte Count (THC) and Differential Haemocyte Count (DHC). The results show that the profile of hemocytes (THC and DHC) of Kijing Taiwan is not polluted. Results from aquaculture pond water quality measurements indicate that the indicators of the water quality i.e. temperature, pH, dissolved oxygen, and ammonia are still in normal limits. However, in TOM test, BOD and soil organic matter has exceeded the normal limits. The existence of organic matter became the medium of life for Kijing Taiwan, due to its role as a biofilter among other organic materials.

Keywords: Hemocytes Profile, Kijing Taiwan, Water Quality.

INTRODUCTION

Public Hatchery Unit (UPR) Sumber Mina Lestari is a regional center for the cultivation of freshwater fish. It is located in Banjartengah, Sumbersekar Village, District Dau, Malang Regency. There are mollusks that live inside Kijing Taiwan. To improve agricultural productivity, farmers are still dependent on the use of various chemicals such as inorganic fertilizers and pesticides [1]. The use of inappropriate dose of chemicals often leaves residues in the environment. Living organisms used as bio motor have the following criteria: are widely spread geographically, have ecological tolerance, are polynomials, have stable population, become indicators of ecosystem, have high pollution tolerance, and are easy to recognize. One living organism that meets the requirements as bio motor in aquaculture ponds of UPR Sumber Mina Lestari is the freshwater mussel or referred to as Kijing Taiwan (*Anodonta woodiana*).

Kijing Taiwan (*A. woodiana*) is a freshwater mussel found in waters with muddy substrate. Kijing Taiwan lives in bottom waters and is relatively settled. Kijing Taiwan is a filter feeder organism that can filter water and is able to survive in polluted environment, so it can be used as a bio-indicator of a body of water. Pollutants that enter the body Kijing Taiwan can affect the haemocyte profile, and thus by analyzing Total Haemocyte Count (THC) and Differential Haemocyte Count (DHC) of Kijing Taiwan in aquaculture ponds of UPR Sumber Mina Lestari, we can examine and analyze the water quality that support the life of Kijing Taiwan. The results show that the profile of haemocyte (THC and DHC) of Kijing Taiwan is not polluted but there has been found hyaline cells in the stage of introduction of foreign objects; thus, it is clear that Kijing Taiwan can be utilized as an early indicator of water pollution [2].

MATERIALS AND METHODS

Study Area and Sampling

The descriptive qualitative method is used in determining haemocyte profile and water quality in freshwater aquaculture ponds at the location of the research. Sampling was conducted at three stations can be seen in Figure 1. Total 30 Kijing Taiwan was taken randomly at each station with the same weight and length criteria.

The study was conducted in aquaculture ponds in UPR Sumber Mina Lestari situated in in Banjartengah, Sumbersekar Village, District Dau, Malang Regency, East Java Province. The area of UPR Sumber Mina Lestari is 1.7 ha. The geographical location of the village of Sumbersekar is 112017'10.90"- 112057'00" EL and 7044'55.11"-8026'35.45" SL at 25-26°C and 630-670 m above

* Correspondence author:
Dyah Ayu Wijayanti
Email : dyah.puny@gmail.com
Address : Graduate School, University of Brawijaya, Jl. Mayjen Haryono No. 169 Malang, 65145

ISSN. 2087-2852
E-ISSN. 2338-1655

sea level. Rainfall in UPR Sumber Mina Lestari is an average of 875-3000 mm per year.

Data Collection and Analysis

Observation is made actively on Total Haemocyte Count (THC) [3] and Differential Analysis Results for Haemocyte Count (DHC) of Kijing Taiwan [4]. Observation on Haemocyte Differential Count (DHC) of Kijing Taiwan was done in three types of haemocyte cells, i.e. granulocytes, semi granulocytes, and hyalinosit. Granulocyte cell consists of granules in the cytoplasm and capable of phagocytosis and move resembles an amoeba, whereas hyaline cells have only a few granules. Semi granule has a larger shape than hyaline, elongated oval-shaped with few number but spread out. To determine the relationship between the environment and the metabolic status of bivalves, haemocyte system, and the development of pollution, bivalve haemocyte can be used as an environmental biomarker [2].

Water Quality

In this study, measurements on water quality in aquaculture ponds were done, because the water quality could support microbial life in it, especially Kijing Taiwan. Water quality (Table 1) parameters including physical parameters (temperature) and chemical parameters (pH, dissolved oxygen, total organic matter, soil organic matter and ammonia). Each parameter was measured thrice for each station.

Figure 1. Location of the Research at Three Stations (**Source:** Google Earth, 2016)

Table 1. Haemocyte Count and Water Quality Measurement

No	Method & Measurement	Tools	Materials
1	Total Haemocyte Count (THC) [3]	- Syringe 1 mL - Eppendorf - Cover glass - Haemocytometer - Microscope - Washing bottle	- Haemocyte of Kijing Taiwan - Trypanblue 0.01% - Tissue - Na-citrate 10% - Aquades
2	Differential Haemocyte Count (DHC) [4]	- Haemocyte preparation - Microscope - Washing Bottle	- Methyl alcohol - Tissue - Giemsa Solution - Aquades
3	Temperature [5]	- Termometer Hg - Stopwatch	- Ropes - Tissue
4	pH [6]	- Standard sheet of pH - Stopwatch	- Ponds water - pH paper
5	Dissolved Oxygen (DO) [7]	- DO bottle - Funnels - Drop pipet - DO meter - Burette - Statif - Washing bottle	- Ponds water - Amylum - $MnS0_4$ - $Na_2S_2O_3$ 0.025 N - NaOH + KI - Aquades - H_2S0_4 - Label paper
6	Total Organic Matter (TOM) [8]	- Erlenmeyer - Statif - Burette - Funnels	- Ponds water - Aquades - $KMnO_4$ - Label paper - H_2SO_4
7	Biological Oxygen Demand (BOD) [9]	- Erlenmeyer - Burette - Statif - Funnels - Winkler bottle - DO bottle - Washing Bottle - Drop pipet	- Ponds water - $MnS0_4$ - NaOH + KI - H_2S0_4 - Amylum - $Na_2S_2O_3$ 0.025 N - Aquades - Label paper - Diluent solution
8	Soil Organic Matter [10]	The organic carbon in the sample is oxidized with dichromate in an acidic atmosphere. The chromium III formed is equivalent to the oxidized C-organic and measured by spectrometry.	
9	Ammonia [11]	Ammonia level was tested with Spectrophotometer in Phenate condition.	

ISSN. 2087-2852
E-ISSN. 2338-1655

RESULTS AND DICUSSION

Total Haemocyte Count (THC)

Based on the research conducted, the granulocyte cells have a larger form and have granules in them. Otherwise, semi granulocyte cells are smaller than the granulocyte cells and larger than the hyaline cells. Hyaline cells have the smallest size and have no granule. The Total Haemocyte Count (THC) can be seen in Table 2.

Table 2. Total Haemocyte Count for Kijing Taiwan

Station	Total Haemocyte Count (cell.ml^{-1})
1	76
2	90.33
3	40.33

Based on the research results, Total Haemocyte Count (THC) for Kijing Taiwan taken in UPR Sumber Mina Lestari ranges from 40.33 x 10^4 to 90.33 x 10^4 cells.mL^{-1}. The THC results indicate that the condition of Kijing Taiwan is unhealthy. It is in accordance with the previous study [12], the value of THC in bivalves must be between 6.4 ± 2.2 x 10^5 cells.mL^{-1} (64 x 10^4 cells.mL^{-1}). THC value above or below the normal range indicate bivalves reproduced in large quantities due to exposure of foreign material and pathogens.

Differential Haemocyte Count (DHC)

The first research result on Haemocyte Differential Count (DHC) is hyalinosit cells. The research results in UPR Sumber Mina Lestari show hyalinosit cells by 54% - 57%. Based on the research results obtained, it is known that Kijing Taiwan at the study site has not been polluted. This is in accordance with the previous study [2] that mentioned the uncontaminated hyalinosit on *Crassotrea gigas* range between 76.3-87.3%. Hyalinosit value obtained in this study is more than 87.3%, showing that granulocytes in Kijing Taiwan have been contaminated, as shown in Table 3.

Table 3. Differential Haemocyte Count for Kijing Taiwan

Haemocyte Cells	Differential Haemocyte Count (%)		
	Station 1	Station 2	Station 3
Hyalinosit	55	57	54
Semi-granulocytes	27	29.67	26.67
Granulocytes	18	13.33	19.33

There are hyaline cells at UPR Sumber Mina Lestari; this happens due to foreign objects or pollutants in UPR Sumber Mina Lestari still in the introduction stage. Hyalineosit is the result of cell growth after going through several stages of maturation into granulocytes [13]. If hyalineosit cells are found more than granulocytes cells, then it can be suspected that the hemocytes are being introduced to foreign substances such as heavy metals and to subsequent encapsulation.

The high percentage of granulocytes and low percentage of hyalineosit will enhance the immune ability that will contribute to reducing vulnerability to disease attacks. At the time of introduction of the hyalineosit cells to foreign materials, the nucleus will release an enzyme called lectins enzymes, i.e. an enzyme that which will react with the surface of cells and increase the PPA (Prophenoloxidase Activating Enzyme). PPA is envisaged as part of the immune system that may be responsible for the introduction of a foreign object in the organism's defense system such as bivalves [13].

One form of organism's defense response to the condition of the body that does not support the increase in phagocytic cells playing role in enhancing the immune response is by increasing the ability of hemocytes cells for phagocytosis [14]. The abundance of circulating hemocytes is influenced by several factors, among others are sex, size, and body weight, and by external factors such as temperature, salinity, and dissolved oxygen [15].

The second result of research on Haemocyte Differential Count (DHC) is semi granulocytes. Semi granulocyte cells are mature form of hyaline cells—in the time of pathogen attacks, hyaline cells play the first role [15]. Based on the research results on Haemocyte Differential Count (DHC), semi granulocyte cells in UPR Sumber Mina Lestari show a value ranges from 26.67% to 29.67%. This happens because of semi granulocyte cells in UPR Sumber Mina Lestari are in the introduction stage to stressors.

Semi granulocyte cells play a major role in the process of encapsulation and a little in the process of phagocytosis [16]. Semi granular cells function more in producing prophenoloxidase, an enzyme that plays a role in non-specific defense system. Activities of prophenoloxidase (PROPO) will free an enzyme from granular cells.

There are mitochondria in haemocytes as an intracellular key to the contamination of foreign objects because they are permeable and highly sensitive. Mitochondria accumulating heavy metals lead to disruption of energy balance. Bivalves have non adaptive immune system and they are able to eliminate pathogens depending on the cooperation of cellular and humoral mechanisms. Hemocytes in shellfish play a role to phagocytosis, especially in the response of immune cells to fight pathogens that enter the body [16]. According to Alifuddin [17], a

ISSN. 2087-2852
E-ISSN. 2338-1655

component of foreign objects can activate cellular defense responses such as phagocytosis and encap-sulation. Cell antibodies can enhance the ability of hemocytes cell phagocytosis. Hemocytes as the immune system fight foreign substances such as heavy metal i.e. Pb, , and Cd through humoral and cellular expressed as Haemocyte Differential Count. Cellular immune response in shellfish contaminated with heavy metals will show different results, and it is possible to result in not only a decrease in the number of haemocytes but also an increase in the number of haemocytes and change the composition of haemocytes.

Based on the research results on granule cells, the granulocyte cells obtained range between 13.33% to 19.33%. Based on these results, granulocyte cells obtained from UPR Sumber Mina Lestari can be said to be free from pollution. This is in accordance with previous study by Soil Research Institute [18], that uncontaminated granulocyte in shellfish shall show a value range between 11.24% to 22.4%. Granulocytes value obtained is more than 22.4% signifying that granulocyte cells in Kijing Taiwan have been contaminated.

The granulocyte cells contained several cell organelles such as lysosomes, where lysosomes serves to hold the metals accumulated. The lysosome is a channel for the metal deposit [19]. Inside lysosomes, there are hydrolytic enzymes that are associated with cytoplasmic granules found in some species of mollusks. There is a trace of metal accumulation in cytoplasmic granules and an increase in the number of granulocytes in shellfish taken from contaminated environments. Granulocyte cells active in phagocytosis in oysters are a sign that there has been a response and internal resistance in the body of the oyster to the environment polluted by heavy metals such as Pb, Cd, and Hg. Several enzymes are found in granulocytes i.e. amylase, glikogenase, lipase, protease, and the complex oxidation systems. Previous study showed that bivalves recast pollutants caused by the increase in the value of circulating hemocytes [20].

This happens because in UPR Sumber Mina Lestari, an introduction of contaminants occurs in hyaline cells. According to previous study [21], encapsulation is a reaction of immune defense against foreign substances and environmental influences. Granulocyte cells contain hydrolytic enzymes that play a role in phagocytosis against microbes that contribute to intracellular death.

Water Quality of the Ponds

In this study, measurements on water quality in aquaculture ponds were done, because the water quality could support microbial life in it, especially Kijing Taiwan. Water quality parameters measured in this study included temperature, pH, dissolved oxygen, TOM, soil OM, and ammonia. The results of water quality measurements carried out in UPR Mina Lestari can be seen in Table 4.

Table 4. Value Range on Water Quality

Parameter	Water Quality	Standards Measurement Result
Temperature (^oC)	25-26	28-32 [17]
Ph	8	7-8.5 [14]
DO ($mg.L^{-1}$)	7-8	≥ 5 [17]
TOM ($mg.L^{-1}$)	28.89-36.67	≥20 [14]
BOD ($mg.L^{-1}$)	2.23-397	3 [20]
Soil Organic Matters (%)		2-3 [12]
Amonia ($mg.L^{-1}$)	0.44-1.16	< 0.02 [20]

Results from water quality measurements indicate that the value of the indicators of the quality of the water, i.e. temperature, pH and dissolved oxygen are still in normal limits. However, TOM, BOD, soil organic matter and ammonia have all exceeded the normal limits. This leads to increased fertility of water due to high organic matter in the aquaculture ponds, so it is natural if the development of Kijing Taiwan happens rapidly because there are many natural food sources for Kijing Taiwan. The description of each indicator of water quality will be explained below.

Temperature

Temperature measurement was done in UPR Sumber Mina Lestari at 08.00 pm. Based on the research results, obtained temperature ranged between 25 to 26°C (Fig. 2). This showed that the temperature was good for the life of aquatic biota. *Taiwan Kijing* likes environment with a temperature of 24 to 29°C. Kijing Taiwan can live in waters with temperatures between 11 to 29°C.

Temperature is a very important factor in regulating the process of life and spread of the organism. The temperature of water is affected by atmospheric conditions, and the intensity of solar radiation entering the waters mainly in the surface layer. Temperature is influenced by seasons, the intensity of sunlight, air circulation, depth, and topography [22]. The life of bivalves is strongly influenced by temperature, which will affect the metabolism of bivalves, and the in-

ISSN. 2087-2852
E-ISSN. 2338-1655

crease in temperature will increase the rate of metabolism.

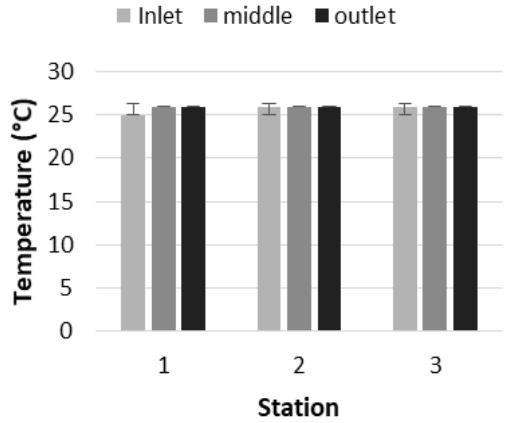

Figure 2. Temperature of Water in Ponds

Changes in temperature can affect the lives of aquatic organisms either directly or indirectly, but the change in the temperature can still be resolved by aquatic biota, where the temperature will affect the rate of metabolism, and the increase in temperature will increase the rate of metabolism [22].

pH

pH measurement in UPR Sumber Mina Lestari was done at 08.00 pm. pH is one of the limiting factors for the life of aquatic biota, one of which is bivalves. Each kind of organism has a different tolerance depending on the saturation levels of dissolved oxygen, alkalinity concentrations, and the type and stage of organisms [23]. Based on the research results, the pH obtained was 8 (Fig. 3). This indicates the pH was good. pH range supporting the life of bivalves must be between 6 to 9 [24]. Therefore, Kijing Taiwan could live well in the study site.

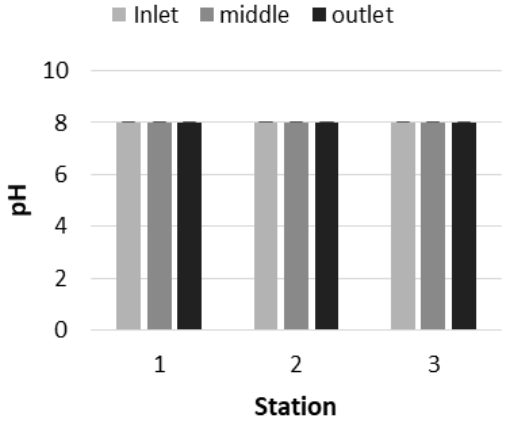

Figure 3. pH of Water in Ponds

The pH value can affect the properties of dissolved heavy metal. At high pH, heavy metals will settle, while at low pH free ions are released into the water or the water column. In addition, pH affects toxicity of chemical compounds, and heavy metals will increase their toxicity at low pH [24].

Dissolved Oxygen (DO)

Measurement of dissolved oxygen carried out in UPR Sumber Mina Lestari at 08.00 pm. Based on the results, obtained dissolved oxygen was 7-8 $mg.L^{-1}$ (Fig. 4). The results were considered good for biota as it was more than 5 $mg.L^{-1}$. Thus, dissolved oxygen is essential for living organisms because it is used for the process of metabolism and respiration. The main source of oxygen in a body of water comes from a process of diffusion of free air and the results of photosynthetic organisms that live in the water.

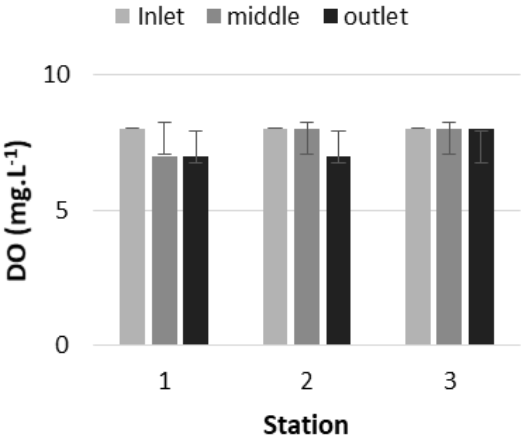

Figure 4. Dissolved Oxygen (DO) of Water in Ponds

The decomposition of organic and inorganic materials can reduce the oxidation of dissolved oxygen in the water until it reaches zero (anaerobic). Effect of dissolved oxygen to heavy metals is inversely proportional, in which the lower the dissolved oxygen, the higher the toxicity of heavy metals, and the vice versa [22].

Total Organic Matter (TOM)

Total Organic Matter (TOM) is the entire organic material that has not been or will undergo decomposition. The organic material is a food source for marine life. Based on the analysis of water quality, the value of total organic matter in Sumber Mina Lestari ranged from 28.89 to 36.67 $mg.L^{-1}$ (Fig. 5).

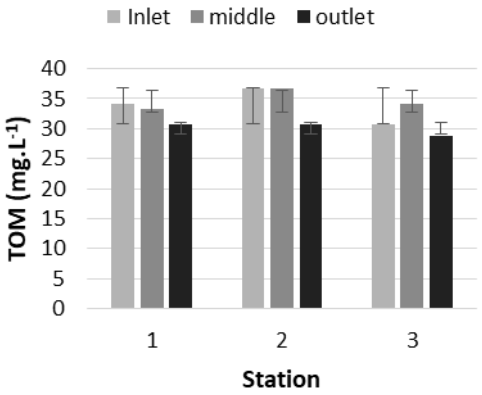

Figure 5. Total Organic Matter of Water in Ponds

Total Organic Matter (TOM) describes the total organic matter content in the water, consisting of dissolved organic matter, particulate, and colloids. The organic material can be used as a backup food for aquatic organisms, especially for organisms that live in bottom waters [25].

Biological Oxygen Demand (BOD_5)

Biological Oxygen Demand (BOD_5) or biological oxygen requirement is the amount of oxygen needed by microorganisms in the water environment to break down organic waste material found in the water environment. Based on the analysis of water quality, the value of Biological Oxygen Demand (BOD_5) in Sumber Mina Lestari ranged between 24 to 45 $mg.L^{-1}$ (Fig. 6) and it has exceeded the normal threshold value at 3 $mg.L^{-1}$ [24].

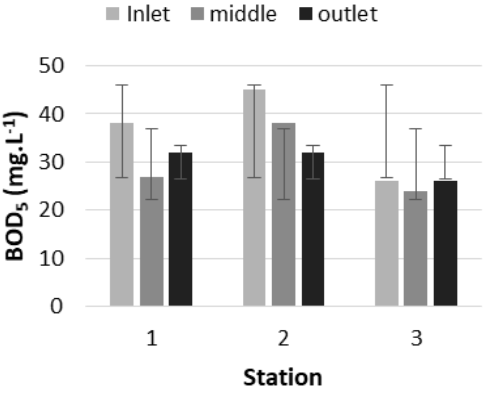

Figure 6. Biologycal Oxygen Demand of Water in Ponds

The high Biological Oxygen Demand (BOD_5) is influenced also by the high value of TOM, as high organic matter breakdown process is in line with the increased use of dissolved oxygen in the water. BOD is the amount of oxygen needed by microorganisms to solve organic materials in the water. BOD examination is required to determine the pollution load due to population or industrial waste water, and to design a water treatment system of polluted biolis. Breakdown of organic matter means that organic materials are used by organisms as food and energy obtained from the oxidation process [26].

Soil Organic Matter

The organic material in the soil of aquaculture ponds in UPR Sumber Mina Lestari was in the range of 2.23 to 3.97%, which indicates that it has exceeded the normal limits set by the Soil Research Institute in 2005 at 3%. See Figure 7.

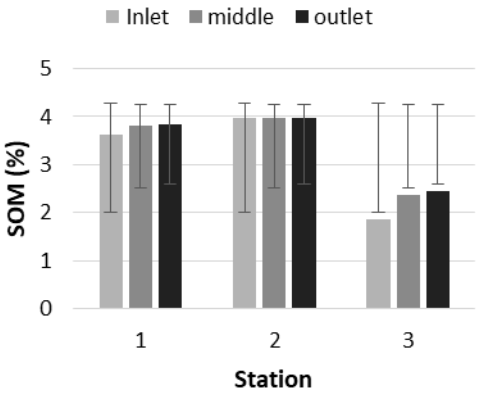

Figure 7. Soil Organic Matter of Water in Ponds

The highest value of soil organic matter was at station 2. This is because station 2 was the main pond used for collecting all the fish seed. Excessive accumulation of organic material in the bottom of the pond, the residual feed and fish feces, make soil organic matter content also increased. Increasing land organic matters will be followed by the high value of ammonia in the water [27].

Ammonia

Measurement of ammonia was also performed in UPR Sumber Mina Lestari. Based on the measurement of ammonia, the results obtained in the study ranging from 0.44 to 1.16 $mg.L^{-1}$. Based on these results, the ammonia value exceeded the quality standard limits [28], which is 0.02 $mg.L^{-1}$. This is caused by the abundant residual fish feed in bottom waters. See Figure 8.

In natural waters, at normal temperature and pressure, ammonia is in the form of gas and will form equilibrium with ammonium ions [22]. In addition to gas, ammonia forms complexes with some metal ions. Ammonia measured in the water is the total ammonia (NH_3 and $NH4^+$). Free

ISSN. 2087-2852
E-ISSN. 2338-1655

ammonia cannot be ionized (ammonia), while ammonium ($NH4^+$) can be ionized. The percentage of ammonia increases with increasing pH value and temperature of water. At pH 7 or less, most of the ammonia will ionize [22].

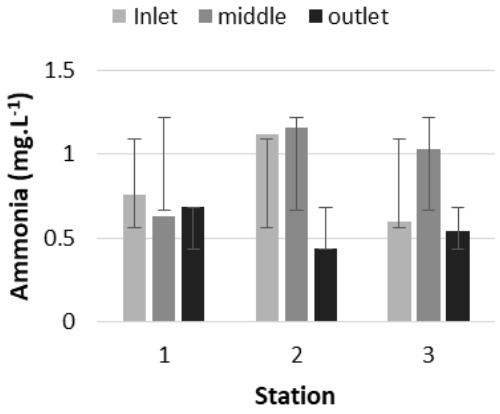

Figure 8. Ammonia of Water in Ponds

CONCLUSION

The results from to show that the profile of hemocytes: THC obtained indicate that the condition of Kijing Taiwan is unhealthy but the THC obtained is part of DHC. The DHC obtained from UPR Sumber Mina Lestari can be said to be free from pollution. Results from aquaculture pond water quality measurements indicate that the indicators of the water quality i.e. temperature, pH and dissolved oxygen are still in normal limits. However, in TOM test, BOD, soil organic matter and ammonia has exceeded the normal limits. The existence of organic matter became the medium of life for Kijing Taiwan, due to its role as a biofilter among other organic materials.

REFERENCES

[1] Personal Communication. 2016. Public Hatchery Unit (UPR) Sumber Mina Lestari. Malang Regency, Dau.

[2] Choi, H.J., J.Y. Hwang, D.L. Choi, M.D. Huh, Y.B. Hur, N.S. Lee, J.S. Seo, M.G. Kwon, H.S. Choi, M.A. Park. 2011. Non-specific defensive factors of the pacific oyster crassostrea gigas against infection with *Marteilioides chuingmuensis*: A Flow-cytometric Study. *Korean J. Parasitol.* XLIX (3). 229-234.

[3] Ekawati, A.W., N. Happy, W. Edi, Marsoedi. 2012. Diatomae *Chaetoceros ceratosporum* dalam formula pakan meningkatkan respon imun seluler Udang Windu (*Penaeus monodon* Fab.). *J. Exp. Life Sci.* 2(1). 1-9.

[4] Tampangallo, B.R., S.P. Chalvyn, A. Rante-tondok. 2012. Respon imun Udang Windu (*Penaeus monodon*) yang dipapar bakteri *Vibrio harveyi*. Proceeding of Seminar on National Fisheries. Fisheries Higher College. Jakarta.

[5] Bloom, J.H. 1998. Analisa mutu air secara kimiawi dan fisika: sebuah laporan tentang pelatihan dan praktek. NUFFIC UB. Faculty of Fisheries and Marine Sciences, University of Brawijaya. Malang.

[6] Subarijanti. 1990. Pemupukan dan kesuburan perairan. Faculty of Fisheries and Marine Sciences, University of Brawijaya. Malang.

[7] Suprapto. 2011. Metode Analisis Parameter Mutu Kualitas Air Untuk Budidaya Udang. Shrimp Club Indonesia. Pacitan.

[8] Indonesian National Standard. 1990. Metode pengukuran kualitas air. Public Work Service. Jakarta.

[9] Tebbutt, T.H.Y. 1992. Priciples of water quality control, 4th Ed. Pergamon Press. Oxford.

[10] Darmono. 2001. Lingkungan hidup dan pencemaran: hubungannya dengan toksikologi senyawa logam. University of Indonesia Press. Jakarta.

[11] Indonesian National Standard. 2005. Cara uji kadar amonia dengan spektrofotometer secara fenat. Office of Indonesian National Standard.

[12] Delaporte, M., P. Soudant, J. Moal, C. Lambert, C. Quere, P. Miner. 2003. Effect of a mono-specific algal diets on immune function in two bivalve species *Crassostrea gigas* and *Ruditapes philippinarum*. *J. Exp. Biol.* 206 (Pt 17): 3053-64.

[13] Ottaviani, C., D. Shapiro, B.I. Goldstein, E.J. Jack, R. Weiss. 2006. Hemodynamic profile, compensation deficit, and ambulatory blood pressure. *Psychophysiology.* 43(1). 46 -56.

[14] Pipe, R.K., S.R. Farley, J.A. Coles. 1997. The separation and characterization of haemocytes from the mussel *Mytilus edilus*. *Cell Tissue Resp.* 289(1). 537-545.

[15] Sari, A.H.W., Y. Risjani, A.P.W. Mahendra. 2012. Efek Konsentrasi sublethal fenol terhadap Total Haemocyte Count (THC) dan histologi insang Kepiting Bakau *(Scylla serata*). *J. Exp. Life Sci.* 2(2). 82-88.

[16] Ekawati, A.W., H. Nursyam, E. Widjayanto, Marsoedi. 2012. Diatomae *Chaetoceros ceratosporum* dalam formula pakan

ISSN. 2087-2852
E-ISSN. 2338-1655

mening-katkan respon imun seluler Udang Windu (*Penaeus monodon* Fab.). *J. Exp. Life Sci.* 2(1). 20-28.
[17] Alifuddin, M. 2002. Immune stimulation in aquatic animal. *J. Aquaculture Indonesia.* 1(2). 87-92.
[18] Soil Research Institute. 2005. Analysis of soil chemistry, plant, water and fertilizers. Agency for Agricultural Research and Development. Department of Agriculture. Bogor.
[19] Giamberini, L., M. Auffret, J.C. Pihan. 1996. Haemocytes the freshwater mussel, *Dreissena polymorpha* Pallas: cytology, cytochemistry and X-Ray microanalysis. *J. Mollusca Stud.* 62(1). 367-379.
[20] Mayrand, E., S.D. Jean, C.C. Simon. 2005. Haemocyte responses of blue mussels (*Mytilus edulils* L.) transferred from a contaminant et site to a reference site: the immune system can recuperate?. *Aquac. Res.* 36. 962-971.
[21] Triana, E., Y.N. Eko. 2006. Novik Test viability of *Lactobacillus* sp. Mar 8 encapsulated. *Biodiversity.* 7(2). 114-117.
[22] Effendi, H. 2003. Telaah Kualitas Air bagi Pengelolaan Sumberdaya dan Lingkungan Perairan. Yogyakarta: Kanisius.
[23] Ruswahyuni. 2010. Populasi dan Keanekaragaman Hayati Bentor Makro pada Perairan Tertutup dan Terbuka di Teluk Awur. Jepara. *Sci. J. Fish. Mar. Resour.* 2 (1). 1-10.
[24] Suwondo, E. F., S. Nurida. 2012. Kepadatan dan Distribusi Mangrove Bivalvia di Pantai Cermin. Sumatera Utara. *J. Biogenesis.* 9(1). 45-50.
[25] Hariyadi, S., Suryadiputra dan B. Widigdo. 1992. Limnologi Metode Kualitas Air. Fakultas Perikanan Institut Pertanian Bogor. Bogor.
[26] Wulandari, R. Y. S. 2011. Kajian Kadar Logam Berat Timbal (Pb) pada Komunitas Periphyton di Enceng Gondok Sungai Lesti Desa Gampingan Kecamatan Pagak Kabupaten Malang. Fakultas Perikanan dan Ilmu Kelautan. Universitas Brawijaya Malang.
[27] Balai Penelitian Tanah. 2005. Analisis Kimia Tanah, Tanaman, Air dan Pupuk. Badan Penelitian dan Pengembangan Pertanian. Departemen Pertanian.
[28] Indonesian Government Regulation. 2001. No.82 about Management of water quality. Republic of Indonesia.

ISSN. 2087-2852
E-ISSN. 2338-1655

Dynamical Analysis of Model for Cholera Disease Spread with Quarantine

Tyas Husadaningsih[1*], Wuryansari Muharini Kusumawinahyu[2], Moch. Aruman Imron[3]

[1]Master Program of Mathematics, Faculty of Mathematics and Natural Sciences, University of Brawijaya, Malang, Indonesia

[2]Department of Mathematics, Faculty of Mathematics and Natural Sciences, University of Brawijaya, Malang, Indonesia

Abstract

In this paper, the model of cholera disease spread with quarantine is discussed. It is assumed that the spread of cholera not only through direct contact between susceptible human populations with bacteria but also through direct contact between susceptible human populations with infected human populations and reduced bacterial populations not only die naturally but can also be done by means of extermination bacteria. Determination of equilibrium points, existence and local stability of equilibrium points are investigated. Numerical simulations are performed to illustrate the results of the analysis.

Keywords: Dynamical Analysis, Model of Spread Cholera, Runge-Kutta Method 4th order, Local Stability, Quarantine.

INTRODUCTION

Cholera disease is a disease caused by drinking water contaminated by poor sanitation or food contaminated by *Vibrio cholera* bacteria. Some symptoms of cholera are watery diarrhea, vomiting and leg cramps. Cholera diseases can be transmitted by direct contact between susceptible populations and the bacterial populations present in the environment [1]. In addition cholera disease can also be transmitted through direct contact between susceptible populations with infected individuals [2].

Cholera disease has spread globally in 1883. Outbreaks of cholera disease in Indonesia occurred since 1992. In 2008-2009 recorded 98,585 people infected with cholera and 4,287 deaths occurred [3]. Based on WHO (World Health Organization) data estimated at 3,000,000-5,000,000 people infected with cholera diseases annually and recorded about 100,000-120,000 cases of cholera suffering death annually [4]. The phenomenon shows that cholera disease poses a global threat to the world, especially in the areas of health, social and economic dynamics.

Based on the history of cholera disease, it is necessary to study the spread of cholera disease. The method used to determine the spread of disease is by using mathematical model of disease epidemic. The epidemic model known since 1927 is often referred to as the SIR type model proposed by Kermack and McKendrick [5]. The SIR model is divided into three compartments, namely S (Susceptible) which states the population is susceptible to disease, I (Infected) which states the population is infected with the disease, and R (Recovered) which states the population is cured of the disease. Furthermore, the model used to determine the spread of cholera disease is the SIRB model (Susceptible-Infected- Recovered -Bacterial) [2,6,7,8]. In the SIRB model [2], it modifies from the SIRB model [8] by adding vaccinations and bacterial eradication. The SIRB model was developed into the SIQRB model (Susceptible, Infected, Quarantine, Recovered, Bacteria) by adding class Q (Quarantine) [1].

In this paper, the cholera disease distribution model will be discussed using the SIQRB type model by modifying from model [1] by adding direct contact of susceptible and infected human populations and bacterial eradication in model [2]. Direct contact between susceptible human populations with infected human populations are added to know that transmission of cholera is not only transmitted through bacteria alone but can be transmitted through infected human populations. Meanwhile, the reduction of bacterial populations can affect the increase of very sharp bacteria. In the modified model, dynamic analysis is done by determining equilibrium point and existence condition, equilibrium point analysis on result of discussion. At the end, a numerical simulation is performed to illustrate the results of the analysis with Runge-Kutta Method 4th order.

* Correspondence address:
Tyas Husadaningsih
Email : tyashusada7@gmail.com
Address : Dept. Mathematics, Faculty of Mathematics and Natural Sciences, University of Brawijaya, Veteran Malang, Malang 65145.

ISSN. 2087-2852
E-ISSN. 2338-1655

MATERIALS AND METHODS

Model Formulation

In this research, we modified the SIQRB model (Susceptible, Infected, Quarantine, Recovered, Bacteria) [1] by adding direct contact of susceptible human populations to infected human populations and bacterial eradication in the SIRB model [2].

Determination of the Equilibrium Point

A dynamical system is a system whose condition in the future will be known if given conditions in the present or past [9]. In completing the dynamic analysis, the first step is to determine the equilibrium point in the mathematical model. The equilibrium point is obtained from equilibrium equations of the system of equations, that is when the population growth rate of SIQRB is zero or equal to zero [10]. From the completion of the equilibrium point that has been obtained it will get the existence of conditions from the point of equilibrium.

Stability of the Equilibrium Point

In this paper, a local equilibrium stability analysis is performed. The determination of local stability begins with a linearization model to be formed Jacobian matrix. From the Jacobian matrix, the roots of characteristic equations or eigen values in the linear system are determined. The stability point is stable locally if the real part of the characteristic roots is negative or equal to zero.

Numerical Simulation

Numerical simulation is done with MATLAB software by applying Runge-Kutta method 4th order. The initial steps taken by determining the value of parameters that fit the terms of existence and the stability requirements of the equilibrium point. Furthermore, in the last step is interpreting the results of numerical simulation in the form of phase portrait graph and the solution curve with time.

RESULT AND DISCUSSION

Model Formulation

In this model, the modifications [1] are made by adding direct contact of susceptible human populations and infected human populations as well as the eradication of bacteria in the model [2]. In the SIRB model and SIQRB model can be written as follows

SIRB Model Formulation [4]

$$\begin{aligned}
\frac{dS}{dt} &= \mu N - \left(\beta_e S\frac{B}{k+B} + \beta_h SI\right) - \mu S \\
&\quad -vS, \\
\frac{dI}{dt} &= \beta_e S\frac{B}{k+B} + \beta_h SI - (\gamma+\mu)I, \qquad (1)\\
\frac{dR}{dt} &= \gamma I - \mu R + vS, \\
\frac{dB}{dt} &= \xi I - \delta B - cB.
\end{aligned}$$

SIQRB Model Formulation [3]

$$\begin{aligned}
\frac{dS}{dt} &= \Lambda - \frac{\beta B}{k+B}S + \omega R - \mu S, \\
\frac{dI}{dt} &= \frac{\beta B}{k+B}S - (\delta+\alpha_1+\mu)I, \\
\frac{dQ}{dt} &= \delta I - (\varepsilon+\alpha_2+\mu)Q, \qquad (2)\\
\frac{dR}{dt} &= \varepsilon Q - (\omega+\mu)R, \\
\frac{dB}{dt} &= \eta I - dB.
\end{aligned}$$

Modified models of equations (1) and (2) become as follows

$$\begin{aligned}
\frac{dS}{dt} &= \Lambda - \frac{\beta_1 B}{k+B}S - \beta_2 SI + \omega R - \mu S, \\
\frac{dI}{dt} &= \frac{\beta_1 B}{k+B}S + \beta_2 SI - (\delta+\alpha_1+\mu)I, \\
\frac{dQ}{dt} &= \delta I - (\varepsilon+\alpha_2+\mu)Q, \qquad (3)\\
\frac{dR}{dt} &= \varepsilon Q - (\omega+\mu)R, \\
\frac{dB}{dt} &= \eta I - dB - cB.
\end{aligned}$$

Diagram of compartment model epidemic cholera of equation (3) can be seen in Figure 1. Description of model parameter of cholera disease can be seen in Table 1 as follows.

ISSN. 2087-2852
E-ISSN. 2338-1655

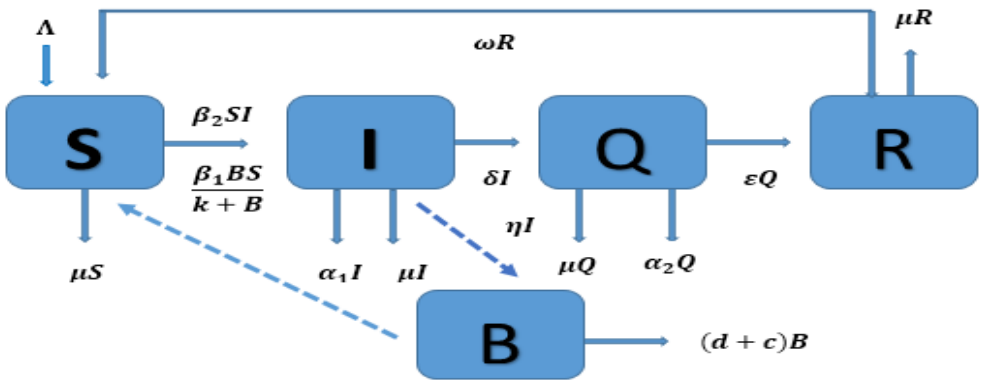

Figure 1. SIQRB Model Compartment Diagram

Table 1. Parameter values and initial conditions for the SIQRB

Parameter	Description
$S(0)$	Susceptible individuals at $t = 0$
$I(0)$	Infected individuals at $t = 0$
$Q(0)$	Quarantined individuals at $t = 0$
$R(0)$	Recovered individuals at $t = 0$
$B(0)$	Bacterial individuals at $t = 0$
Λ	Recruitment rate (birth and migration)
μ	Natural death rate
β_1	Environment-to-human transmission rate
β_2	Human-to-human transmission rate
k	Half saturation constant
ω	Immunity waning rate
δ	Quarantine rate
ε	Recovery rate
α_1	Death rate (infected)
α_2	Death rate (quarantined)
η	Shedding rate (infected)
d	Bacteria death rate
c	Disinfection rate

Stability of Equilibrium Points

The equilibrium point of model (3) is obtained when

$\frac{dS}{dt} = \frac{dI}{dt} = \frac{dQ}{dt} = \frac{dR}{dt} = \frac{dB}{dt} = 0$, that is,

$E_0^*\left(\frac{\Lambda}{\mu}, 0,0,0,0\right)$

$E_1^*(S_1^*, I_1^*, Q_1^*, R_1^*, B_1^*)$

where

$k_1 = \delta + \alpha_1 + \mu, \qquad k_3 = \omega + \mu,$

$k_2 = \varepsilon + \alpha_2 + \mu, \qquad k_4 = d + c,$

$k_5 = \frac{\omega\varepsilon\delta - k_1 k_2 k_3}{\mu k_2 k_3} < 0,$

$A = \frac{\beta_2 \eta k_5}{k_4} < 0,$

$B = \left(\frac{\beta_1 \eta}{k_4} + \kappa\beta_2\right) k_5 + \frac{\eta}{k_4}\left(\frac{\beta_2 \Lambda}{\mu} - k_1\right),$

$C = \frac{\beta_1 \eta \Lambda}{k_4 \mu} + \kappa\left(\frac{\beta_2 \Lambda}{\mu} - k_1\right).$

So that is obtained the value of endemic equilibrium point as follows.

$S_1^* = \frac{\Lambda}{\mu} + k_5 I_1^*,$

$I_1^* = \frac{-B - \sqrt{B^2 - 4AC}}{2A}$, if $\frac{\beta_2 \Lambda}{\mu} > k_1$

$Q_1^* = \frac{\delta I_1^*}{k_2},$

$R_1^* = \frac{\varepsilon\delta I_1^*}{k_2 k_3},$

$B_1^* = \frac{\eta I_1^*}{k_4}.$

The local stability analysis of the system equilibrium point (3) is determined by linearization. Jacobian matrix on model (3) is

$$J(E^*) = \begin{pmatrix} a_{11} & a_{12} & 0 & a_{14} & a_{15} \\ a_{21} & a_{22} & 0 & 0 & a_{25} \\ 0 & a_{32} & a_{33} & 0 & 0 \\ 0 & 0 & a_{34} & a_{44} & 0 \\ 0 & a_{52} & 0 & 0 & a_{55} \end{pmatrix}, \quad (5)$$

ISSN. 2087-2852
E-ISSN. 2338-1655

where

$a_{11} = -\frac{\beta_1 B}{\kappa+B} - \beta_2 I - \mu,\ a_{12} = -\beta_2 S,\ a_{14} = \omega,\ a_{15} = -\frac{\beta_1 S}{\kappa+B} + \frac{\beta_1 SB}{(\kappa+B)^2},\ a_{21} = \frac{\beta_1 B}{\kappa+B} + \beta_2 I,\ a_{22} = \beta_2 S - k_1,\ a_{25} = \frac{\beta_1 S}{\kappa+B} - \frac{\beta_1 SB}{(\kappa+B)^2},\ a_{32} = \delta,\ a_{33} = -k_2,\ a_{34} = \varepsilon,\ a_{44} = -k_3,\ a_{52} = \eta,\ a_{55} = -k_4.$

Theorem 1. The disease free equilibrium point E_0^* on system (3) is as follow.

Proof. The Jacobian matrix at point E_0^* is obtained by substituting the equilibrium point E_0^* in the matrix $J(E^*)$ is obtained.

$$J(E_0^*) = \begin{pmatrix} b_{11} & b_{12} & 0 & b_{14} & b_{15} \\ 0 & b_{22} & 0 & 0 & b_{25} \\ 0 & b_{32} & b_{33} & 0 & 0 \\ 0 & 0 & b_{34} & b_{44} & 0 \\ 0 & b_{52} & 0 & 0 & b_{55} \end{pmatrix},$$

where

$b_{11} = -\mu,\ b_{12} = \frac{-\beta_2 \Lambda}{\mu},\ b_{14} = \omega,\ b_{15} = \frac{-\beta_1 \Lambda}{\mu\kappa},\ b_{22} = \frac{\beta_2 \Lambda}{\mu} - k_1,\ b_{25} = \frac{\beta_1 \Lambda}{\mu\kappa},\ b_{32} = \delta,\ b_{33} = -k_2,\ b_{34} = \varepsilon,\ b_{44} = -k_3,\ b_{52} = \eta,\ b_{55} = -k_4.$

The eigen value of $J(E_0^*)$ is obtained by solving . The characteristic equation $|J(E_0^*) - \lambda I| = 0$

$$-(\mu+\lambda)(k_3+\lambda)(k_2+\lambda)\begin{pmatrix} \frac{\beta_2\Lambda}{\mu} - k_1 - \lambda & \frac{\beta_1\Lambda}{\mu\kappa} \\ \eta & -k_4 - \lambda \end{pmatrix} = 0,$$

Then generated three roots equation of negative characteristic is $\lambda_1 = -\mu, \lambda_2 = -k_3$, and $\lambda_3 = -k_2$ while the other eigen value is the eigen values of the matrix

$$X = \begin{pmatrix} \frac{\beta_2\Lambda}{\mu} - k_1 & \frac{\beta_1\Lambda}{\mu\kappa} \\ \eta & -k_4 \end{pmatrix}.$$

It is seen that the matrix X has a value

$$\det(X) = k_4\left(k_1 - \frac{\beta_2\Lambda}{\mu}\right) - \frac{\eta\beta_1\Lambda}{\mu\kappa}$$

and $trace\,(X) = \frac{\beta_2\Lambda}{\mu} - k_1 - k_4$

Based on [9], the equilibrium point E_0^* is asymptotically stable when the value

$$\det(X) = k_4\left(k_1 - \frac{\beta_2\Lambda}{\mu}\right) - \frac{\eta\beta_1\Lambda}{\mu\kappa} > 0$$

and $trace\,(X) = \frac{\beta_2\Lambda}{\mu} - k_1 - k_4 < 0$. Stability require-ments E_0^* causing existence condition E_1^* is not fulfilled

Theorem 2. The endemic Equilibrium point E_1^* on system (3) is as follow.

Proof. The Jacobi matrix at point E_1^* is obtained by substituting the equilibrium point E_1^* in matrix $J(E^*)$ is obtained

$$J(E_1^*) = \begin{pmatrix} c_{11} & c_{12} & 0 & \omega & c_{15} \\ c_{21} & c_{22} & 0 & 0 & c_{25} \\ 0 & d & -k_2 & 0 & 0 \\ 0 & 0 & \varepsilon & -k_3 & 0 \\ 0 & \eta & 0 & 0 & -k_4 \end{pmatrix}.$$

where

$c_{11} = -\frac{\beta_1 B^*}{\kappa+B^*} - \beta_2 I^* - \mu,\ c_{21} = \frac{\beta_1 B^*}{\kappa+B^*} + \beta_2 I^*,\ c_{12} = -\beta_2 S^*,\ c_{22} = \beta_2 S^* - k_1,\ c_{15} = -\frac{\beta_1 S^*}{\kappa+B^*} + \frac{\beta_1 S^* B^*}{(\kappa+B^*)^2},\ c_{25} = \frac{\beta_1 S^*}{\kappa+B^*} - \frac{\beta_1 S^* B^*}{(\kappa+B^*)^2}.$

The eigen value of $J(E_1^*)$ is obtained by solving $|J(E_1^*) - \lambda I| = 0$, that is

$$\lambda^5 + A_1\lambda^4 + A_2\lambda^3 + A_3\lambda^2 + A_4\lambda + A_5 = 0$$

where

$$\begin{aligned} A_1 &= -c_{11} + k_2 + k_3 + k_4 - c_{22}, \\ A_2 &= -k_3c_{22} + c_{11}c_{22} - k_2c_{22} - \eta c_{25} - c_{11}k_2 + k_3k_4 + k_2k_4 - c_{11}k_3 + k_2k_3 - \\ &\quad - c_{22}k_4 - c_{21}c_{12}, \\ A_3 &= -c_{11}k_2k_3 + c_{11}c_{22}k_3 - c_{11}k_3k_4 + c_{11}c_{22}k_2 - c_{11}k_2k_4 + c_{11}c_{22}k_4 + \eta c_{11}c_{25} - c_{22}k_2k_3 \\ &\quad + k_2k_3k_4 - k_3k_4c_{22} - \eta k_3c_{25} - k_2k_4c_{22} - \eta k_2c_{25} - \eta c_{21}c_{15} - c_{21}c_{12}k_4 \\ &\quad - c_{21}c_{12}k_2 - c_{21}c_{12}k_3, \\ A_4 &= -c_{21}d\varepsilon\omega + c_{11}c_{22}k_2k_3 - c_{11}k_3k_4k_2 + c_{11}c_{22}k_3k_4 + \eta c_{11}c_{25}k_3 + c_{11}c_{22}k_2k_4 \\ &\quad + \eta c_{11}c_{25}k_2 - c_{22}k_2k_3k_4 - \eta c_{25}k_2k_3 - \eta c_{21}c_{15}k_3 - \eta c_{21}c_{15}k_2 \\ &\quad - c_{21}c_{12}k_2k_4 - c_{21}c_{12}k_3k_4 - c_{21}c_{12}k_2k_3, \\ A_5 &= -c_{21}d\varepsilon\omega + c_{11}k_2k_3k_4c_{22} + c_{11}k_2k_3\eta c_{25} - c_{21}c_{15}\eta k_3k_4 - c_{21}c_{12}k_2k_3k_4. \end{aligned}$$

The values of the characteristic equations are solved using the Routh-Hurwitz criterion [11]. The root of the characteristic equation has a

ISSN. 2087-2852
E-ISSN. 2338-1655

negative real part if it qualifies several of the following criteria :

1. Requirements for $A_1 > 0$,
2. Requirements for $A_5 > 0$,
3. Terms for $A_1A_2 - A_3 > 0$,
4. Terms for $(A_1A_2 - A_3)A_3 - {A_1}^2A_4 > 0$,
5. Terms for $(A_1A_4 - A_5)(A_1A_2A_3 - A_3^2 - A_1^2A_4) - A_5(A_1A_2 - A_3)^2 - A_1A_5^2 > 0$.

Numerical Method and Simulations

The numerical method of epidemic model of spreading cholera disease of SIQRB is solved using MATLAB R 2010a software with Runge-Kutta method of order 4. The simulation is done in order to illustrated the result of analysis result so that the behavior of system solution (3) can be depicted graphically. There are two simulated cases that are numerical simulations showing the stability of the equilibrium point $E_0^*\left(\frac{\Lambda}{\mu}, 0,0,0,0\right)$ and numerical simulations showing the stability of the equilibrium point $E_1^*(S_1^*, I_1^*, Q_1^*, R_1^*, B_1^*)$.

The first parameter is chosen to simulate the first equilibrium point is

$\Lambda = 0.009,\ \mu = 0.0002,\ \beta_1 = 0.8,\ \beta_2 = 0.00001,\ \kappa = 10^6,\ \omega = 0.02,\ \delta = 0.05,\ \varepsilon = 0.2,\ \alpha_1 = 0.015,\ \alpha_2 = 0.001,\ \eta = 5,\ d = 0.03,\ c = 1.$

The condition is indicated by modifying various initial values

$NA_1 = (15, 20, 15, 0, 0),\ NA_2 = (22, 10, 5, 10, 5),\ NA_3 = (26, 5, 5, 10, 5),$

and $NA_4 = (24, 15, 5, 5, 10)$

as shown in Figure 1 and Figure 2. Figure 2 illustrates the subpopulation change between by using 4 initial values. It appears that the number of susceptible human populations can survive while the human population is infected, the human population is quarantined, the human population recovered. While the bacterial population is extinct. This condition can be said that the bacteria of *V. cholera* and infected population did not successfully infect the vulnerable population.

Based on the parameter values, the stability condition of the equilibrium point E_0^* is

$det = 0.0644425 > 0$ and
$trace = -1.09475 < 0$

then the number of each subpopulation will go to equilibrium-free equilibrium point $E_0^* = (45, 0, 0, 0, 0)$. Therefore E_0^* is stable asymptotically local.

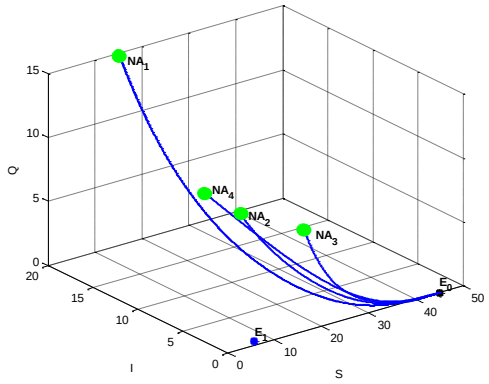

(a) Point phase SIQ

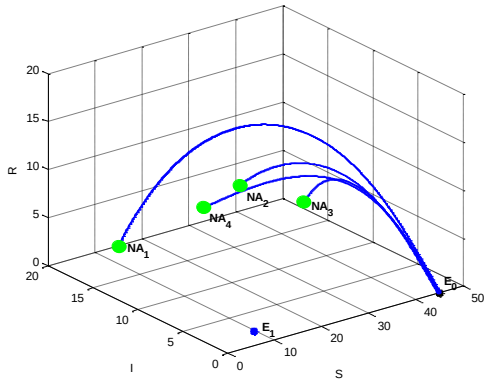

(b) Point phase SIR

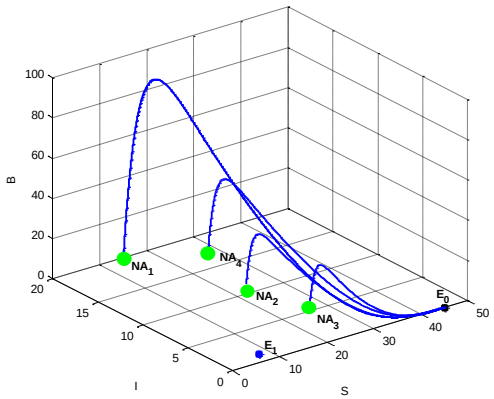

(c) Point phase SIB

Figure 1. Stability the disease free equilibrium E_0^* for NA_1, NA_2, NA_3 and NA_4

ISSN. 2087-2852
E-ISSN. 2338-1655

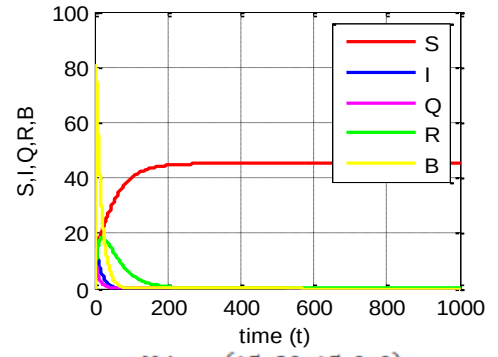

(a) $NA_1 = (15, 20, 15, 0, 0)$

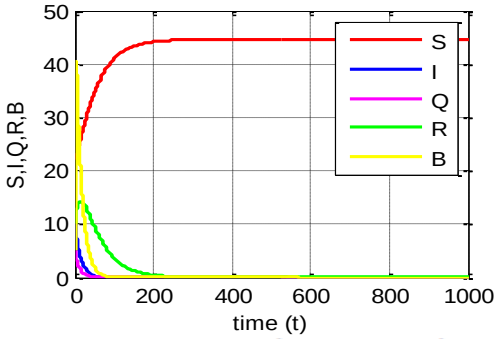

(b) $NA_2 = (22, 10, 5, 10, 5)$

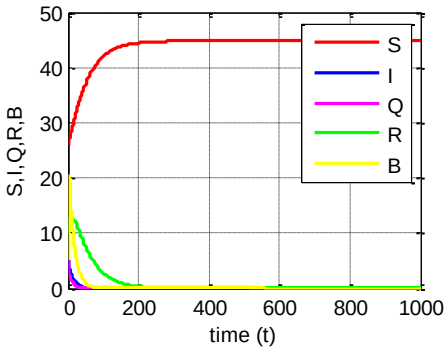

(c) $NA_3 = (26, 5, 5, 10, 5)$

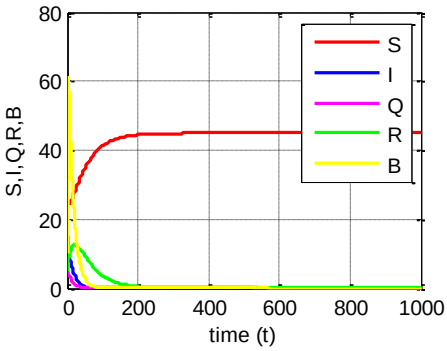

(d) $NA_4 = (24, 15, 5, 5, 10)$

Figure 2. The solution curve of endemic equilibrium point to time $0 \leq t \leq 1000$

Select the parameter value endemic E_1^* by changing the parameter value $\beta_2 = 0.01$ while the other parameter values are the same as the first parameter value, then the stability condition of equilibrium point E_0^* is not fulfilled. While the conditions of existence and stability E_1^* are qualify that is the local asymptotic stable. The condition is shown by using various initial values $NA_1 = (15, 20, 15, 0, 0)$, $NA_2 = (22, 10, 5, 10, 5)$, $NA_3 = (26, 5, 5, 10, 5)$, and $NA_4 = (24, 15, 5, 5, 10)$. As shown on figure 3 and figure 4.

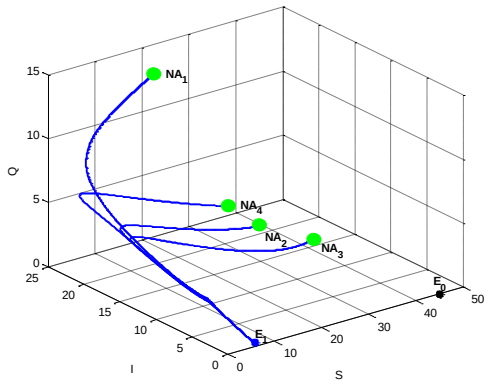

(a) Point phase SIQ

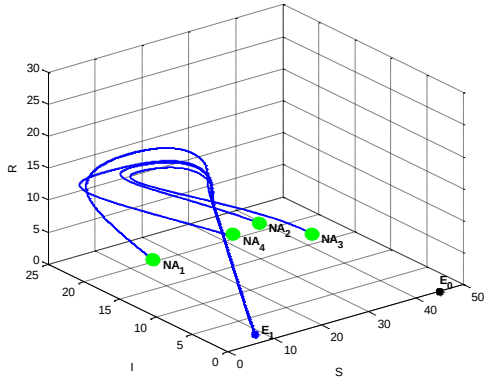

(b) Point phase SIR

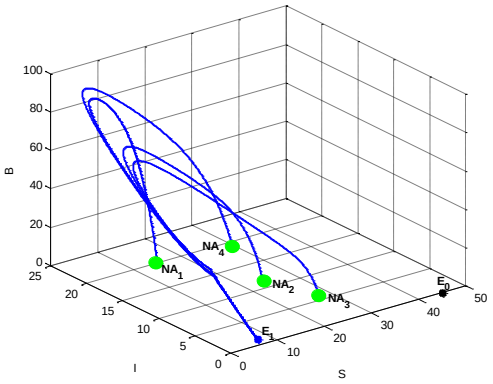

(c) Point phase SIB

Figure 3. Stability the endemic equilibrium E_1^* for NA_1, NA_2, NA_3 and NA_4

ISSN. 2087-2852
E-ISSN. 2338-1655

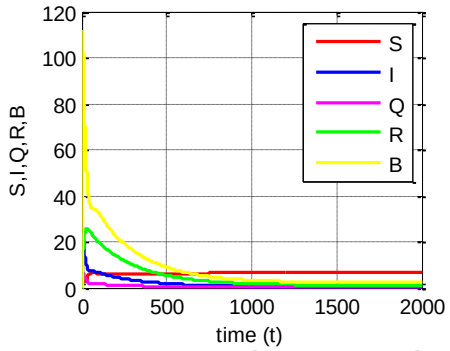

(a) $NA_1 = (15, 20, 15, 0, 0)$

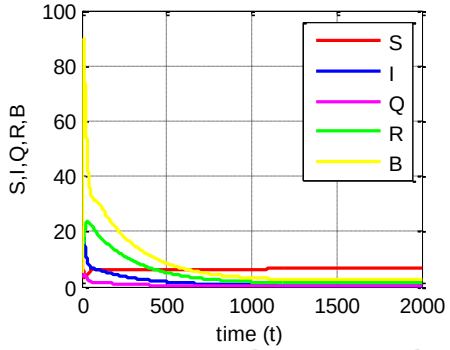

(b) $NA_2 = (22, 10, 5, 10, 5)$

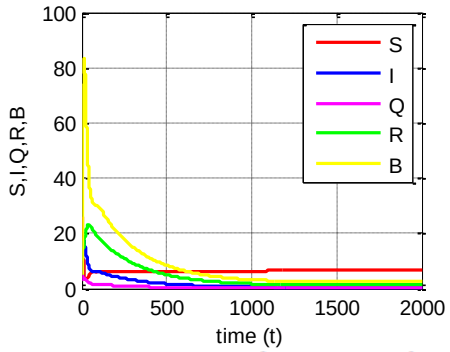

(c) $NA_3 = (26, 5, 5, 10, 5)$

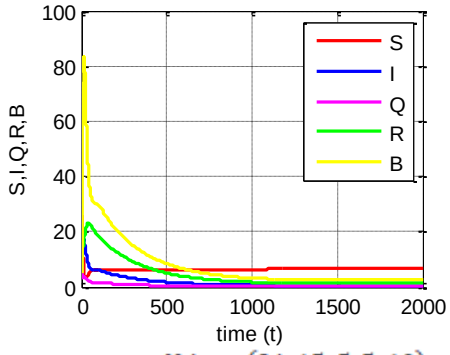

(d) $NA_4 = (24, 15, 5, 5, 10)$

Figure 4. The solution curve of endemic equilibrium point to time $0 \leq t \leq 2000$

Figure 4 illustrates the subpopulation change between $0 \leq t \leq 2000$ by using 4 initial values.

It appears that the human population is susceptible (S), the human population is infected (I), the human population is quarantined (Q), the human population recovered (R), and the bacterial population (B) can survive. This condition can be said that the bacteria vibrio cholera and infected population have been infected the vulnerable population.

Based on the parameter values, the stability condition of the equilibrium point E_1^* is

$$A_1 = 1.256443742 > 0,\ A_5 = 0.0000007190869874 > 0,\ A_1A_2 - A_3 = 0.2941765335 > 0,\ (A_1A_2 - A_3)A_3 - A_1{}^2A_4 = 0.001542449551 > 0,\ (A_1A_4 - A_5)(A_1A_2A_3 - A_3^2 - A_1^2A_4) - A_5(A_1A_2 - A_3)^2 - A_1A_5^2 = 0.0000001174750234 > 0$$

then the number of each subpopulation will go to the equilibrium point of endemic disease

$$E_1^* = (6.51746895,\ 0.4813232099,\ 0.11961131237,\ 1.184288354,\ 2.336520436)$$

Therefore E_1^* is the local asymptotic stable.

CONCLUSION

The SIQRB model is a modification of the model [1] by adding direct contact of susceptible human populations to infected human population and bacterial eradication in model [2]. SIQRB model obtained 2 equilibrium point value that is equilibrium point of disease E_0^* and endemic point of disease E_1^*. Equilibrium points E_0^* and E_1^* are asymptotically stable locally on terms already discussed in the previous discussion. The equilibrium point results are investigated using numerical simulations according to the analysis.

REFERENCES

[1] Lemos-Paiao, A.P., C.J. Silva., D.F.M. Torres. 2017. An epidemic model for cholera with optimal control treatment. *J. Comput. Appl. Math.* 318. 168-180.

[2] Sun, G., J. Xie, S. Huang, Z. Jin, M. Li, L. Liu. 2017. Transmission dynamics of cholera: Mathematical modeling and control strategis. *J. Commun. Nonlinear. Sci. Numer. Simulat. Elsevier B. V.* 45.b235-244.

[3] Mukandavire Z., S. Liao, J. Wang, H. Gaff, D.L. Smith, J.G. Morris. 2011. Estimating the reproductive numbers for the 2008-2009

cholera outbreaks in Zimbabwe. DOI: 10.1073/pnas.1019712108.

[4] World Health Organization (WHO). 2011. Cholera Fact Sheet. Geneva: World Health Organization. Available at: http://www.who.int/mediacentre/factsheets/fs107/en/index.html.

[5] Shuai, Z., J.H. Tien. 2012. Cholera models with hyperinfectivity and temporary immunity. *Bull. Math. Biol.* 74. 2423-2445.

[6] Cheng, Y., J. Wang, X. Yang. 2012. On the global stability of a generalized cholera epidemiological model. *J. Biol. Dynamics.* 6(2). 1088-1104.

[7] Khan, M.A., A. Ali, L.C.C. Dennis, T. Gui. 2015. Dynamical behavior of cholera epidemic model with non-linear incidence rate. *Appl. Math. Sci.* 9(20). 989-1002.

[8] Wang, J., C. Modnak. 2011. Modeling cholera dynamics with controls. *Canadian Appl. Math. Quarterly.* 19(3), 255-273.

[9] Panfilov, A. 2004. Qualitative of differential equation. Utrect University. Utrecht.

[10] Boyce, W.E., R.C. Diprima 2012. Elementary differential equation and boundary value problems, 9th Ed., John Willey and Sons, Inc. United State of America.

[11] Murray, J.D. 2002. Mathematical biology: an introduction, 3rd Ed. Springer-Verlg, Inc. Berlin.

ISSN. 2087-2852
E-ISSN. 2338-1655

Dynamical Analysis of HIV/AIDS Epidemic Model with Treatment

Badria Ulfa[1], Trisilowati[2*], Wuryansari Muharini Kusumawinahyu[2]

[1]Master Program of Mathematics, Faculty of Mathematics and Natural Sciences, University of Brawijaya, Malang, Indonesia
[2]Department of Mathematics, Faculty of Mathematics and Natural Sciences, University of Brawijaya, Malang, Indonesia

Abstract

In this article, an epidemic model of HIV/AIDS with treatment is observed. This model consists of five populations: susceptible, educated susceptible, exposed, HIV infected, and AIDS infected. Antiretroviral therapy (ART) is one type of treatment that can be given to individual that is infected by HIV. This medication can prevent the growth of the virus. Exposed individuals are given short term antiretroviral treatment called Post Exposure Profilaxis (PPP), while for infected individuals are given treatment by combining two or three types of antiretroviral drugs. Dynamical analysis is performed by determining equilibrium points and local stability analysis. Based on the analysis results, two equilibrium points are obtained, namely disease free equilibrium point and endemic equilibrium points. The stability analysis shows that the free equilibrium point is locally asymptotically stable if $R_0 < 1$ and the endemic equilibrium point is locally asymptotically stable under certain conditions. Numerical simulations show that giving two medications together has a greater effect in reducing the spread of the disease.

Keywords: antiretroviral, dynamical analysis, HIV/AIDS.

INTRODUCTION

In medical science, diseases are differentiated into infectious and non infectious diseases. Infectious diseases are diseases caused by bacteria, fungi, viruses, and parasites that can spread through various media. Infectious diseases are a big problem because they can lead to high relative mortality rates, as example is HIV/AIDS.

AIDS (Acquired Immuno Deficiency Syndrome) was first identified in 1981 in Los Angeles, USA. Furthermore, in 1983 has identified the virus that causes AIDS is HIV (Human Immunodeficiency Virus), which is a virus that attacks and damage the human immune system [1]. The spread of HIV virus can occur through several media, such as sexual contact with HIV positive individuals, by sharing needles, by blood transfusions from HIV positive individuals, and through the vertical transmission process, which is mother to child HIV transmission [2].

Treatments that can be done to deal with the spread of HIV/AIDS is the treatment of post exposure prophylaxis (PPP) and antiretroviral (ART). Exposure is an event that causes the risk of transmission. PPP treatment is a short term antiretroviral treatment used to prevent infection after a risk incident. This treatment should be given as soon as possible after exposure, which is in the range of two to four hours. It is stated that the provision of PPP after seventy two hours is declared ineffective [3], so it is recommended to provide treatment by combining two or three types of antiretroviral drugs. ARV treatment works by inhibiting the progression of HIV in $CD4^+$ T-cells, so it can depress the course of the disease and improve the quality of life [2].

Some mathematical models related to the spread of HIV/AIDS have been studied by some researchers. In 2000, Culshaw [4] discussed a delay time differential equation model of HIV infection of $CD4^+$ T-cells. In his study, Culshaw proposed a model for the spread of HIV infection in three compartments, i.e T, I, and V.

In 2009, Cai [5] analyzed the model and stability of the HIV/AIDS epidemic with treatment. The process of transmission of the disease occurs due to the presence of susceptible individuals who interact with individuals exposed and infected with HIV. In this model, the HIV/AIDS epidemic is divided into four compartments, that is $SIJA$. Each compartment states the subpopulation of susceptible individuals (S), exposed (I), infected (J), and AIDS infectious (A).

In 2014, Mahato [6] analyzed the mathematical model of HIV/AIDS with vertical transmission. In this study, the disease epidemic model are expressed in four compartments, i.e S, E, I, A, with the spread of the disease affected by verti-

* Correspondence address:
Trisilowati
Email : trisilowati@ub.ac.id
Address : Dept. Mathematics, Faculty of Mathematics and Natural Sciences, University of Brawijaya, Veteran Malang, Malang 65145.

ISSN. 2087-2852
E-ISSN. 2338-1655

cal transmission, that is transmission from pregnant mother to the baby.

Furthermore, in 2015, Basak [7] proposed a model of the HIV/AIDS epidemic which is expressed in four compartments, namely S, I_1, I_2, A. The process of spreading of the disease is assumed to occur due to the interaction between susceptible individuals with exposed and infected individuals.

In 2016, Huo [8], examined the epidemic model of HIV/AIDS by providing treatment for infected individuals. Huo divided the compartment model of HIV/AIDS epidemic into five parts, namely subpopulation of susceptible individuals (S), infected (I), AIDS infectious (A), therapy recipients (T), and subpopulations for individuals who change sexual habits (R). In this model, HIV transmission occurs when there are susceptible individuals who interact with HIV infected individuals, thus forming a subpopulation of I without exposed compartment.

In 2016, Marsudi [9], analyzed the sensitivity of the HIV virus transmission model with the effect of screening and therapy. The disease model distribution compartment is divided into six, that is susceptible (S), educated susceptible (E), unaware infectives (I_1), aware infectives (I_2), therapy infectives (T), and AIDS infectious (A). The spread of the virus is declared to occur due to the interaction between susceptible individuals with individual unaware infectives, aware infectives, and therapy infectives [9].

Different from previous research, this article examines the epidemic model of HIV/AIDS disease transmission with treatment based on modified results from previous studies of Huo [8] and Marsudi [9]. Modification is done by assuming the disease transmission occurs because of the interaction between susceptible individuals and infected individuals [8]. In addition, treatment is given directly to exposed and infected individuals without forming a subpopulation of individual therapy. In this paper, dynamical analysis is performed by determining the equilibrium points and analyzing their local stability. Finally, numerical simulations are performed to verify the analytical results.

MATERIALS AND METHODS

Contruction Model

In this article, the epidemic model of HIV/AIDS with treatment is expressed in five compartments. Each compartment describes the process of spreading the disease from one compartment to another compartment that is affected by time (t). In this study, the HIV/AIDS epidemic model is in the form of a nonlinear autonomous system.

Determination of the Equilibrium Point

In dynamical analysis, the first step is determining the equilibrium point of the model. The equilibrium point can be done by solving nullcline. In general, the equilibrium point of the disease distribution model is divided into two types, namely the point of disease free equilibrium and endemic equilibrium, with each point representing whether or not there is a disease in a population.

Stability of the Equilibrium Point

Stability analysis is done by linearizing the system of equations to form a Jacobian matrix. Linearization is done with purpose to transform the nonlinear system into linear, so the stability of the equilibrium points can be observed easily. Furthermore, based on the Jacobian matrix, the eigenvalue of the characteristic equation can be determined. If all eigenvalue are negative then the equilibrium point is locally asymptotically stable. On the other hand, it is unstable if at least there is one negative eigenvalue.

Numerical Simulation

Numerical simulations was performed to verify the analytic results and illustrate the behavior of the model. This step is done by using fourth order Runge Kutta method with MATLAB software. The parameter values should be choosen in order that can support the calculation result analytically.

RESULT AND DISCUSSION

Model Formulation

The epidemic model of HIV/AIDS with treatment is obtained based on modified studies [8] and [9]. Modification is done on the process of the spread occurrence of the illness which is assumed as in the previous study [8]. The treatment is given directly to subpopulation of exposed and infected individuals with the aim of reducing the spread of the disease.

The model consists of five subpopulations: subpopulation of susceptible individuals (S), educated susceptible (E), exposed (I_1), HIV infected (I_2), and AIDS infected (A). Each population SEI_1I_2A is positive because it states population density. The compartment diagram of the epidemic model SEI_1I_2A with treatment is described in Figure 1.

The rate of change in the number of individuals susceptible subpopulation (S) is influenced by

ISSN. 2087-2852
E-ISSN. 2338-1655

several conditions, namely the birth rate denoted by Λ, educational programs for susceptible individuals at rate η, and natural death at rate μ. In addition, when susceptible individuals come in contact with HIV infected individuals, they become infected at rate β_1 and then move to the exposed compartment.

In educated susceptible subpopulation which is denoted by (E), the rate of change individuals number is affected by the presence of educated susceptible individuals at rate η, natural death at rate μ and the rate of exposed individuals become HIV infected individuals because of the effect of interacting with HIV infected individuals at rate β_2. Furthermore, this subpopulation changes in the number of individuals are also affected by the presence of exposed individuals become susceptible individual again after receiving PPP treatment at rate u_1.

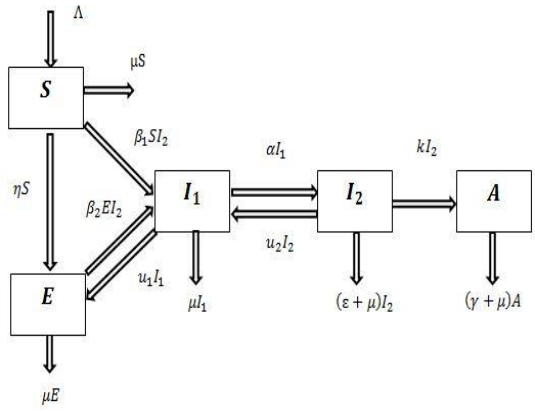

Figure 1. Compartment diagram of HIV/AIDS epidemic model with treatment.

The number of exposed subpopulation individuals (I_1) is increased due to effective contact between susceptible individuals (S) and HIV infected individuals (I_2) at rate $\beta_1 S$ as well as due to effective contact between educated susceptible individuals (E) and HIV infected individuals (I_2) at rate $\beta_2 E$. Besides that, this compartment is influenced by the rate of exposed individuals become HIV infected individuals at rate α, natural death at rate μ, PPP treatment for exposed individuals at rate u_1, and there are HIV infected individuals which become exposed individual again after getting antiretroviral treatment (ART) at rate u_2.

HIV infected subpopulation (I_2) is affected by parameters: α, k, μ, and ε. Parameter α represents HIV transmission rate, k is the transmission rate from HIV infected subpopulation to AIDS infected subpopulation. Furthermore, there is an antiretroviral treatment (ART) for HIV infected individuals at rate u_2.

Finally, the change rate of AIDS subpopulation (A) is influenced by several parameters, such as, k and μ defined as before and γ denotes the death rate due to AIDS infection.

Based on the description above, it is obtained the following differential equation system

$$\begin{aligned}
\frac{dS}{dt} &= \Lambda - \beta_1 S I_2 - (\eta + \mu)S, \\
\frac{dE}{dt} &= \eta S - \beta_2 E I_2 - \mu E + u_1 I_1, \\
\frac{dI_1}{dt} &= \beta_1 S I_2 + \beta_2 E I_2 - (\alpha + \mu + u_1) I_1 + u_2 I_2, \\
\frac{dI_2}{dt} &= \alpha I_1 - (k + \varepsilon + \mu + u_2) I_2, \\
\frac{dA}{dt} &= k I_2 - (\mu + \gamma) A,
\end{aligned} \tag{1}$$

with $\beta_2 < \beta_1$.

Equilibrium Point of Model

In dynamical analysis, determining the equilibrium point of the epidemic model SEI_1I_2A is obtained by solving the equation $\frac{dS}{dt} = \frac{dE}{dt} = \frac{dI_1}{dt} = \frac{dI_2}{dt} = \frac{dA}{dt} = 0$. Based on the system (1), it is obtained the disease free equilibrium point

$$X_0 = (S_0, E_0, I_{10}, I_{20}, A_0) = \left(\frac{\Lambda}{\eta+\mu}, \frac{\eta\Lambda}{\mu(\eta+\mu)}, 0,0,0\right).$$

The equilibrium point X_0 means that there is no infected individual of HIV/AIDS in a population, so that the subpopulation of infected individuals, that is (I_1, I_2, A) are zero. Endemic equilibrium point is stated as

$$X^* = (S^*, E^*, I_1{}^*, I_2{}^*, A^*) \text{ with}$$

$$S^* = \frac{\Lambda}{\beta_1 I_2^* + \eta + \mu},$$

$$E^* = \left(\frac{\eta\Lambda\alpha + u_1 I_2^*(k + \varepsilon + \mu + u_2)(\beta_1 I_2^* + \eta + \mu)}{(\beta_1 I_2^* + \eta + \mu)(\beta_2 I_2^* + \mu)\alpha}\right),$$

$$I_1{}^* = \frac{(k + \varepsilon + \mu + u_2) I_2^*}{\alpha},$$

$$A^* = \frac{k I_2^*}{(\mu + \gamma)}.$$

and the equilibrium point I_2^* is obtained by solving the third degree polynomial equation as follows.

$$I_2^3 K + I_2^2 L + I_2 M = 0. \tag{2}$$

Equation (2) is equivalent to

ISSN. 2087-2852
E-ISSN. 2338-1655

$$I_2 = 0 \quad \text{or} \quad I_2^2 K + I_2 L + M = 0. \qquad (3)$$

with

$$\begin{aligned}K =&(\alpha k\beta_1\beta_2 + \alpha\varepsilon\beta_1\beta_2 + \alpha\mu\beta_1\beta_2 + \mu k\beta_1\beta_2\\ &+\mu\varepsilon\beta_1\beta_2 + \mu^2\beta_1\beta_2 + \mu u_2\beta_1\beta_2),\end{aligned}$$

$$\begin{aligned}L =&(\alpha k\beta_1\mu + \alpha k\beta_2\eta + \alpha k\beta_2\mu + \alpha\varepsilon\beta_1\mu + \alpha\varepsilon\beta_2\eta\\ &+\alpha\varepsilon\beta_2\mu + \alpha\mu^2\beta_1 + \alpha\mu\beta_2\eta + \alpha\mu^2\beta_2 + \mu^2 k\beta_1\\ &+\mu k\beta_2\eta + \mu^2 k\beta_2 + \mu^2\varepsilon\beta_1 + \mu\varepsilon\beta_2\eta + \mu^2\varepsilon\beta_2\\ &+\mu^3\beta_1 + \mu^2\beta_2\eta + \mu^3\beta_2 + \mu^2 u_2\beta_1 + \mu u_2\beta_2\eta\\ &+\mu^2 u_2\beta_2 + u_1 k\beta_1\mu + u_1\varepsilon\beta_1\mu + u_1\mu^2\beta_1\\ &+u_1 u_2\beta_1\mu - \beta_1\beta_2\Lambda\alpha),\end{aligned}$$

$$\begin{aligned}M =&(\alpha k\eta\mu + \alpha k\mu^2 + \alpha\varepsilon\eta\mu + \alpha\varepsilon\mu^2 + \alpha\mu^2\eta + \alpha\mu^3\\ &+\mu^2 k\eta + \mu^3 k + \mu^2\varepsilon\eta + \mu^3\varepsilon + \mu^3\eta + \mu^4 + \mu^2 u_2\eta\\ &+\mu^3 u_2 + u_1 k\eta\mu + u_1 k\mu^2 + u_1\varepsilon\eta\mu + u_1\varepsilon\mu^2\\ &+u_1\mu^2\eta + u_1\mu^3 + u_1 u_2\eta\mu + u_1 u_2\mu^2 - \beta_1\Lambda\mu\alpha\\ &-\beta_2\eta\Lambda\alpha).\end{aligned}$$

To simplify the solution step, first simplified equation (3) becomes

$$I_2^2 + I_2\frac{L}{K} + \frac{M}{K} = 0,$$

which can be written in form

$$I_2^2 + I_2 Q + R = 0, \qquad (4)$$

with

$$Q = \frac{L}{K}, \qquad \text{and} \qquad R = \frac{M}{K}.$$

Based on equation (4) we obtained several possible equilibrium points I_2^* as follows.

In order to obtain an equilibrium point I_2^* a positive real number, it must satisfy

$$Q^2 - 4R \geq 0,$$

and the solution is divided into four cases:

1. $R > 0$ and $Q < 0$,
   i. If $Q^2 = 4R$, then there are two positive twin roots, that is

$$I_{2_\pm} = \frac{-Q}{2}.$$

   ii. If $Q^2 > 4R$, then there are two different positive roots, that is

$$I_{2_\pm} = \frac{-Q \pm \sqrt{Q^2 - 4R}}{2}.$$

2. If $R < 0$ and $Q < 0$, then one positive root is obtained, that is

$$I_2 = \frac{-Q + \sqrt{Q^2 - 4R}}{2}.$$

3. If $R = 0$, and $Q < 0$, then obtained two positive roots, that is

$$I_2 = -Q$$

4. If $R < 0$, and $Q > 0$, then one positive root is obtained, that is

$$I_2 = \frac{-Q + \sqrt{Q^2 - 4R}}{2}.$$

The equilibrium point X^* states that (I_1, I_2, A) exsist in the population. This condition represents that in the population epidemic of HIV/AIDS disease will occur.

Stability of the Equilibrium Point

The stability analysis of the equilibrium point is investigated by linearizing of system (1). From this linearization, it is obtained the following Jacobian matrix

$$J = \begin{pmatrix} -\beta_1 I_2 - (\eta+\mu) & 0 & 0 & -\beta_1 S & 0\\ \eta & -\beta_2 I_2 - \mu & u_1 & -\beta_2 E & 0\\ \beta_1 I_2 & \beta_2 I_2 & -(\alpha+\mu+u_1) & (\beta_1 S + \beta_2 E + u_2) & 0\\ 0 & 0 & \alpha & -(k+\varepsilon+\mu+u_2) & 0\\ 0 & 0 & 0 & k & -(\mu+\gamma) \end{pmatrix}.$$

The Jacobian matrix of the disease free and endemic equilibrium points is obtained by substituting each equilibrium point in the Jacobian matrix.

Teorema 1. The disease free equilibrium point (X_0) of epidemic model SEI_1I_2A is locally asymptotically stable if $R_0 < 1$.

Proof. If it is given a disease free equilibrium point $X_0 = (S_0, E_0, I_{10}, I_{20}, A_0) = \left(\frac{\Lambda}{\eta+\mu}, \frac{\eta\Lambda}{\mu(\eta+\mu)}, 0, 0, 0\right)$, then the Jacobian matrix X_0 is as follows

$$J(X_0) = \begin{pmatrix} -(\eta+\mu) & 0 & 0 & -\frac{\beta_1\Lambda}{\eta+\mu} & 0\\ \eta & -\mu & u_1 & -\frac{\beta_2\eta\Lambda}{\mu(\eta+\mu)} & 0\\ 0 & 0 & -(\alpha+\mu+u_1) & \left(\frac{\beta_1\Lambda}{\eta+\mu} + \frac{\beta_2\eta\Lambda}{\mu(\eta+\mu)} + u_2\right) & 0\\ 0 & 0 & \alpha & -(k+\varepsilon+\mu+u_2) & 0\\ 0 & 0 & 0 & k & -(\mu+\gamma) \end{pmatrix}.$$

The eigenvalues of the $J(X_0)$ matrix are obtained by solving the characteristic equation

$$|J(X_0) - \lambda I| = 0.$$

The eigenvalues of the above matrix are $\lambda_1 = -(\eta+\mu)$, $\lambda_2 = -\mu$, $\lambda_3 = -(\mu+\gamma)$, whereas for λ_4 and λ_5 are obtained by determining *trace* value and determinant of the submatrix

$$J_1(X_0) = \begin{pmatrix} -(\alpha+\mu+u_1) & \left(\frac{\beta_1\Lambda}{\eta+\mu} + \frac{\beta_2\eta\Lambda}{\mu(\eta+\mu)} + u_2\right)\\ \alpha & -(k+\varepsilon+\mu+u_2) \end{pmatrix},$$

$$trace\ J_1(X_0) = -(\alpha + 2\mu + u_1 + k + \varepsilon + u_2) < 0,$$

and

ISSN. 2087-2852
E-ISSN. 2338-1655

$$det\, J_1(X_0) = (\alpha+\mu+u_1)(k+\varepsilon+\mu+u_2) - (\alpha)\left(\frac{\beta_1\Lambda}{\eta+\mu}+\frac{\beta_2\eta\Lambda}{\mu(\eta+\mu)}+u_2\right),$$

$$(\alpha+\mu+u_1)(k+\varepsilon+\mu+u_2) - (\alpha)\left(\frac{\beta_1\Lambda}{\eta+\mu}+\frac{\beta_2\eta\Lambda}{\mu(\eta+\mu)}+u_2\right) > 0,$$

$$(\alpha+\mu+u_1)(k+\varepsilon+\mu+u_2) > (\alpha)\left(\frac{\beta_1\Lambda}{\eta+\mu}+\frac{\beta_2\eta\Lambda}{\mu(\eta+\mu)}+u_2\right),$$

$$1 > \left(\frac{\alpha\mu\beta_1\Lambda+\alpha\beta_2\eta\Lambda+\alpha u_2\mu(\eta+\mu)}{\mu(\eta+\mu)(\alpha+\mu+u_1)(k+\varepsilon+\mu+u_2)}\right).$$

Suppose

$$\left(\frac{\alpha\mu\beta_1\Lambda+\alpha\beta_2\eta\Lambda+\alpha u_2\mu(\eta+\mu)}{\mu(\eta+\mu)(\alpha+\mu+u_1)(k+\varepsilon+\mu+u_2)}\right) = R_0,$$

then

$$R_0 < 1.$$

Based on above description, if R_0<1 then all eigenvalues are negative. It indicates that the disease free equilibrium point is locally asymptotically stable.

Teorema 2. The endemic equilibrium point (X^*) of epidemic model SEI_1I_2A is locally asymptotically stable if and only if $a_n > 0, \forall_n = 0,1,2,3$ and $a_1a_2 - a_0a_3 > 0$.

Proof. If an endemic equilibrium point is given $X^* = (S^*, E^*, I_1^*, I_2^*, A^*)$, then the Jacobian $J(X^*)$ matrix is obtained as follows

$$J(X^*) = \begin{pmatrix} -\beta_1 I_2^* - (\eta+\mu) & 0 & 0 & -\beta_1 S^* & 0 \\ \eta & -\beta_2 I_2^* - \mu & u_1 & -\beta_2 E^* & 0 \\ \beta_1 I_2^* & \beta_2 I_2^* & -(\alpha+\mu+u_1) & (\beta_1 S^* + \beta_2 E^* + u_2) & 0 \\ 0 & 0 & \alpha & -(k+\varepsilon+\mu+u_2) & 0 \\ 0 & 0 & 0 & k & -(\mu+\gamma) \end{pmatrix}$$

The eigenvalues of the $J(X^*)$ matrix are obtained by solving the equation

$$|J(X^*) - \lambda I| = 0.$$

The eigenvalues of this matrix are $\lambda_1 = -(\mu+\gamma)$, $\lambda_2 = -(\beta_2 I_2^* + \mu)$, while for λ_3, λ_4, and λ_5 are obtained based on the solution of a third degree polynomial which is easier solve by using Routh Hurwitz criterion on [10].

The general form of a polynomial equation of third degree is

$$a_0\lambda^3 + a_1\lambda^2 + a_2\lambda + a_3 = 0. \quad (5)$$

By using Routh Hurwitz criterion, from equation (5) the root of the real part is negative if and only if $a_n > 0, \forall_n = 0,1,2,3$ and $a_1a_2 - a_0a_3 > 0$. Thus, the endemic equilibrium point is locally asymptotically stable.

Numerical Method and Simulations

In this section, the simulation results show the change of the number of individuals in each subpopulation S, E, I_1, I_2, A against time. Numerical simulation is executed using MATLAB software which are presented in the following figures (see Fig. 2, Fig. 3, Fig. 4a, Fig. 4b and 4c).

Figure 2 is conducted by using the following parameter values,

$\Lambda = 10, \beta_1 = 0.00005, \beta_2 = 0.0000001, \eta = 0.003, \mu = 0.01, \alpha = 0.2, k = 0.01, \varepsilon = 0.05, \gamma = 0.02,$

$u_1 = 0, u_2 = 0$. Based on these parameter values, it is obtained $R_0 = 0.5236 < 1$. The graph is shown with two different initial values,

$(250, 200, 100, 100, 10)$ and
$(400, 220, 180, 120, 85)$ with each solution convergent toward the point

$(769.23, 230.77, 0, 0, 0)$. The solution behavior of the subpopulation S convergent toward point 769.23 and E converget to point 230.77, while subpopulation $I1, I2, A$ tend to zero. This means, that all solutions move toward the point of disease free equilibrium (X_0) and the numerical simulations obtained are consistent with the results of the analysis that X_0 is locally asymptotically stable. This condition indicates that there is no transmission of disease in the population.

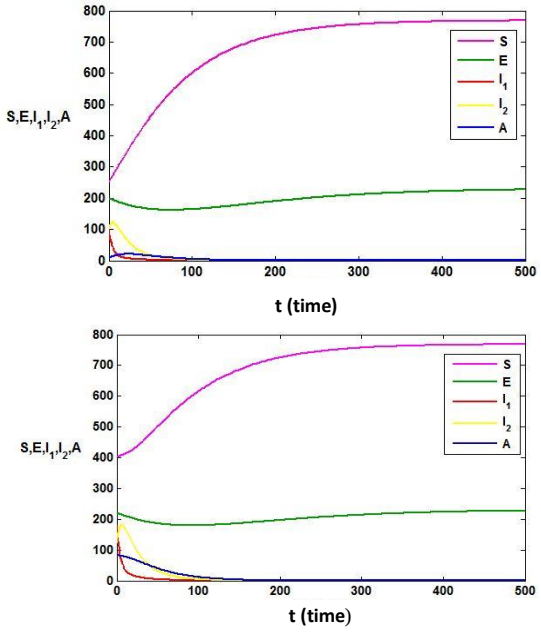

Figure 2. The solution of epidemic model SEI_1I_2A at the equilibrium point X_0.

Figure 3 is illustrated to show the stability of the endemic equilibrium. Parameter values

ISSN. 2087-2852
E-ISSN. 2338-1655

$\Lambda = 100, \beta_1 = 0.0001, \beta_2 = 0.00005, \eta = 0.003, \mu = 0.01, \alpha = 0.5, k = 0.05, \varepsilon = 0.05, \gamma = 0.02, u_1 = 0.03, u_2 = 0.02$

are used in this simulation. These parameters satisfy case two with $R = -1.764618117 \times 10^5$ and $Q = -544.2451155$, which implies the endemic will occur in the population. Moreover, it is obtained

$a_2 = 0.06054611822, a_3 = 0.004265827497,$ and $a_1 a_2 - a_0 a_3 = 0.04183534505$.

By Theorem 2, this indicates that the endemic equilibrium point is locally asimtotically stable which is supported by numerical simulation (Fig. 3). The initial value used in this simulations are

$(250, 175, 150, 75, 50)$ and $(400, 220, 180, 120, 85)$,

it can be seen that all solution convergent to the point

$$(1107.87, 192.26, 200.89, 772.64, 1287.73).$$

Based on these initial condition, the exposed and infected subpopulation convergent toward point 200.89 and 772.64 respectively as time tends to infinity. This condition implies that the disease remains in the population.

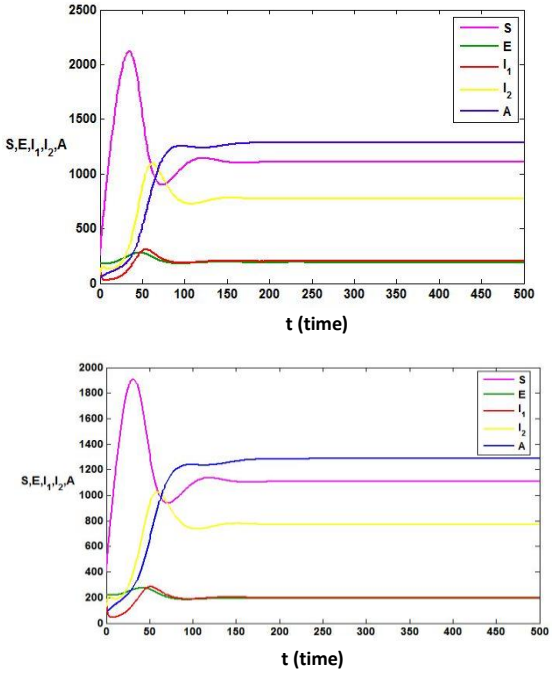

Figure 3. The solution of SEI_1I_2A f at the endemic equilibrium X^* when $R < 0$ and $Q < 0$.

In the HIV/AIDS epidemic model, it is introduced the parameters u_1 and u_2 representing PPP and antiretroviral treatment respectively which is used to help reducing the number of individuals exposed and HIV infected. Figure 4 (a, b, c) states that the changes in parameter values of u_1 and u_2 give a significant effect on the number of HIV infected individuals (I_2).

This is indicated by increasing the values of u_1 and u_2 in the model will result in decreasing the number of infected population. Even the infected population tends to zero along with the increasing the values u_1 and u_2 simultaneously as indicated in Figure 4c. The changing of the value u_1 and u_2 is given in the legend of the figure. Figure 4c also shows that by applying the PPP treatment (u_1) and ARV treatment (u_2) together give a greater effect than applying PPP treatment only on Figure 4a or ARV treatment only on Figure 4b. Therefore, to reduce the number of individuals I_2 is better if both treatments are applied together in order to obtain optimal results.

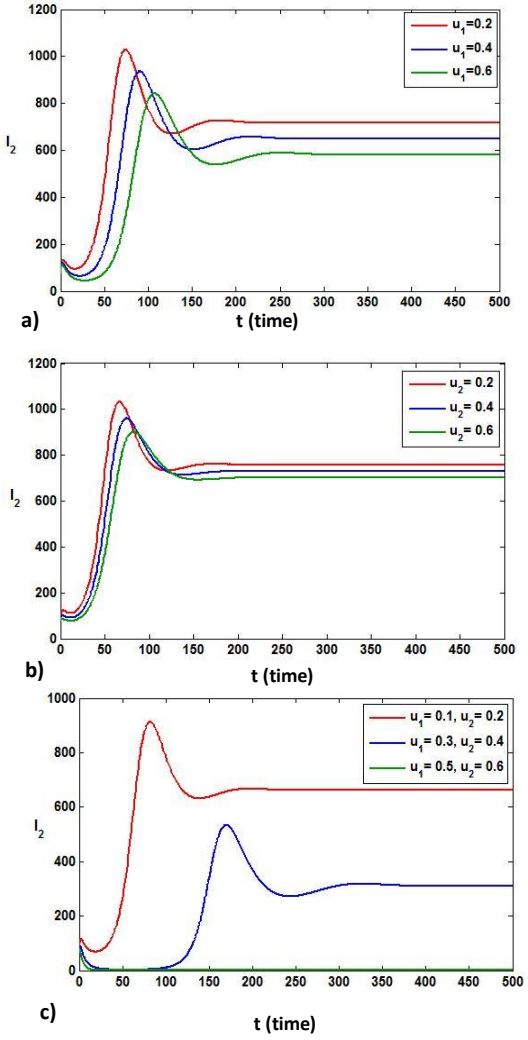

Figure 4. The Effect of Changing Values. a) u_1 on the subpopulation I_2, b) u_2 on the subpopulation I_2, and c) u_1 and u_2 on the subpopulation I_2

ISSN. 2087-2852
E-ISSN. 2338-1655

CONCLUSION

In this study, a HIV/AIDS epidemic model has been observed. The analysis results show that there are two equilibrium points of the model, namely the disease free equilibrium point which is locally asymptotically stable if $R_0 < 0$ and an endemic equilibrium point which is locally asymptotically stable under certain conditions.

The numerical simulation performed support the the analytical result that has been obtained at the result and discussion section, so that both free disease and endemic solutions provide the appropriate results. In addition, the presence of antiretroviral treatment denoted by u_1 and u_2 indicates that PPP and ARV treatment can be used to assist in reducing the number of HIV infected.

REFERENCES

[1] UNAIDS and WHO. 2003. A history of the HIV/AIDS epidemic with emphasis on Africa. Department of Economic and Social Affairs United Nations Secretariat. New York.

[2] UNESCO. 2012. Sexually transmitted infections and HIV/AIDS: supplementary guidebook for reproductive health technicians. UNESCO Indonesia. Jakarta.

[3] Indonesian Department of Health. 2007. Antiretroviral therapy: guidelines for clinical management of HIV infection in adults and adolescents. Indonesian Department of Health. Jakarta.

[4] Culshaw, R.V., S. Ruan. 2000. A delay differential equation model of HIV infection of 〖CD4〗 ^+ T-cells. *Math. Biosci.* 165. 27-39.

[5] Cai, L., X. Li, M. Ghosh, B. Guo. 2009. Stability analysis of an HIV/AIDS epidemic model with treatment. *Comput. Appl. Math.* 229. 313-323.

[6] Mahato, B., B.K. Mishra., A. Jayswal, R. Chandra. 2014. A mathematical model on Acquired Immunodeficiency Syndrome. *The Egypt. Math. Soc.* 22. 544-549.

[7] Basak, U.S., B.K. Datta, P.K. Ghose. 2015. Mathematical analysis of an HIV/AIDS epidemic model. *Am. J. Math. Stat.* 5(5). 253-258.

[8] Huo, H.F., R. Chen, X.Y. Wang. 2016. Modelling and stability of HIV/AIDS epidemic model with treatment. *Appl. Math. Model.* 40. 6550-6559.

[9] Marsudi, R.B.E. Wibowo, N. Hidayat. 2016. A sensitivity analysis of the impact of educational campaign, screening and therapy on the spread of HIV infection. *Nonlinear Anal. Differential Equations.* 4. 327-341.

[10] Murray, J.D. 2002. Mathematical biology I: an introduction, 3rd Ed. Springer Verlag. Berlin Heidelberg.

ISSN. 2087-2852
E-ISSN. 2338-1655

Analysis of Genotype and Phylogenetic of Koi Herpesvirus (KHV) on Carp (*Cyprinus carpio*) in Lombok Island of West Nusa Tenggara Province Based on Thymidine Kinase Sequence

Amira Baihani[1*], Uun Yanuhar[2], Maftuch[3]

[1]Master Program of Fisheries and Marine Sciences, Faculty of Fisheries and Marine Sciences, University of Brawijaya, Malang, Indonesia
[2]Faculty of Fisheries and Marine Sciences, University of Brawijaya, Malang, Indonesia

Abstract

Koi herpesvirus (KHV) is a virus that usually infects carp and koi causing mass mortality, as well as economic and social loss. The results of varied test are often found in its development. Allegedly, there are mutation or genetic variation of KHV in Indonesia. Based on these problems, this research aims to understand the genetic variation and kindship of KHV isolate in the carp (*Cyprinus carpio*) in Lombok Island of West Nusa Tenggara Province based on thymidine kinase sequence. Water quality of fish pond was checked. KHV clinical symptom was checked visually in each fish sample, then sacrifices the organ (gill) for PCR analysis and DNA sequencing. The research results show that clinical symptoms that appear are pale fish gill and bleeding on the surface of the body. The temperature in the research site shows an optimum range for KHV development. The results electrophoresis of carp suspected with KHV shows five positives out of a total six samples. Genetically, KHV isolates from Lombok Island of West Nusa Tenggara Province is identical with the GenBank isolate code KHV-J/U/I and Indo_0C05WNT2.

Keywords: Carp, Koi herpesvirus, Phylogenetic, Thymidine kinase,.

INTRODUCTION

Koi herpesvirus (KHV) is a virus that usually infects carp and koi which lead to their mass death [1]. This virus was identified for the first time in 1998 as the cause of mass mortality of koi fish both juvenile and adult stages cultivated in Israel, United States and Germany [2,3]. KHV entered Indonesia in 2002 through cross-country fish trade [4].

This virus caused mass mortality which reached 80-95% population and has impacts of economic and social loss. This disease caused material loss about 15 billion rupiah in the first three months since the incidence of the disease on March to September 2002 [5]. KHV has been an outbreak in carp and koi almost all over Indonesia. According to the government of Republic of Indonesia, this disease has crossed spread almost all areas of carp farming in Indonesia [6].

Based on the result of the observation in 2016 by the Fish Quarantine Station of Quality Control and Safety Fishery Products Class II Mataram, it was found that quarantine pests and disease of fish in koi and carp namely Koi herpesvirus (KHV). Fish mortality amounted to ± 1,992 fishes showed the mortality pattern that occurred quickly without showing any early symptom of fish disease attack. The review on KHV has been done by several researchers in several centers of cultivation in Lombok. The research results of their studies are the only incident report, until the detection phase using polymerase chain reaction (PCR) [7].

The results of varied test are often found in its development. Allegedly, there are mutation or genetic variation of KHV in Indonesia. According to Walker [8], genetic variation due to mutation of the nucleotide sequence can prevent the binding of primer PCR on the target sequence. Thorough research related to the amplicon sequencing KHV and the amount of geographic location variation of the genome's origin in the future will be useful in distinguishing some KHV isolates based on geographic location [8].

Koi herpesvirus (KHV) has and produces at least four genes encoding the same proteins expressed by the poxvirus: thymidylate monophosphate kinase, ribonucleotide reductase (RNR), thymidine kinase (TK) and B22R-like gene [9]. The use of conventional PCR based on the targeting of the thymidine kinase (TK) gene has been shown to be specific to KHV. The method distinguishes KHV (CyHV-3) from two other herpes viruses, CyHV-1 and CyHV-2 [10]. Based on differences in nucleotide sequence and insertion

* Correspondence address:
Amira Baihani
Email : amirabaihani20@gmail.com
Address : Faculty of Fisheries and Marine Sciences, University of Brawijaya, Veteran Malang, Malang 65145.

ISSN. 2087-2852
E-ISSN. 2338-1655

and deletion pattern among 3 CyHV-3 isolates obtained from Japan (KHV-J), US (KHV-U) and Israel (KHV-I), KHV forms two lineages: J lineage and U/I [11].

Therefore, this research aims to determine the genetic and phylogenetic variation of Koi herpesvirus (KHV) in carp (*C. carpio*) in Lombok Island of West Nusa Tenggara based on sequence analysis of thymidine kinase. It provides the clues on growing variants and their pathogens related to the virus transmission pattern, thereby providing the information for both its prevention and control.

MATERIALS AND METHODS

The research conducted from March to April 2017 at the cultivation location in an area with the KHV epidemic occurrence. Location of cultivation pool of freshwater fish used in this research are Mataram, East Lombok, West Lombok and Central Lombok. The laboratory test conducted at the Fish Quarantine Test Laboratory, Quality Control and Safety Fishery Products Class II Mataram, Fish Quarantine Center, Quality Control and Safety of Fishery Product Class I Surabaya II and First Base Laboratories (molecular biology service) Malaysia.

Samples of fish that have been taken immediately examined of its clinical symptoms such as behavioral observation, and the appearance of the external or internal organs. Furthermore, the fish samples sent to the laboratory for analysis. Examination of clinical symptoms and water quality performed as preliminary data on the determination of KHV infection in carp.

DNA extraction

Fish gill that suspected as infected with KHV virus is cut into small pieces/finely crushed, inserted into a sterile Eppendorf tube and added 1 mL of Tri-Reagent. Tri Reagent tissue and solution are homogenized using pellet pastel, incubated at room temperature for 5 minutes and then centrifugate at 14,000 rpm at room temperature for 5-10 minutes. After centrifugation, collect 200 µL of the supernatant and inserted into new Eppendorf tube. Then, 0.5 mL of 100% alcohol is added to homogeneous and centrifuged at 10,000 rpm, at room temperature for 5 minutes.

The supernatant then eliminated and the pellet washed by adding 1 mL of 70% alcohol and centrifuged at 10,000 rpm, at room temperature for 5 minutes. This method was repeated three times or until the color of yellowish pigment disappears. For the last step, remove the supernatant and dry the pellet of DNA using aerated and dissolved with ddH_2O or Nuclease-Free Water by 25 µL and immediately followed by amplification [12].

PCR Test

KHV tested using PCR test after DNA from fish tissue extracted and determined its concentration. PCR amplification using primer Thymidine kinase [10] with its forward base 5'-GGGTTACCTGTACGAG-3' and reverse 5'-CACCCAGTAGATTATGC-3' with target band of 409 bp (based pairs). The process of amplification begins with the initial denaturation at 95°C for about 5 minutes (1 cycle), and then 30 cycles of amplification consists denaturation at 95°C for about 30 seconds, annealing at the temperature of 50°C for about 30 seconds and extension at the temperature of 72°C for about 30 seconds, terminated with extra elongation at 72°C for about 7 minutes (1 cycle).

After the amplification process completed, 10µL of every sample taken (as well as the marker) then added 2µL of staining solution (6x loading dye) and mixed well on the parafilm. Ten microliters of the sample mixture are inserted into each well on the agarose slowly and carefully. Electrophoresis is carried out with electric power of 100 V, 400 mA for 25 minutes. Immerse the gel in the buffer that added with 0.05% ethidium bromide (EtBr) for 15 minutes. The gel is placed on the gel documentation to observed and documented [12].

DNA Sequencing

Positive PCR product contains DNA KHV packed for sequencing. Sequencing done at First Base Laboratories (molecular biology service) Malaysia.

Data analysis

PCR test results in KHV-positive fishes presented in the form of a picture. Furthermore, the sequenced data are analyzed and edited using the Bioedit [13]. The sequence consensus result is matched with the sequence in GenBank NCBI (National Center for Biotechnology Information) available online through the BLAST (Basic Local Alignment Search Tool) method. Then, using computer software MEGA ver. 3 in align with the data from GenBank assisted using Clustal W computer software [14]. The construction of phylogenetic trees is determined using Neighbour-Joining (NJ-tree) method [15].

ISSN. 2087-2852
E-ISSN. 2338-1655

RESULT AND DISCUSSION

The presence of the virus within the host cell can determinated through the appearance of clinical symptoms or abnormalities in the infected host organ. According to the visual observation of KHV-infected fishes show the increasing of respiratory disorder frequency behavior, swimming toward the water surface, or gathering at the water surface, and weak movement. Observation of the external disorder of some infected fishes show the presence of bleeding and wound on the fish's body, erosion of the gill, color of the gill and pale body and excessive mucus secretion (Fig. 1 and 2).

Clinical symptoms of KHV are often not specific and causes mortality attack in 24-40 hours subsequently. Another study showed that KHV infection causes gill erosion and the appearance of pale, lethargy (fish's mouth always pointing out to the surface), sunken eyes, excessive mucus secretion, discoloration, fish skin peeling and Increased respiratory rates [16,17]. The main clinical symptom of KHV is skin peeling, pale and necrotic of skin and gill [18].

Fish gill damage showed by behavioral disorder such as always swim and gather at the surface or gather at the water surface and increase respiratory frequency, meanwhile, damage of the brain and fish nervous system showed by the aimless movement where both organs are the target of KHV [1,17,19,20].

The symptom of excessive mucus secretion is one of the fish's body-protection responses to the invasion of pathogenic agents including KHV and its environmental change. Mucus in the skin found in the epidermis layer that serves as the body's defense of fish. Moreover, in the epidermal layer, there are also cells that can migrate freely such as lymphocytes and macrophages that play a role in skin immunity and in the epidermal layer, that cells secrete immunoglobulin into the skin mucus [21,22].

Other symptoms found on the fish's body surface are bleeding and skin wound. Bleeding symptom occurs due to the rupture of the blood vessel. In the artery or vein, it can caused by several things such as trauma, inflammation, or erosion of blood vessel wall. Wound or skin damage can caused by the rough treatment and ectoparasitic infestation resulting in elevated sensitivity to secondary infection. Some ectoparasites causes of skin abrasion, although it's not severe, the wound can be the entrance of infectious agents [21].

Water temperature has a role in disease attack in aquatic animals such as being able to increase viral replication in the host while suppressing host immune processes [23]. The most definitive factor affecting KHV virulence is water temperature [19]. That carp lives in the temperature range between 18-30°C and grow optimum between 20-28°C [24]. Water temperature at the study site showed at Figure 3.

Figure 1. The Carp's Gill Infected with KHV are Eroded and Appear Pale

Figure 2. Hemorrhagic and Wound on the Surface of the Fish Body

Optimal temperature of KHV development that can cause death is between 18-27°C. This factor also has something to do with the change of seasons either from the rainy season to the dry season or vice versa, which play a role in the incidence of KHV disease [1].

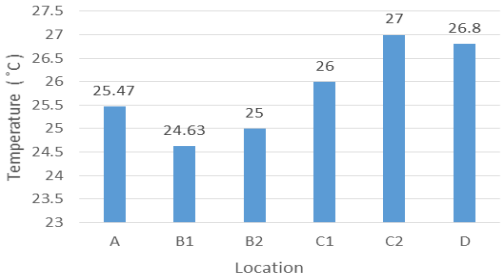

Figure 3. The Temperature at the Study Site. Highest temperature was West Lombok (C2) at 27°C and lowest temperature was East Lombok (B1) at 24.63°C. **Description:** A= Mataram, B1= East Lombok, B2= East Lombok, C1= West Lombok, C2= West Lombok, D= Central Lombok.

ISSN. 2087-2852
E-ISSN. 2338-1655

PCR test performed to ensure that fish test was infected by KHV. The samples that show specific clinical symptoms from one study site was collected and then extracted. Furthermore, they are amplified to produce 409 bp PCR product. The final result obtained KHV positive results of 5 samples representing each location (Table 1).

Table 1. Results of PCR

No	Region	Location	Result of PCR
1.	Mataram	UPR (A)	Positive KHV
2.	East Lombok	BPBIAT (B2)	Positive KHV
		UPR (B2)	Positive KHV
3.	West Lombok	UPR (C1)	Positive KHV
		UPR (C2)	Negative KHV
4.	Central Lombok	UPR (D)	Positive KHV

Note: the PCR test of fish sample with clinical symptom of KHV showed that five was positively infected.

PCR method used in this study proof the presence of KHV in carp, even long after the outbreak. This PCR test [10] where he conducted a research on cloning of the Thymidine kinase gene and state that Thymidine kinase as a standard method to diagnose KHV. PCR test using Thymidine kinase to detect at least 10 femtogram of KHV DNA against 30 virions, while the PCR method by previous study [17,20] used the primary design of the of fragment sequence of DNA restriction at the non-coding region of DNA virus. Its may not match the KHV strain, so the result is undetectable [25].

Accordingly, suggests that PCR using the primary design of the thymidine kinase gene of the KHV genome has higher sensitivity than the two previous methods. Based on the result of the test using PCR method, Electrophoresis gel visualization showed the DNA band banding, the positive result obtained by 409 bp band or parallel to the positive control (Fig.4).

Figure 4. Results of Electrophoresis Visualization of the fish sample suspected to be attacked by KHV. **Description:** M= Marker 100 bp, K+= Positive Control, K- = Negative Control, A to D = Gill Sample.

The result of DNA sequencing from the KHV-infected fish template in the form of the nucleotide sequence (adenine, cytosine, guanine, and thymine) are later used to determine the percentage of the similarity between isolate genotypic examined based on the database GenBank. Isolated KHV from GenBank can be used as the reference for related analysis with genomic data from the existing isolate to predict the evolution speed that occurs and to be reconstructed by the evolutionary relationship between one organism and another.

Based on the multiple alignments (Fig. 5) it can be said that KHV isolate from the Lombok Island has high homology with all four isolates comparatively. Another study reported that phylogenetic analysis using the same methode indicate that isolate of MG, CK and VK (from Indonesian) had close relations of association with KHV strain J isolates and of variant A1 of Asian genotype, whereas KV3 isolates have a close relationship of kinship with the U/I strain KHV isolate and the variant E1, E2, E3 of European genotype [26].

Genetic variation in the virus is one natural way to adapt to environmental changes. Viruses must face its change constantly in their host, as well as passing from one host to another. They must deal with a defense response or immune system of the host. Avoiding the host defense is a central feature of the defensive strategy in all viruses [8].

Mutation can happened at anytime in the growth of a virus population. It may occur spontaneously or may be induced by physical and chemical agents against the DNA. The spontaneous may result from inter-pair faults during DNA replication or during reparation of the DNA. Also, it can occur due to *meaningless* changes in the DNA base, low radiation level, the bases in depuration or deamination or recombination that spontantly change [8].

With regards to genetic analysis of KHV obtained from DNA sequencing and phylogenetic tree construction (Fig. 6), it can illustrated how the relationship between DNAKHV from various locations and can predict the possibility of the outbreak. Sample isolate has a relatively high or very high resemblance, may come from the same source. The increasing inter-regional carp trade in the Lombok Island region or between provinces bring the possibility of spreading the KHV variants that previously found in another location.

A study reported that on isolation and characterization of the first KHV isolates from koi

ISSN. 2087-2852
E-ISSN. 2338-1655

and carp in Indonesia [4]. Clinical symptoms, morphology, histopathology, and thevirions are similar from other countries. Phylogenetic analyses using the thymidine kinasegene from each collected samplesfrom KHV outbreaks throughout Indonesia suggest that Indonesia's are closer to KHV Asian offspring than in Europe [4].

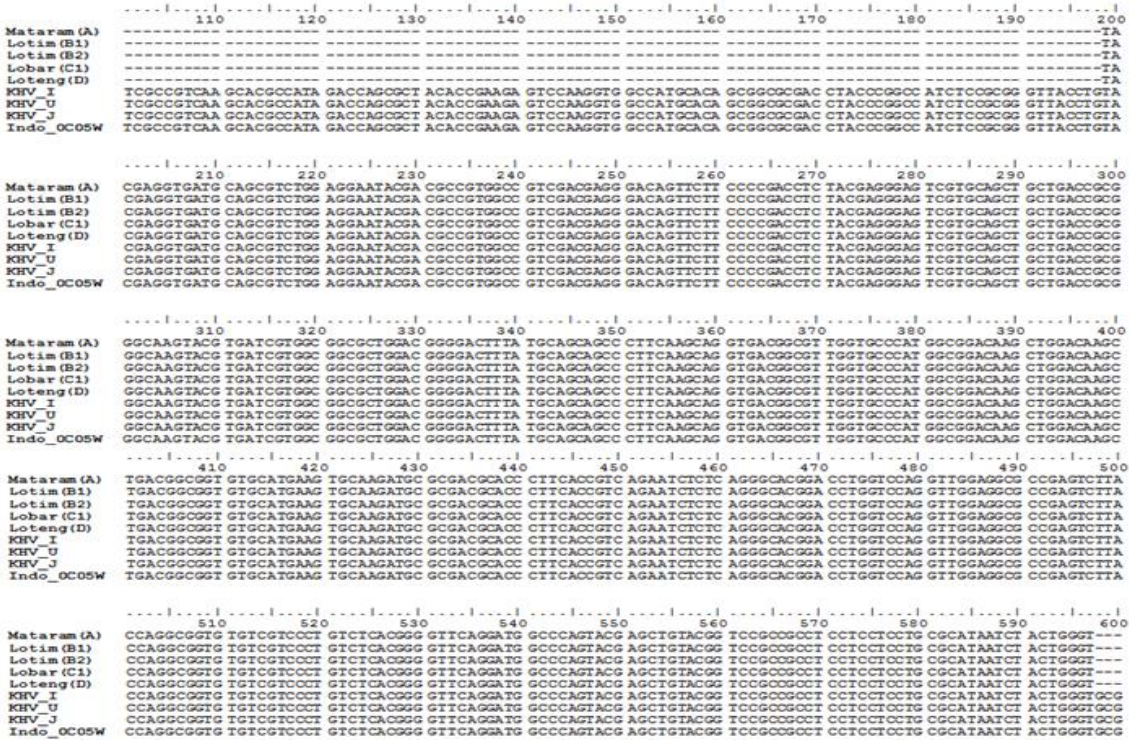

Figure 5. The Result of Multiple Alignments

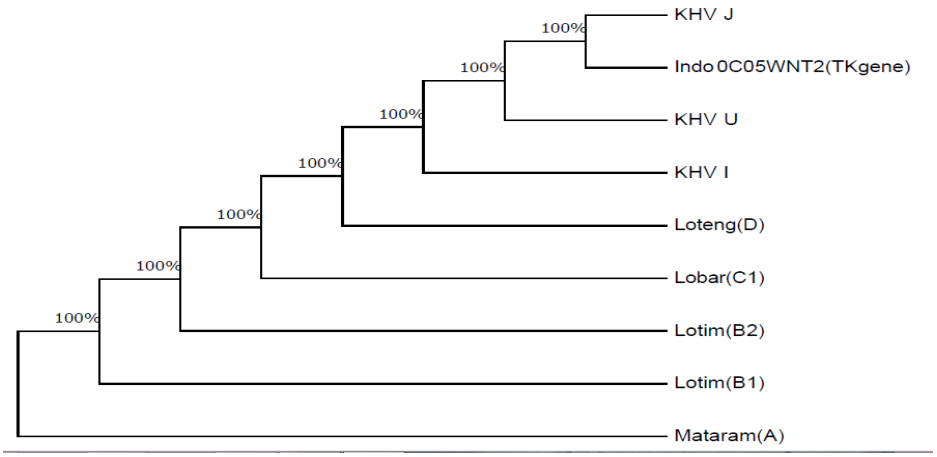

Figure 6. Construction of KHV Isolate Phylogenetic Tree and Comparative Isolate by Neighbors-Joining Method

CONCLUSION

The research shows that clinical symptoms that appear are the pale grill and bleeding on the surface of the body. The results electrophoresis of carp suspected with KHV shows five positives out of a total six samples. Genetically, KHV isolates from Lombok Island of West Nusa Tenggara Province is identical with the GenBank isolate code KHV-J/U/I and Indo_0C05WN.

REFERENCES

[1] Hedrick, R.P., O. Gilad, S. Yun., J.V. Spangenberg, G.D. Marty, R.W. Nordhausen, M.J. Kebus, H. Bercovier, A. Eldar. 2000. A herpesvirus associated with mass mortality of juvenileand adult koi, a strain of common carp. *J. Aquat. Anim. Health*. 12. 44-57.

ISSN. 2087-2852
E-ISSN. 2338-1655

[2] Bretzinger, A., T. Fischer-Scherl, M. Oumouma, R. Hoffmann, U. Truyen. 1999. Mass mortalities in Koi, *Cyprinus carpio*, associated with gill and skin diseases. *Bull. Eur. Assoc. Fish Pathol.* 19(5). 182-199.

[3] Hedrick, R.P., G.D. Marty, R.W. Nordhausen, M.J. Kebus, H. Bercovier, A. Eldar. 1999. A herpesvirus associated with mass mortality of juvenile and adult Koi *Cyprinus carpio*. Fish Health Newsletter, Fish Health Section. American Fisheries Society. California. 12. 44-57.

[4] Sunarto, A., Taukhid, A. Rukyani, I. Koesharyani, H. Supriyadi, L. Gardenia, H. Huminto, D.R.A. Priyono, F.H. Pasaribu, Widodo, D. Herdikiawan, D. Rukmono, S.B. Prayitno. 2005. Field investigations on a serious disease outbreak among koi and common carp (*Cyprinus carpio*) in Indonesia. In: Walker, P.J., R.G. Lester, M.G. Bondad-Reantaso (Eds). Diseases in Asian Aquaculture V. Fish Health Section, Asian Fisheries Society, Manila, Philippines. 125-136.

[5] Sunarto, A. 2004. Epidemiologi penyakit koi herpesvirus (KHV) di Indonesia. Laboratory of Fish Health Research, Research Center of Marine and Fisheries. Jakarta.

[6] Ministry of Marine and Fiheries. 2015. Decision No. 81/KEPMEN-KP/2015. Penetapan area yang tidak bebas penyakit ikan karantina, golongan, dan media pembawanya di wilayah negara Republik Indonesia. Ministry of Marine and Fiheries. Jakarta.

[7] BKIPM Mataram. 2016. Annual Repport 2016. Fish Quarantine Station of Quality Control and Safety Fishery Products Class II. Mataram.

[8] Walker, P.J. 2000. Introduction of virology. CSIRO Tropical Agriculture, Indooroopilly, Queensland, Australia.

[9] Ilouze, M., A. Dishon, T. Kahan, M. Kotler. 2006. Cyprinid herpes virus-3(CyHV-3) bears genes of genetically distant large DNA viruses. *FEBS. Lett.* 580. 4473-4478.

[10] Bercovier, H., Y. Fishman, R. Nahary, S. Sinai, A. Zlotkin, M. Eyngor, O. Gilad, A. Eldar, R.P. Hedrick. 2005. Cloning of the koi herpesvirus (KHV) gene encoding thymidine kinase and its use for a highly sensitive PCRbased diagnosis. *Bio. Med. Central Microbiol.* 5. 13.

[11] Aoki, T., I. Hirono, K. Kurokawa, H. Fukuda, R. Nahary, A. Eldar, A.J. Davidson, T.B. Waltzek, H. Bercovier, R.P. Hedrick. 2007. Genome sequences of three Koi herpesvirus isolates representing the expanding distribution of an emerging disease threatening koi and common carp worldwide. *J. Virol.* 5058-5065.

[12] Fish Quarantine Center. 2008. Metode standar pemeriksaan HPIK golongan virus Koi Herpesvirus (KHV). Puskari Publisher. Jakarta.

[13] Hall, T.H. 1999. Bioedit: a user-friendly biological sequence alignment editor and analysis program for Windows 95/98/NT. *Nucleic Acid Symp. Ser.* 4. 95-98.

[14] Thompson, J.D., D.G. Higgins, T.J. Gibson, 1994. W: Improving the sensitivity of progressive multiple sequence alignment through sequence weighting, position specific gap penalties, and weight matrix choice. *Nucleic Acids Res.* 22. 4673-4680

[15] Nei, M. 1987. Molecular evolutionary genetics. Columbia University Press. New York.

[16] Bondad, M.G. 2002. Transboundary aquatic animal disease focus on Koiherpesvirus (KHV). Aquatic Animal Research Pathologist at the Cooperative Oxford Laboratory of the Maryland, Dept. Natural Resources in Oxford. Maryland.

[17] Gray, W.L., L. Mullis, S.E. LaPatra, J.M. Groff, A. Goodwin. 2002. Detection of koi herpesvirus DNA in tissues of infected fish. *J. Fish Dis*. 25. 171-178.

[18] Oh, M.J., S.J. Jung, T.J. Choi, R. Kim, K.V. Rajendran, Y.J. Kim, M.A. Park, S.K. Chun. 2001. A viral disease occurring in cultured carp *Cyprinus carpio* in Korea. *Fish Path.* 36. 147-151.

[19] Gilad, O., S. Yun, M.A. Adkison, K. Way, N.H. Willits, H. Bercovier, R.P. Hedrick. 2003. Molecular comparison of isolates of an emerging fish pathogen, koi herpesvirus, and the effect of water temperature on mortalityof experimentally infected koi. *J. General Virol.* 84. 2661-2668.

[20] Gilad, O., S. Yun, F.J.Z. Vergara, C.M. Leutenegger, H. Bercovier, R.P. Hedrick. 2004. The Concentration of koi herpesvirus (KHV) in tissues of experimentally infected *Cyprinus carpio* koi as assessed by real-time TaqMan PCR. *Dis. Aquat. Organ.* 60. 179-187.

[21] Roberts, R.J. 2001. Fish Pathology, 3rd Ed. W.B. Saunders. London.

[22] Takashima, F., T. Hibiya. 1995. An atlas fish histology, normal and pathological features,

ISSN. 2087-2852
E-ISSN. 2338-1655

2nd Ed. Kodansha Ltd. Tokyo. Pathological features, 2nd Ed. Kodansha Ltd. Tokyo.

[23] Alcorn, S.W., AI Murray, J.R. Pascho. 2002. Effect on rearing temperature on immune function in sockeye salmon Oncorhynchus nerka. Fish Shellfish Immunol. 12. 303-304.

[24] Serdiati, 1988. Pengaruh padat penebaran terhadap pertumbuhan ikan mas (*Cyprinus carpio)* yang dipelihara dalam keramba pada kolam dengan input air limbah rumah tangga. Bachelor Thesis. Faculty of Animal Husbandry. Hasanuddin University. Makassar.

[25] Haenen, O.L.M, K. Way, S.M. Bergmann, E. Ariel. 2004. The emergence of koi herpesvirus and its significance to European aquaculture. *Bull. Eur. Ass. Fish. Pathol.* 24. 293-307.

[26] Pratiwi, G. 2016. Analisis variasi genotip dan filogenetik koi herpesvirus di Indonesia berdasarkan dua penanda molekuler dan sekuen gen thymidine kinase. Bachelor Thesis. Faculty of Fisheries. Gajah Mada University. Yogyakarta.

ISSN. 2087-2852
E-ISSN. 2338-1655

Effect of 17β-Estradiol on Feminization, Growth Rate and Survival Rate of Pasific White Shrimp (*Litopenaeus vannamei*, Boone 1931) Postlarvae

I Nengah Gde Sugestya[1*], Maheno Sri Widodo[2], Agoes Soeprijanto[2]

[1]Master Program of Fisheries and Marine Sciences, Faculty of Fisheries and Marine Sciences, University of Brawijaya, Malang, Indonesia

[2]Faculty of Fisheries and Marine Sciences, University of Brawijaya, Malang, Indonesia

Abstract

This study was therefore aimed to determine the effect of different concentration of estrogen hormone, 17β-estradiol (E_2) on feminization for the production of all female, growth rate and survival rate of Pasific white shrimp (*Litopenaeus vannamei*) postlarvae (PL). *L. vannamei* PL_1 were stocked randomly at a density of 10 ind.L^{-1} into a 10 L of seawater for each experimental flask with three replicates each. PL_1 was immersed in seawater containing 0.5, 1.0 and 1.5 mg.L^{-1} estrogen hormone, E_2 for 4 hours. The experiment was continued for 30 days for larval rearing. At the termination of experiment, the specimens in each treatment groups were weighed and measured individually for their wet body weight (BW) and total length (TL) for the mean weight gain, length gain and the specific growth rate (SGR) estimation. The mean sex ratio values of male to female postlarvae obtained from control till the highest E_2 hormone concentration of 0, 0.5, 1.0 and 1.5 mg.L^{-1} were 1:1, 1:2, 0:1 and 0:1 respectively. The weight gain and length gain were 40605% and 606% for control, 46310% and 647% for 0.5 mg.L^{-1} concentration, 49310% and 663% for 1.0 mg.L^{-1} concentration and 45048% and 628% for 1.5 mg.L^{-1}. The mean SGR BW and SGR TL for control till the highest E_2 hormone concentration of 0, 0.5, 1.0 and 1.5 mg.L^{-1} were 20.00 and 6.51, 20.46 and 6.70, 20.67 and 6.77 and 20.37 and 6.62 respectively. The mean survival rate for E_2 hormone concentration of 0, 0.5, 1.0 and 1.5 mg.L^{-1} were 52.67%, 54.33%, 54.67% and 52.33% respectively. The study shows that while the concentration of E_2 hormone increased, the female sex ratio of L. vannamei PL also increased but the growth rate and survival rate decreased at concentration of 1.5 mg.L^{-1}. Thus the optimum concentration of this hormone usage was 1.0 mg.L^{-1} immersed for 4 hours.

Keywords: 17β-estradiol, feminization, growth rate, *Litopenaeus vannamei*, postlarvae, survival rate.

INTRODUCTION

In Indonesia, as in many countries, aqua-culture plays an important role in increasing seafood production. Penaeid shrimp is one of the fastest growing aquaculture production sectors [1]. The Pacific white shrimp (*Litopenaeus vannamei*) production has rapidly increased in Asia [2]. In 2006, 88% of penaeid shrimp came from Asia, with the top five producers such as China, Thailand, Vietnam, Indonesia and India are accounting for 81% of world production [3].

Thus, an efficient biotechnology for producing all female penaeid shrimp populations is required especially in Indonesia, in which shrimp farming economically constitute an important source of income [4]. Due to the economic importance of penaeid shrimp worldwide, especially in aquaculture base production, great efforts had been developed for suitable and useful techniques. It is in order to increase the total of harvesting production goal [5]. Thus, the requirement of market demand for shrimps in more uniform sizes, the monosex culture of female penaeid shrimps could be a strategy to produce larger shrimp is become necessary [6].

Commonly, females penaeid shrimp are growing faster and achieve a larger ultimate size than males as they are observed in wild populations [7,8,9]. Possibly, the larger size of females penaeid shrimp also exibhit sex-dependent dimorphic growth pattern that influence females growing faster than the males [10], because females have higher food efficiency utilization and apparent digestibility of energy [7, 11]. Therefore, there is a technique that potential for monosex females culture of penaeid shrimps for decreasing growth period, increasing pond yield, and also provide significantly higher growth rate [12].

The productions of monosex population can be applied through sex reversal achieved by administering androgens or estrogens hormone. While 17β-estradiol has been shown to be an effective feminization hormone in some fish [13], the administration of the steroid in crustaceans focused on reproduction has been attemped but the results are varied and sometime inconsistent [14,15].

* Correspondence address:
I Nengah Gde Sugestya
Email : gdesugestya@gmail.com
Address : Faculty of Fisheries and Marine Sciences, University of Brawijaya, Veteran Malang, Malang 65145.

ISSN. 2087-2852
E-ISSN. 2338-1655

Some study to reverse sex in penaeid shrimps from male to female had reported successful by administering steroid hormone 17β-estradiol through prepared feed in *Penaeus monodon* [16] and banana shrimp (*Fenneropenaeus merguiensis*) [17] during postlarvae stages. But none administration of steroid hormone 17β-estradiol through immersion were reported. Thus, this study aimed to determine the effect of different concentration of immersions estrogen hormone, 17β-estradiol on feminization, survival rate and growth rate of *L. vannamei* postlarvae.

MATERIALS AND METHODS

Sea Water Supply and Water Treatment

This experiment was conducted at National Broodstock Center for Shrimp and Mollusc Karangasem, Bali, Indonesia, where the Pacific white shrimp (*L. vannamei*) postlarvae also obtained. The sea water source was from coastal water of Lombok Strait and pumped to the sedimentation tank and left overnight. The water was desinfected with 30 ppm calcium hypochlorite for 16 hours without aeration, then full aeration was blown throughout the tank for 8 hours. Before use, the sea water was checked with o-Tolidine to make sure there was no chlorine left. When the o-Tolidine test result showed yellowish water, the sea water then de-chlorinated with sodium thiosulfate. After that, 5 ppm EDTA added as chelating agents of heavy metals in the water. The cotton filterbag (50 µm) was used to filter detritus, small organisms and turbid water while sea water being used.

Experimental Design

The culture design consisted of 12 flasks containing each 10 L sea water. All the flasks were put in the 8000L tank containing freshwater which act as the water bath and covered with black hollow plastic to maintain stable temperature of 28-32^{o}C throughout the experimental period. Aeration was distributed from a controled air blower to each flask through transparent long rubber hose which provide with an air stone. *Litopenaeus vannamei* postlarvae day 1 (PL_1) were stocked randomly at a density 10 ind.L^{-1}, so the number of postlarvae stocked in each experimental flask is 100 individuals. The experiment consisted of immersed postlarva containing three consentrations of E_2 at 0.5, 1.0 and 1.5 mg.L^{-1} with three replicates for each treatment. Twenty five PL samples were weighted and measured randomly to obtain the initial body weight (BW) and total length (TL) and recorded.

Hormone Immersions

The hormone solution prepared by following method described by [18,19]. Stock solution of hormone prepared by weighting the amount of 0.5, 1.0 and 1.5 mg.L^{-1} E_2 hormone (Argent Laboratories Inc. Philippines) and dissolved in 1 mL 95% ethanol (Merck) each. The hormon solution then poured in 1 L sea water each and aerated for 30 minutes to evaporate ethanol odor. Amount of PL_1 *L. vannamei* were immersed for 4 hours in hormone solution. After completion of hormone immersion, the flasks were emptied, washed and filled with 10 L filtered sea water. The experiment were maintained until the end of study in this flasks.

Larval Rearing

The daily amount of feed, which include quantity and number of feeding times, were adjusted for growth and survival compensation depend on the age of shrimps. The fed were given four times a day at 07.00 am, 12.00 am, 05.00 pm and 10.00 pm at the rate of 10% wet body weight.day^{-1} [20]. The experiment was continued for 30 days. Water exchange were done by siphoned out 40-50% water and also to removed uneaten food and faeces then replaced with new clean treated and filtered water.

During the study, the parameters of sea water were maintained at 28-32 ppt of salinity, more than 4 mg.L^{-1} for DO, temperature 28-30^{o}C and 7.5-8.5 for pH. After 30 days, the shrimp postlarvae in each flasks were harvested by firstly siphoned out until the depth of water level about 2/3 left and finally shrimps collected using smooth scoop net. Postlarvae harvested from each flask was counted to determine their survival rate, and their weight and length also measured for the growth rate analysis. The shrimp postlarvae were preserved in 10% formaldehyde and put in the bottle sample according to their each concentration of treatment until their sexes observed.

Sex Determination and Sex Ratio

These external sex differentiation of each shrimp between male and female *L. vannamei* in this present study determined by examining the morphological sex structures following the protocol of previous study [10]. The females PL had a pair of oblique sharp ridges on the anterior part of sternite XIV (between the fourth and fifth pereiopods) that characterizes the female thelycum of this species. While the males PL had a masculine appendix at the second pair of pleopods and tubular appendage developed the

ISSN. 2087-2852
E-ISSN. 2338-1655

gonophores complex at the medially of fifth pereiopods.

Size Increasements and Spesific Growth Rate

At the termination of the experiment (after 30 days), the biological measurement of wet body weight (BW) and total length (TL) of random 25 PL *L. vannamei* from each treatment group were weighted and measured individually to estimate the mean final body weight and total length, and the spesific growth rate (SGR). A digital weighing machine (Kern brand) with an accuracy of 0.0001 g and a vernier calliper (Tricke Brand, Shanghai China) with an accuracy of 0.1 mm were use to measure the BW and TL of each PL shrimp, respectively. The SGR of PL was calculated using formula by [21].

$$SGR = \frac{100(\text{in mean final}\frac{BW}{TL} - \text{In mean initial}\frac{BW}{TL})}{\text{Culture Period (days)}}$$

Description:
SGR = Spesific Growth Rate
BW = Body Weight
TL = Total Length

Survival rate

The survival *L. vannamei* PL were also counted at the termination of the study. Survival rate (%) is equal to number of PL harvested divided by number of PL stocked multiply by 100% [22].

Statistical analysis

To determine the differences among treatments, One way Analysis of variance (ANOVA) was used. Post host test and Tukey's test were used to determine the significantly different among treatment. The significance level of the results was set at ($P < 0.05$). All statistics were performed using SPSS (version 16).

RESULT AND DISCUSSION

Sex Ratio

The sex ratio of experimentals groups hormone-treated *L. vannamei* gained from the mean of 25 individuals PL for the three replicates of each treatment. The comparison of mean sex ratio values of male : female gained from control to the highest E_2 hormone concentration of 0, 0.5, 1.0 and 1.5 mg.L^{-1} that is 1:1, 1:2, 1:9 and 0:1, respectively. In this study, as the concentration of E_2 hormone increased from control treatment (0 mg.L^{-1}) until the highest treatment concentration (1.5 mg.L^{-1}), the mean sex ratio values of male to female were also increased. The results obtained were significantly different ($P<0.05$) among the treatments. The sex ratio of experimental groups hormone-treated *L. vannamei* were shown in Figure 1.

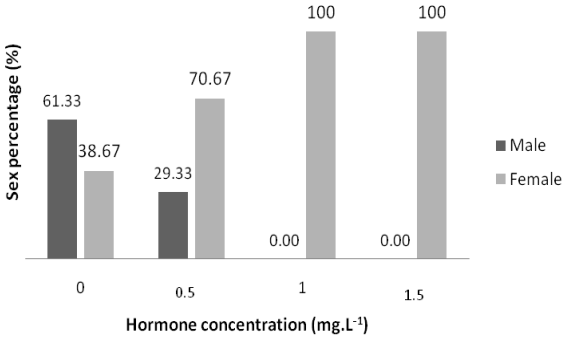

Figure 1. Sex ratio percentage of *L. vannamei* larvae between all hormone concentration (mg.L^{-1}) treatments

This study, showed the administration of E_2 hormone can increase the sex reversal of the male *L. vannamei* PL into 100% females. A similar result was also obtained by previous study in blue gill sunfish, *Lepomis macrochirus* [23]. Thus, it can be stated that E_2 hormonal administration can produce sex reversal not only for fish species but also for Penaeid shrimps. Other studies shown consider successful feminization of tiger shrimp (*Penaeus monodon*) [16] and banana shrimp (*Feneropenaeus merguiensis*) [17] as their mean sex ratio values of male reverse to female increased as the concentration of E_2 hormone increased from control treatment to the highest treatment concentration when administration of E_2 hormone through feed was done during the early stages of their lives.

Growth Rate

The mean SGR BW for control treatment of *L. vannamei* PL after 30 days of culture was 20.00, while for E_2 hormone concentration treatments of 0.5, 1.0 and 1.5 mg L^{-1} were 20.46, 20.67 and 20.37 respectively (Fig. 2). All hormone treatment shrimp shows higher SGR BW than control with the highest SGR BW was 1.0 mg.L^{-1} hormone treatment. The same situation was obtained from SGR TL result (Fig. 3) which showed all hormone treatment shrimp have higher SGR TL than control. The results for control, 0.5, 1.0 and 1.5 mg.L^{-1} treatment were 6.51, 6.70, 6.77 and 6.62 respectively. Immersions through 1.0 mg.L^{-2} E_2 concentration showed the highest SGR TL from all treatments. This study showed the same results obtained from the study on bluegill sunfish, *L. macrochirus* that shown consider successful in administration

ISSN. 2087-2852
E-ISSN. 2338-1655

of E_2 hormone not only on sex reversal but as a growth promoter [23].

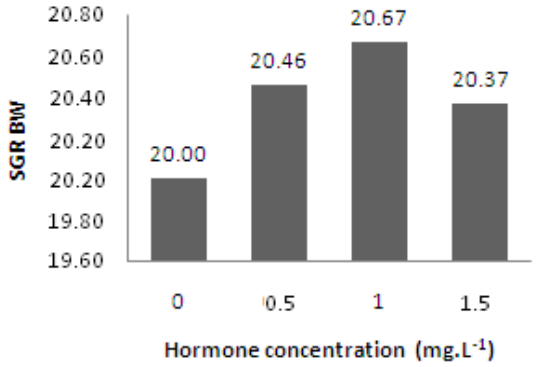

Figure 2. Mean SGR BW of *L. vannamei* larvae between all hormone concentration (mg.L^{-1}) treatments

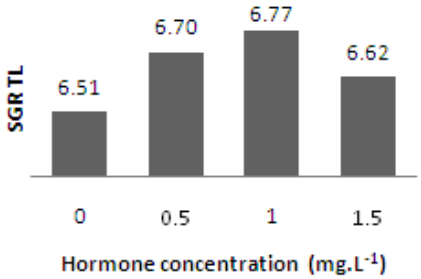

Figure 3. Mean SGR TL of *L. vannamei* larvae between all hormone concentration (mg.L^{-1}) treatments

The weight gain and length gain for control and all treatment were shown in Table 1 and Table 2. Control shows the lowest value of both weight gain and length gain. Hormone concentration of 1.0 mg.L^{-1} showed the highest weight gain and length gain followed by 0.5 and 1.5 mg.L^{-1} hormone concentration respectively. Highly significant difference (P>0.05) was detected among the treatments.

Results of weight gain and length gain were expected to show that the hormone treatment of *L. vannamei* larvae gain weight and length higher and faster than normal or control larvae because E_2 also have been proved to accelerate the growth of coho salmon [24], *Penaeus monodon* [16] and *Fenneropenaeus merguiensis* [17].

The increased E_2 doses (0.5 and 1.0 mg.L^{-1}) had also increased the growth and size of *L. vannamei* PL due to the increasing somatic growth rate for each individual of the monosex population. In monosex population, the shrimp body will concentrate the energy from feed more on somatic growth than in the gonad development [22,25].

Meanwhile, mean SGR BW and SGR TL and also weight gain and length gain at 1.5 mg.L^{-1} E_2 concentration decreased. One of the possible reason for their decreasing because of the high concentration of E_2, as also reported that 17β-estradiol at 62.5 µg.L^{-1} and higher levels may cause growth suppression and low survival rate for mysid shrimp *Americamysis bahia* [26].

Table 1. Weight Gain (%) *L. vannamei* Larvae Between All Hormone Concentration (mg.L^{-1}) Treatments

Hormone doses (mg.L^{-1})	Initial mean weight (g)	Final mean weight (g)	Weight gain (%)
0.0	0.0007 ± 0.0003	0.2849 ± 0.047	40605
0.5	0.0007 ± 0.0003	0.3249 ± 0.018	46310
1.0	0.0007 ± 0.0003	0.3459 ± 0.024	49310
1.5	0.0007 ± 0.0003	0.3160 ± 0.011	45048

Table 2. Length Gain (%) *L. vannamei* Larvae Between All Hormone Concentration (mg.L^{-1}) Treatments

Hormone doses (mg.L^{-1})	Initial mean length (mm)	Final mean length (mm)	Length gain (%)
0.0	5.05 ± 0.74	35.30 ± 2.10	606
0.5	5.05 ± 0.74	37.30 ± 0.83	647
1.0	5.05 ± 0.74	38.20 ± 1.36	663
1.5	5.05 ± 0.74	36.40 ± 0.65	628

Survival Rate

Survival rate of each treatment group was calculated based on mean of three replicates. The highest mean percentage of survival rate was recorded for 1.0 mg.L^{-1} E_2 hormone treatment at 54.67 ± 1.53% while the lowest mean percentages was recorded for 1.5 mg.L^{-1} E_2 at 52.33 ± 3.79%. The survival rate was increase started from 0.5 mg.L^{-1} E_2 at 54.33 ± 1.15 % to 1.0 mg.L^{-1} E_2 at 54.67 ± 1.53 % and slightly decreased at 1.5 mg.L^{-1} E_2 at 52.33 ± 3.79 % (Fig. 4). Highly significant difference (P>0.05) was detected among the treatments.

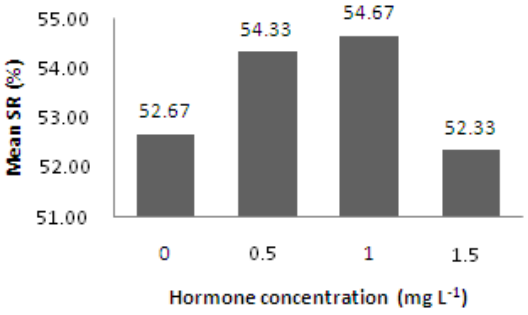

Figure 4. Mean Survival Rate of *L. vannamei* PL Immersed with Different E_2 Hormone Concentration.

The survival rate of 1.5 mg.L^{-1} E_2 hormone treated *L. vannamei* postlarvae were slightly lower comparing with control. It was not surprising because 17β-estradiol treatments result in higher mortality of most aquaculture

ISSN. 2087-2852
E-ISSN. 2338-1655

spesies [27-31]. It was suggested that the *L. vannamei* PL are in the stress with the increasing of E_2 concentrations in their body that will over react their body metabolism thus produced lower survival rate. Based on those result, we conclude that the optimum concentration for the growth and survival rates was 1.0 $mg.L^{-1}$ of E_2.

CONCLUSION

The present study demonstrates that the usage of estrogen hormone, 17β-estradiol through immersion can be an effective method for the production of 100% female *L. vannamei* PL at lowest concentration of 1.0 $mg.L^{-1}$ E_2. The results also showed that E_2 hormone can be acted as a growth promoter in penaeid shrimp (*L. vannamei*) PL either the growth rate and survival rate decrease when the hormone concentration increasing. It also concludes that the optimum concentration of 17β-estradiol was 1.0 $mg.L^{-1}$ for the best feminization, growth and survival rate of *L. vannamei*.

ACKNOWLEDGEMENT

This study was fully funded by a research grant from BPSDMKP, Ministry of Fisheries and Marine Affair. The authors wish to thank all the staff from National Broodstock Center for Shrimp and Mollusc Karangasem, Bali and Faculty of Fisheries and Marine Science for all the help which made this study possible.

REFERENCES

[1] Jiang, S.G., J.H. Huang, F.L. Zhou, X. Chen, Q.B. Yang, W.G. Wen, Z.M. Ma. 2009. Observations of reproductive development and maturation of male *Penaeus monodon* reared in tidal and earthen ponds. *Aquaculture.* 292. 121-128.

[2] FAO. 2010. The state of world fisheries and aquaculture. Available at: www.fao.org/ docrep/013/i1820e/i1820e01.pdf.

[3] FAO. 2008. The state of world fisheries and aquaculture. Available at: ftp://ftp.fao.org /docrep/fao/009/a0699e/a0699e.pdf.

[4] Sagi, A., E.D. Aflalo. 2005. The androgenic gland and monosex culture in Taiwan: A biotechnological perspective. *Aquacult. Res.* 36. 231-237.

[5] Franco, A.R., J.G. Ferreira, A.M. Nobre. 2006. Development of a growth model for penaeid shrimp. Aquaculture. 259. 268-277.

[6] Gomelsky, B. 2003. Chromosome set manipulation and sex control in common carp: A review. *Aquatechnol. Living Resour.* 16. 408-415.

[7] Gopal, C., G. Gopikrishna, G. Krishna, S.S. Jahageerdar, M. Rye, B.J. Hayes, S. Paulpandi, R.P. Kiran, S.M. Pillai, P. Ravichandran, A.G. Ponniah, D. Kumar. 2010. Weight and time of onset of female-superior sexual dimorphism in pond reared *Penaeus monodon*. *Aquaculture.* 300. 237-239.

[8] FAO. 2006. Cultured aquatic species information programme *Penaeus vannamei* (Boone, 1931). Fishery Statistics. Italy.

[9] Perez-Rostro, C.L., A.M. Ibarra. 2003. Heritabilities and genetic correlations of size traits at harvest in sexually dimorphic Pacific White Shrimp (*Litopenaeus vannamei*) grown in two environments. *Aquacult. Res.* 34. 1079-1085.

[10] Campos-Ramos, R., R. Garza-Torres, D.A. Guerrero-Tortolero, A.M. Maeda-Martinez, H. Obregon-Barboza, 2006. Environmental sex determination, external sex differentiation and structure of the androgenic gland in the Pacific White Shrimp, *Litopenaeus vannamei* (Boone). *Aquacult. Res.* 37. 1583-1593.

[11] Moss, D.R., S.M. Moss. 2006. Effects of gender and size on feed acquisition in the Pacific White Shrimp *Liptopenaeus vannamei. J. World Aquac.Soc.* 37. 161-167.

[12] Hansford, S.W., D.R. Hewitt. 1994. Growth and nutrient digestibility by male and female *Penaeus monodon*: evidence of sexual dimorphism. *Aquaculture.* 125. 147-154.

[13] Padian, T.J., S.G. Sheela. 1995. Hormonal induction of sex reversal in fish. *Aquaculture.* 138. 1-22.

[14] Okumura, T. 2004. Perspective on hormonal manipulation of shrimps reproduction. *Jpn. Agric. Res. Q.* 38. 49-54.

[15] Wilder, M.N., T. Subramoniam, K. Aida. 2002. Yolk protein of Crustacea. In: Raikhel, A.S, T.W. Sappington (Eds). Reproductive Biology of Invertebrates Vol. XIIA Progress in Vitellogenesis. Science Publishers, Enfield, NH, USA. 131-174.

[16] Hafiz, M.B., M. Hidayah, A.Y. Yusdianatu, M.A. Ambak, A.B. Abol-Munafi, M. Ikhwanuddin. 2012. Effect of estrogen Hormone, 17β-Estradiol on feminization, survival rate and growth rate of Tiger Shrimp, *Penaus Monodon* (Fabricius, 1798) Postlarvae. *Borneo Sci.* 30. 70-80.

[17] Hafiz, M.B., J. Safiah, A.B. Abol-Munafi, M. Ikhwanuddin. 2012. Effect of estrogen

ISSN. 2087-2852
E-ISSN. 2338-1655

hormone, 17β-estradiol on feminization, survival and growth rate of Banana Shrimp, *Fenneropenaeus merguiensis* (De Man, 1888) Postlarvae. UMT 11th International Annual Symposium on Sustainability Science and Management. Terengganu, Malaysia. 84-90.

[18] Rosmaidar, D. Aliza, J. Ramadhanita. 2014. Pengaruh lama perendaman dalam hormon metiltestoteron alami terhadap pembentukan kelamin jantan larva Ikan Nila (*Oreochromis niloticus*). *Jurnal Medika Veterinaria.* 8(2). 853-1943.

[19] Aktas, M., M.A. Genc. 2011. The effect of 17β-Estradiol on growth, survival and feminization of Green Tiger Shrimp, *P. semisulcatus* (Decapoda: Penaeidae). *J. Anim. Vet. Adv.* 10(5). 562-565.

[20] Kian, A.Y.S., S. Mustafa, R.A. Rahman. 2004. Use of enriched live prey in promoting growth and maturation of Tiger Shrimp (*Penaeus monodon*). *NAGA, Worldfish Center Q.* 27 (1&2). 55-59.

[21] Bautista-Teruel, M.N., P.S. Eusebio, T.P. Welsh. 2003. Utilization of feed Pea, *Pisum Sativum*, meal as a protein source in practical diets for juvenile Tiger Shrimp, *Penaeus monodon*. *Aquaculture.* 225. 121-131.

[22] Ikhwanuddin, M., A.D. Talpur, O. Zulizah, A.M. Hidayah, A.A. Shamsuddin, A.B. Abol-Munafi, 2012. The masculine effect of the androgen hormone, 17α - methyltesterone for the production of all male postlarvae of tiger shrimp, *Penaeus monodon* (Fabricius, 1798) postlarvae. *Int. J. Current Res.* 4(10). 59-64.

[23] Wang, H.P., Z. Gao, B. Beres, J. Ottobre, G. Wallat, L. Tiu, D. Rapp, P. O'Bryant, H. Yao. 2008. Effects of Estradiol-17β on survival, growth performance, sex reversal and gonadal structure of Bluegill Sunfish, *Lepomis macrochirus*. *Aquaculture.* 285. 216-223.

[24] Ashby, K.R. 1957. The effect of steroid hormones on the brown trout (*Salmo trutta* L.) during the period of gonadal differentiation. *J. Embryol. Exp. Morphol.* 5. 225-249.

[25] Sagi, A., E.D. Aflalo. 2005. The androgenic gland and monosex culture of Freshwater Prawn *Macrobrachium rosenbergii* (De Man): a biotechnological perspective. *Aquac. Res.* 36. 231-237.

[26] Hirano, M., H. Ishibashi, N. Watanabe, N. Matsumura, A. Watanabe. 2004. Effects of 17β-estradiol on survival, growth, sexual development and molting cycles of the marine Crustacean Mysid Shrimp, *Amerycamysis bahia*. *Environ. Sci.* 11. 259-268

[27] Karayucel, I., O.K. Orhan, S. Karayucel. 2006. Effect of different levels of 17α-methyltestosterone on growth and survival of Angelfish (*Pterophyllum scalare* Lieechtenstein, 1923) fry. *J. Anim. Vet. Adv.* 5. 244-248.

[28] Kirankumar, S., V. Anaty, T.J. Pandian. 2003. Hormonal induction of super male golden rosy barb and isolation of Y-chromosome specific markers. *Gen. Comp. Endocrinol.* 134. 62-71.

[29] Kim, D.S., Y.K. Nam, J.Y. Jo. 1997. Effect of 17β-estradiol immersion treatment of sex reversal of Mud Loach *Misgurnus mizolepis* (Gunther). *Aquacult. Res.* 28. 941-946.

[30] Herman, R.L., H.L. Kincaid. 1988. Pathological effects of orally administered estradiol to Rainbow Trout. *Aquaculture.* 72. 165-172.

[31] Sower, S.A., W.W. Dickhoff, J. Mighell, T. Flagg, C. Mahnken. 1984. Effects of estradiol and diethylstilbestrol on sex reversal and mortality in Atlantic Salmon (*Salmo salar*). *Aquaculture.* 43. 75-82.

ISSN. 2087-2852
E-ISSN. 2338-1655

Physical Properties of Turpentine and Gum Rosin *Pinus merkusii* Jungh et de Vriese Tapped Oleoresin by Borehole Method

Agus Sukarno

Faculty of Forestry, Malang Agriculture University, Malang, Indonesia

Abstract

This study was conducted to determine the physical properties of turpentine and gum rosin derived from oleoresin tapped with borehole method. The research material is derived oleoresin from Aceh provenance pine and Jember landrace. The test results of the physical properties of turpentine are as follows; color: clear, specific gravity 0.84-0.85, refraction index 1.46, negative fatty oil, flash point 34-35.5°C, residual evaporation 1.2-1.6%, and optical round + 32.2-32.4^{o}. Result of test of physical properties of gum rosin: color X (main), softening point 76.0-76.5°C, impurity 0.0014-0.0051%, acid value 179.5-188.5, saponification value 188.7-194.3, iodine number 9.6-9.8, ash content 0.001-0.005% and volatile tupentine content 2.1-2.4%.

Keywords: Aceh provenance pine, borehole method, gum rosin, turpentine.

INTRODUCTION

Pinus merkusii is one of the native tree species of Indonesia with its natural distribution in Aceh, Tapanuli and Kerinci. The products of pine oleoresin are gum rosin and turpentine. Gum rosin and turpentine export opportunities are still wide open because the world's largest producer is dominated by three countries, Cina, Brazil and Indonesia. Indonesia's gum rosin and turpentine export markets are India, the United States, France, Cameroon, and the Netherlands which they are only able to meet less than 10% of the market demand [1].

According to Langenheim, the use of turpentine is limited only as a paint thinner, whose economic value is low [2]. Currently, turpentine benefits are becoming more important for the chemical industry, if it is in the form of its derivatives. The mixture between alpha pinene and beta pinene contained within the turpentine is required as a glue, transparent tape and similar products. Insecticides and bactericides require alpha pinene and champena. The current widespread use is as a raw material for synthetic fragrances such as orange flavor, menthol, nutmeg flavor, deodorant and cooling effect of cosmetics (lipstick). Gum rosin is traditionally required by the *batik*, soap and paper industries, today more widely used such as plaster softeners and dental dressing mixtures, eyeshadow blends and eyelash reinforcement, adhesives, colors in the printing industry (ink) and paint [4].

Physical properties of turpentine-gum rosin related to the quality of these products and affect the sale value. Physical properties are also related to technical processing and raw materials. The physical properties of a product must meet the quality requirements of the established quality standard. Until now, the processing of the oleoresin becomes turpentine and gum rosin is produced by the gum rosin and turpentine processing factory, whose raw material comes from tapping the quare method, and the resulting oleoresin is mixed with various impurities. In this research, the oleoresin was obtained by tapping the borehole method on Aceh provenance pine and Jember landrace. The purpose of this research is to know the difference of physical properties of turpentine and gum rosin Aceh provenance pine and Jember landrace.

MATERIALS AND METHODS

Location and Time of Research

Oleoresin material obtained from the tapping of Aceh provenance pine in the Seedling Seeds Orchard, Sumberjati Forest Management Resort (*Resort Pemangkuan Hutan* – RPH), Sempolan Sub Unit of Forest Management (*Bagian Kesatuan Pemangkuan Hutan* – BKPH), Jember Unit of Forest Management (*Kesatuan Pemangkuan Hutan* – KPH). The Jember landrace oleoresin is obtained from pine tapping of the plants in Plot 21e, RPH Garahan, BKPH Sempolan KPH Jember.

* Correspondence address:
Agus Sukarno
Email : sukarnoagus59@gmail.com
Address : Faculty of Forestry, Malang Agriculture University, Malang.

ISSN. 2087-2852
E-ISSN. 2338-1655

Tools and Objects

The tool used consists of mini distillers capacity of 1.5 kg. Objects of the study are Aceh provenance pine and Jember landrace.

Tapping the Oleoresin

Oleoresin tapping with borehole method were done by following step. The oleoresin that directly comes out of the tree in the container were put into the plastic bag and accommodated in a plastic container. Oleoresin required as much as 6 kg, for four times cooking (replication).

Cooking of Oleoresin

Cooking oleoresin with temperature 160-180^{o}C for 2 hours. Turpentine that comes out in the glass were measured and gum rosin accommodated in a place made of zinc size 17 x 14 x 9 cm.

Test the Physical Properties of Turpentine

The physical properties of turpentine were tested according to SNI 01-5009.12-2001 standard in Non-Timber Forest Product Laboratory of Perum Perhutani Divre I Semarang, covering test specifications: Specific weight at 25^{o}C, Refraction Index at 25^{o}C, Oil and Fat, Evaporation Time, Color visually and Optical Rounds.

Test the Physical Properties of Gum Rosin

Physical properties of gum rosin are tested according to SNI 01-5009.12-2001 consisting of color, softening point, impurity, acid value, saponification value, iodine value, ash content of Heraeus Furnace method and the remaining volumes of oil content (volatile oil content). Physical properties test is conducted in Laboratory Non-Timber Forest Product Perum Perhutani Divre I Semarang.

Data Analysis

The results of the laboratory test of the physical properties of gum rosin-turpentine are then analyzed in a descriptive manner.

RESULT AND DISCUSSION

Physical Properties of Turpentine

The physical properties of turpentine are influenced by the production process and raw materials (oleoresin). The production process with raw materials mixed with other ingredients such as leaves, skin flakes, soil, water and other mixtures, requires a gradual cleaning process until the production of Oil Pine Resin (OPR) is ready for cooking. This is done at a oleoresin processing plant. According to Sukarno [8], clean raw materials, tapping oleoresin with borehole method, oleoresin cooking can be done without going through the process of cleaning the oleoresin material. The production process in the factory, both the tool and the operating procedure, has followed the established standards and has obtained ISO-9001-2008 certification.

In this research, the processing of oleoresin is still using the old way of direct heating, the difference is not using a fire heater but with an electric heater. The reason for using direct heating means is to simplify the tool, but without reducing the function as a destilator. The raw materials are considered good because of the oleoresin result of tapping with the borehole [9].

The physical properties of turpentine have been tested with SNI 01-5009.12-2001 standard. Table 1 shows that of the seven specifications tested, the physical properties of the Aceh provenance pine turpentine and the Jember landrace have met the standards required by SNI 01-5009.12-2001. The resulting density ranges from 0.85. Specific gravity is the weight ratio of an object with the same weight of water at the same temperature, so that the volume of 1 liter turpentine weighs equal to 0.85 kg. Refractive index at 25°C. We did not found fatty oil content (negative results).

Table 1. The Results of physical properties on Turpentine of Aceh and Jember Pine

Specifications test	Standard	Aceh			Jember
	SNI 01-5009.12-2001	Takengon	Blangkejeren	Jantho	
Specific gravity on 25°C	0.848 – 0.865	0.857	0.857	0.857	0.858
Refraction index on 25°C	1.464 – 1.478	1.465	1.465	1.465	1.465
Fatty oil	Negative	Negative	Negative	Negative	Negative
Flash point	33°C – 38°C	34.0°C	35.5°C	35.2°C	35.0°C
Residual evaporation	Grade A: ≤ 2% Grade B : > 2%	1.50%	1.18%	1.44%	1.58%
Color	Clear	Clear	Clear	Clear	Clear
Optical round	Grade A : +≥ 3° Grade B : +<3°	+ 32.38°	+ 32.37°	+ 32.32°	+ 32.33°

Notes: Analysis in Laboratory of Non Timber Forest Products, Industrial Perum Perhutani Divre I Semarang in 2011

ISSN. 2087-2852
E-ISSN. 2338-1655

Flashpoint on the turbulent in Takengon shows the numbers below the turbulent Blangkejeren, Jantho and Jember landrace, but still above the required minimum. The remainder of evaporation and optical rotation are included in the quality criteria A (excellent quality). Clear turpentine color, meaning turpentine is not oxidized or not mixed with water, optical rotation including A (prime) quality. Although the production process using a simple tool, but the results are in accordance with the required standard.

Physical Properties of Gum Rosin

Color

The quality of gum rosin first used as an indicator is color, because this physical nature is the visible first impression. If the color shown the criteria that have been set, it will affect the price and attractiveness for consumers. The color of gum rosin in SNI-01-5009.4.2001 is classified as: Main (color X); First (color WW); Second (color WG) and third (color N). The X = Extra (Rec) gum rosin clear color of yellowish; WW = water white, yellow; WG = the glass window is brownish yellow and N = Nancy is brownish, based on the color standard through the Lovibond tool. Color is determined by the raw materials and the production process. The gum rosin and turpentine processing factory (PGT) obtained raw materials, derived from tapping oleoresin through quare method which oleoresin mixed with various impurities.

In this study, the raw material comes from tapping with borehole method, so that the impurities mixed in the oleoresin can be minimized. Oleoresin directly cooked without going through the process of cleaning dirt and dilution sap. Given the very simple tool (mini-scale), it still raises quality color of two opposite choices, if the color is good, then the softening point is less than the standard. The results of physical properties of gum rosin presented in Table 2.

Table 2. The Results of physical properties on Gum Rosin of Aceh and Jember Pine

Specifications test	Standard SNI 01-5009.12-2001	Aceh Provenance			Jember
		Takengon	Blangkejeren	Jantho	
Color	X/WW/WG/N	X	X	X	X
Softening Point	X = ≥ 78°C WW = ≥ 78°C WG = ≥ 76°C N = ≥ 74°C	76.5°C	76.5°C	76.0°C	76.0°C
Impurity	X= ≤ 0.02 % W = ≤ 0.05% WG = ≤ 0.07% N = ≤ 0.10%	0.0014%	0.0036%	0.0040%	0.0051%
Acid Value	160 – 190	179.46	183.62	188.50	182.06
Saponification value	170 – 220	188.72	190.49	194.27	191.87
Iodine Value	5 – 25	9.68	9.78	9.61	9.70
Ash Content	X = ≤ 0.01 % WW= ≤ 0.04 % WG= ≤ 0.05 % N = ≤ 0.08 %	0.0013%	0.0046%	0.0030%	0.0043%
The volatile turpentine contents	X = ≤ 2 % WW = ≤ 2 % WG = ≤ 2.5 % N= ≤ 3 %	2.365%	2.168%	2.122%	2.212%

Notes: Analysis in Laboratory of Non Timber Forest Products, Industrial Perum Perhutani Divre I Semarang in 2011.
X= Rex, WW= Water White, WG= Windows Glass, N= Nancy

Table 2 showed that the color of gum rosin produced shows the main color (U) that is extra color (X), this is suspected because the raw material of the oleoresin is derived from tapping by borehole method, so it is a clean raw material. This is as delivered by Wiyono that the raw material is very decisive to the color of gum rosin [5]. The quality of gum rosin produced is determined by the quality of the processed oleoresin [6]. Fresh oleoresin will produce better quality gum rosin compared with that derived from oleoresin that has been stored for long, let alone stored in open space, causing the oleoresin to be oxidized [5]. Pine oleoresin is a complex compound that is acidic and very sensitive to time and damage due. The cooking process also greatly determines the color of gum rosin, especially the temperature setting and the length

ISSN. 2087-2852
E-ISSN. 2338-1655

of the cooking time. In practice, people are often more interested in paying attention to color first, although not always, color reflects the quality of others [7].

Soft Point

The soft point is closely related to the remaining turpentine in gum rosin, the less the remaining turpentine, the higher the soft point and vice versa. Gum rosin with turpentine content is still remaining much, then the gum rosin will be less fragile (crumb), according to SNI standard, the required softening point is ≥ 78°C. The result of physical properties test in laboratory (Table 2) shows soft point of gum rosin from Aceh provenance pine (Takengon and Blangkejeren) 76.5°C, while Jantho and Jember landrace 76°C, so based on SNI standard soft point is still less 1.5 - 2°C . Physically, the soft spot between 76-76.5°C gum rosin looks no different, hard (not flabby), brittle (crumb), so it still meets the required physical quality standards. This is in accordance with the opinion of Khadafi et al., that good quality gum rosin according to the consumer is not easy to soften at room temperature, brittle (fragile) and does not change physically from time to time (during storage) [7].

Average gum rosin droppings produced by PGT. Rejowinagun (direct interview with head of the factory, 2010) is 0.0229% has met the standard set by the SNI that is the lowest ≤ 0.02%. This is because the process of cleaning the oleoresin from the dirt has been done through several stages of filtering and washing oleoresin. The results when compared with the factory, it shows a much lower result that is Takengon 0.0014%, Blangkejeren 0.0036%, Jantho 0.0040% and Jember landrace 0.0051%. This suggests that tapping the oleoresin by borehole will produce gum rosin with very low levels of impurities.

CONCLUSION

Based on the test results of physical properties of turpentine and gum rosin, both Aceh provenance pine and Jember landrace has similar physical properties. The physical properties of the turpentine of the seven specifications tested have shown the range of numbers required under SNI 01-5009.12-2001. Meanwhile, the physical properties of gum rosin of the eight specifications tested have also shown the range of numbers required under SNI 01-5009.12-2001. Therefore, the borehole method produce a clean oleoresin and has less damage towards the pine trees to meet the standard.

ACKNOWLEDGEMENT

The author would like to thank Prof. Muh. Na'iem, Dr. Sri Nugroho Marsoem and Dr. Eko Bhakti Hardiyanto, who has provided the opportunity and guidance to the to complete this research. I also thank all parties who have helped this research.

REFERENCES

[1] State Forest Enterprise. 2011. Industri Gondorukem dan Terpentin Perum Perhutani. Laboratory of Industry and Marekting Bureau. Perum Perhutani Unit I Jawa Tengah.

[2] Langenheim, J.H. 2003. Plant Resin: chemistry, evolution, ecology and ethnobotany. Timber Press. Cambridge.

[3] Lenny, S. 2006. Senyawa Terpenoida dan Steroid. Sciantific Paper. Faculty of Mathematics and Naturan Sciences. University of North Sumatera.

[4] [Sjostrom, E. 1998. Kimia Kayu: dasar-dasar dan penggunaannya, 2nd Ed. Hardjono Sastrohamidjojo, H. (Transl). Gadjah Mada University Press. Yogyakarta.

[5] Wiyono, B. 2007. Pengaruh konsentrasi bahan kimia maleat anhidrida terhadap gondorukem maleat dari getah *Pinus merkusii*. *Jurnal Penelitian Hasil Hutan.* 25. (1). 28-40.

[6] Nasnedi, B.D., A.F. Mas'ud (Eds). 2001. Kajian teknis ekonomis pengolahan gondorukem dalam rangka peningkatan nilai tambah: studi kasus di PGT Peninggaran dan PGT Cimanggu. Center of Forestry Research and Development. Department of Foretsry.

[7] Khadafi, M., I. Rostika, T. Hidayat. 2014. Pengolahan gondorukem menjadi bahan pendarihan sebagai aditif pada pembuatan kertas. *Jurnal Selulosa.* 4(1). 17-24.

[8] Sukarno, A., E.B. Hardiyanto, S.N. Marsoem, M. Na'iem. 2012. Pengaruh perbedaan kelas umur terhadap produktivitas getah *Pinus merkusii* Jungh et de Vriese ras lahan Jawa melalui penyadapan getah metode bor. *Jurnal Pembangunan dan Alam Lestari.* 3(1). 28-31.

[9] Sukarno A., E.B. Hardiyanto, S.N. Marsoem, M. Na'iem. 2015. Oleoresin production, turpentine yield and components of *Pinus merkusii* from various Indonesian Provenances. *J. Trop. Forest Sci.* 27(1). 136-141.

ISSN. 2087-2852
E-ISSN. 2338-1655

The Effects of Rosella Extract (*Hibiscus sabdariffa*) against the *n-carboxymethyl-lysine*, NF-κβ, TNF-α in the Rats Heating Food Diets

Batmomolin Pia Bataif[1*], Setyawati Soeharto K[2], Edi Widjajanto[3], Ardhiyanti Puspita Ratna[1], Silvy Amalia[1]

[1]Biomedical Sciences Program, Faculty of Medicine, University of Brawijaya, Malang, Indonesia
[2]Laboratorium of Pharmacology, Faculty of Medicine, University of Brawijaya, Malang, Indonesia
[3]Laboratorium of Pathology Clinic, Faculty of Medicine, University of Brawijaya, Malang, Indonesia

Abstract

The food processing by heating can increase the formation of AGEs (Advanced Glycation End Products). AGEs are compounds that formed from a non-enzymatic continuous glycation reaction between proteins and sugar residues. The CML (*N-carboxymethyl-lysine*) is used as a marker for AGEs cause most commonly found in vivo. The bond of AGEs and RAGE (reseptor for AGEs) induce various signaling pathways that trigger inflammation and increase oxidative stress. The AGE and RAGE interaction activate the transcription factor of NF-κβ. NF-κβ activate gene transcription to release proinflammatory cytokines such as TNF-α. Anthocyanins are compounds that can prevent the formation of AGEs and muffle the adverse effects of AGEs. Rosella contains anthocyanin such as : delphinidin-3-O-glucoside, delphinidin-3-O-sambubioside, and cyanidin-3-O-sambubioside. This study is to determine whether the daily intake of Rosella extract can reduce the levels of *n-carboxymethyl-lysine* in serum, expression of NF-κβ and TNF α in the rats fed with heated food. This study applied experimental *post test control* using *Rattus norvegicus* Wistar strain. The samples were divided into 5 groups: KN (negative control/fed without heating), KP (positive control/fed heated food but not treated by Rosella extract), R_1 (fed heated food and treated by 200 mg.kg^{-1}BW Rosella extract), R_2 (fed heated food and treated by 300 mg.kg^{-1}BW Rosella extract), and R_3 (fed heated food and treated by 400 mg.kg^{-1}BW Rosella extract). The *n-carboxymethyl-lysine* levels were measured by using the ELISA, the expression of NF-κβ is analyzed by using immunofluorescence, and expression of TNF - α is observed by immunohistochemistry. There was significantly decreased the levels of *n-carboxymethyl-lysine* in all groups which were treated by Rosella extracts (R_1,R_2,R_3); p= 0.000, α = 0.05 (p< α). Decreased activation of NF-κβ in all groups which were treated by Rosella extract is significant (p = 0.000), and decreased expression of TNF α in all groups which were treated by Rosella extract is also significant (p = 0.000). Rosella extract can reduce the levels of *n-carboxymethyl-lysine*, expression of NF-κβ, and TNF α.

Keywords: AGEs, anthocyanin, Rosella flower extract, *n-carboxymethyl-lysine*, NF-κβ, TNF α.

INTRODUCTION

There are two sources of AGEs (Advanced Glycation End Products) namely exogenous derived from consumed food and beverages and endogenous formed in the body as part of normal metabolism. Raw foods derived from plants and animals containing AGEs, however within the limits that can be tolerated by the body considering the body that has homeostatic system.

Foods processing that contain sugar, lipid or fat, and protein through a heating process such as fried, grilled, and roasted can increase AGEs. The processing using dry heat methods can increase the formation of AGEs up to 100-fold, compared to the amount of AGEs found in raw foods.

The amount of AGEs of food consumption is greater than the total amount of AGEs normally contained in plasma and tissue [1]. The average total AGEs dietary exposure to healthy people which did not cause adverse effects was approximately 16,000 AGEs kU.day^{-1} [2]. Consumption of processed foods with warming will lead to increased exposure to AGEs, thus exceeding 20,000 kU.day^{-1} [3].

The accumulation of AGEs in the body, will cause oxidative stress and chronic inflammation, which in turn will further enhance the endogenous formation of AGEs. Accumulation of AGEs will also increase the susceptibility to damage tissue [4].

Giving AGEs dietary may increase its circulation thus exceeding the normal limit that can be tolerated. The increase of AGEs in circulation will activate RAGE (Receptor of AGEs). AGE and RAGE interaction causes the activation

* Correspondence address:
Batmomolin Pia Bataif
Email : piabatmomolin@yahoo.co.id
Address : Biomedical Sciences Program, Faculty of Medicine, University of Brawijaya, Veteran Malang, Malang 65145.

ISSN. 2087-2852
E-ISSN. 2338-1655

of MAPKs and PI3-K, which will then activate the transcription factor of NF-κβ. Once activated, NF-κβ moves from the cytoplasm to the nucleus and activate gene transcription to release proin-flammatory cytokines, growth factors and adhesive mole-cules, such as TNF-α, IL-6 and VCAM1 [5,6].

CML (*N-carboxymethyl-lysine*) is a type of AGEs which is mostly used as a marker for the formation of AGEs. CML is a type of AGEs which is most commonly found in vivo, best known for its characterizations [5] and most representable structure of AGEs both quantitative and patho-physiologic [7].

AGEs's bad consequences can be avoided by prevent the formation, build up on the network, and overcome the inflammatory reactions and oxidative stress of AGEs. The use of ingredients that work as AGE inhibitors and breakers can prevent the formation and accumulation of AGEs in the body tissues [8,9].

Anthocyanin is a type of flavonoid poly-phenols in the group known as antioxidants. The mechanism of anthocyanin which can be indi-cated as inhibitor formation of AGEs is through the inhibition of auto-oxidation monosacaride [10] which prevent lipid peroxidation and inhibition of polyol pathway [11]. Anthocyanins also inhibit the binding of AGEs to its receptor (RAGE) [12].

Rosella contains phenolics, organic acids, sterols, terpenoids, polysacharides and some minerals. Its fenolic content consists of antho-cyanins as delphinidin-3-O-glucoside, delphinidin-3-O- sambubioside, and cyanidin-3-O-sambubio-side [13]. This study was conducted to determine whether daily intake of Rosella extract could reduce the levels of CML in serum, activation of NF-κβ, and expression of TNF α in Wistar rats' aorta fed by heating food diets.

MATERIALS AND METHODS

Object Study

This study was an experimental research laboratories used *Rattus norvegicus* Wistar strain and designed *post test control group*. The study used 25 male rats**,** ages 3-4 months old with 100-150 gram initial body. The rats is randomly devide into 5 groups, KN (negative control), KP (positive control), R_1 (treated by 200 mg.kg^{-1}BW Rosella extract) R_2 (treated by of 300 mg.kg^{-1}BW Rosella extract), and R_3 (treated by 400 mg.kg^{-1} BW Rosella extract). KN fed without heating, while KP, R_1, R_2, and R_3 fed by heating food for 8 weeks. The Rosella extract is given once a day. Rosella that used in this study was purchased from Materia Medika Batu. Rosella extract is the result of Rosella flower extraction using 70% ethanol solvent.

Data Collection

The levels of CML was examined after 8 weeks. The feeding for all groups was continued until 12 weeks. At the end of the treatment, the mice were fasted, anaesthetized and then dissected. The serum was taken to measure CML level by using ELISA method (used ELISA kit for CML , No. CATALOG E1374Ra). The aorta was taken to analyze the activation of NF-κβ by using immunoflouroescence method (using primary antibody NF-κβ P65 ThermoFisher no catalog MA5-15160) and to observe the expression of TNF-α by using immunohisto-chemistry method (dyes by DAB and Mayer's Hematoxilen).

Data Analysis

Data were statistically analyzed. Test for normality using the Shapiro-Wilk test, homogeneity test using Levene's Test. Data comparison using One-way ANOVA, followed by LSD (Least Significant Difference) 5%. Compa-risons between groups using multiple compari-son test. The test results said to be significant if the p value <0.05.

RESULT AND DISCUSSION

The Effect of Rosella Extract against CML Levels

The results of ANOVA was obtained p-value for 0000 which was smaller than α=0.05 (p<0.05). It can be concluded that there was significant influence of Rosella extract on the levels of CML. The LSD 5% test results showed that the significant decrease of CML's levels occurred in all groups which were treated by Rosella extract. The lowest average levels of CML was obtained in R_1. The highest average level of CML was obtained in KP and R_2, average value of CML levels were not significantly different with KN. On the other words, the provision of rosella extract at a dose of 300 mg.kg^{-1}BW can lower the levels of CML to the rats given feed without heating (Fig. 1).

The results showed that there was significant decline of the CML levels in all groups of mice which were treated by Rosella extract. This could occur because the Rosella extract contained anthocyanin. These results were consistent with the previous studies which stated that the antioxidant is a type of flavonoid that can inhibit the formation of AGEs [12]. This result also showed that anthocyanin in the Rosella extract

ISSN. 2087-2852
E-ISSN. 2338-1655

could break the CML. This fits with previous research which states that the phenolic antioxidant can function as a *breaker* AGEs [13].

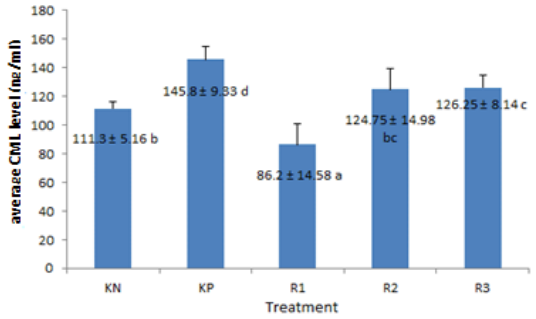

Figure 1. The average levels of CML (ELISA method) using ANOVA test.

Description:

KN = negative control/fed without heated

KP = positive control/fed heated food but not treated by Rosella extract

R_1 = fed heated food, treated by 200 mg.Kg^{-1}BW Rosella extract

R_2 = fed heated food, treated by 300 mg.Kg^{-1}BW Rosella extract

R_3 = fed heated food, treated by 400 mg.Kg^{-1}BW Rosella extract.

p-value = 0.000

This study found that in the higher dose of Rosella extract, its ability become low for reducing the levels of CML. This might be because this study were still used a crude of Rosella extract rather than the type of anthocyanins of Rosella that have been isolated. The crude extract of rosella that had been used had many other compounds besides the anthocyanin, i.e. fatty acids (saturated and unsaturated), protein, carbohydrates, minerals, organic acids (citric, hydroxycitric, Hibiscus, malik, tartaric, oxalate, and ascorbate), anthocyanins, polysaccharides and flavonoids [10,14].

With the wide range of content in the Rosella ekstract, an increase in dosage also increases the activity of another material, thus the effect of anthocyanins reduced. Previous research suggested that there are many precursors to form the CML, among others, *Polysaturated fatty acid* (PUFA), and *ascorbic acid*. CML formation pathways other than through the Maillard reaction also through the reaction between PUFA or ascorbic acid with lysine residues derived from proteins. Researchers suspect that when the dose of Rosella is increased likely not due to the inability of anthocyanins to break the CML that causes its levels increased, but rather because there have been more CML formation in the body through a reaction between lysine and PUFA, as well as ascorbic acid. So then, although anthocyanins have the ability to break down the CML but since its number is formed mounting so that the CML levels tend to remain high.

The Effect of Rosella Extract against the Activation of NF-κβ

Based on the results of ANOVA, p-value was obtained for 0000, smaller than α= 0.05 (p<0.05). The LSD 5% test results indicated that the lowest activation of NF-κβ was in KN and the highest in KP. There was significant decrease of the activation of NF-κβ in all groups which were treated by Rosella extract compared with KP. The lowest average of activation of NF-κβ was obtained in rats which were treated by 200 mg.kg^{-1} BW Rosella extract (R_1) (Fig. 2).

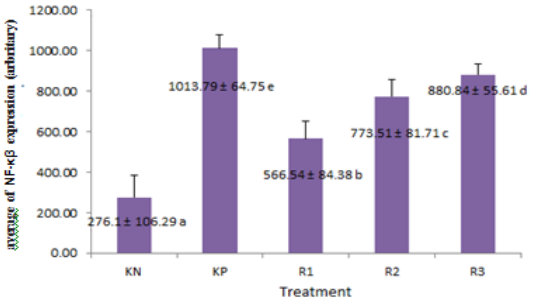

Figure 2. The average of NF-κβ expresion (immuno-flouroescence method) using ANOVA test.

Description:

KN = negative control/fed without heated

KP = positive control/fed heated food but not treated by Rosella extract

R_1 = fed heated food, treated by 200 mg.Kg^{-1}BW Rosella extract

R_2 = fed heated food, treated by 300 mg.Kg^{-1}BW Rosella extract

R_3 = fed heated food, treated by 400 mg.Kg^{-1}BW Rosella extract.

p-value = 0.000

These results indicated a decline in the activation of NF-κβ significantly in all groups which were treated by Rosella extract. This happened because the extract of Rosella flower containing anthocyanin.

This decreased activation of NF-κβ agrees with the theory that the intake of anthocyanins may decrease the activation of the transcription factor NF-κβ and the expression of several cytokines and proinflammatory mediators [15]. These results are also consistent with several other studies which stated that the Rosella flower extract has an effect as an antioxidant, and the compound suspected to have effect as an antioxidant and inhibits the activation of NF-κβ is its fenolic content which is flavonoid-

compound anthocyanin [16]. The mechanism of inhibition on the activation of NF-κβ is to prevent loss of p50 and p65 binding so there is no translocation of p50/p65 into the nucleus. Moreover, it can be worked as an inhibitor of NADPH oxidase which produces superoxide anion radicals. Anthocyanins can inhibit the activation of NF-κβ by inhibiting the degradation of Iκβ, and also inhibition on the activation of Iκβ kinase enzyme that prevent phosphorylation of NF-κβ (p50 and p65) dimer result which do not separate each other, and subsequently p50 and p65 translocation into the nucleus will not occur.

The results of this study are also consistent with other studies mentioned that the anthocyanins in the dried petals of Rosella extract (*H. sabdariffa Linn*) were able to inhibit oxidative stress-induced activation of NF-κβ [17]. Anthocyanins and flavonoids have been proven to inhibit LDL oxidation and the activation of NF-κβ, and decrease inflammation. Mechanism of anthocyanin in inhibiting Ox-LDL is to fight free radicals, eliminate oxidant product, inhibite the oxidation of lipids, lipoproteins, liposomes and DNA, and suppress production of radicals and their precursors both in vivo and in vitro. In addition, anthocyanins can increase the production of endogenous antioxidants such as superoxide dismutase, Gluthation Peroxidase and Catalase. The ability of anthocyanins to reduce the activation of NF-κβ can be solved through AGEs/CML. The breakdown of AGEs reduces the amount of AGEs so then it was inadequate to carry out the binding to RAGE. Moreover, it can be done through binding of AGEs/CML with its receptor which is RAGE.

From the various doses of Rosella which are given, it turns out that the most effective dose that lowers the activation of NF-κβ is a dose of 200 mg.kg^{-1} BW Rosella extract. This study shows that with the addition dose of Rosella extract, its extract ability to decrease activation of NF-κβ decreases. This may be due to the formation of AGEs/CML increases with the increasing doses of Rosella extract so that the amount of AGEs/CML which binds to RAGE increases. The increasing amount of AGEs which binding to RAGE will increase the number of activation of NF-κβ.

The Effect of Rosella Extract against TNF-α Expression

Based on the results of ANOVA, p-value was obtained for 0000, smaller than α= 0.05 (p<0.05). The LSD 5% test results showed that KP had the highest average expression of TNF-α. The decreased expression of TNF-α were significantly demonstrated in all group treated by Rosella extract.

In comparison of KN with the R_1 and R_2, p-value was obtained greater than 0.05 (p>0.05). This means there was no significant difference in the average expression of TNF-α between KN and R_1 and R_2. In comparison of KP with R_1, the p-value of R_2 and R_3 was obtained less than 0.05. This proved that the group that treated by Rosella extract at the dose of 200, 300, and 400 mg.kg^{-1}BW can lower the expression of TNF-α significantly. KP had the highest average value of the expression of TNF-α, while the average expression of TNF-α decreased in all groups which were treated by Rosella extract. The lowest average expression of TNF-α was obtained in rats which were treated by Rosella extract 200 mg.kg^{-1}BW (R_1) (Fig. 3).

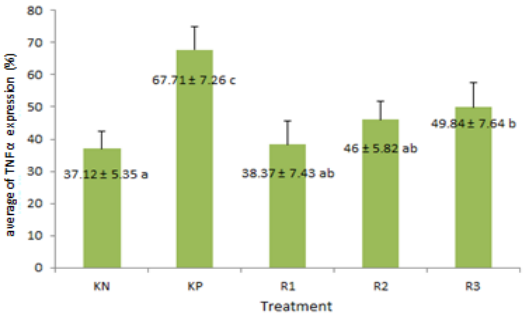

Figure 3. The average of TNF-α expression (immunohistochemistry method) using ANOVA test.

Description:

KN = negative control/fed without heated

KP = positive control/fed heated food but not treated by Rosella extract

R_1 = fed heated food, treated by 200 mg.Kg^{-1}BW Rosella extract

R_2 = fed heated food, treated by 300 mg.Kg^{-1}BW Rosella extract

R_3 = fed heated food, treated by 400 mg.Kg^{-1}BW Rosella extract.

p-value = 0.000

The results showed that the expression of TNF-α in all groups of mice which were treated by Rosella extract decreased. The type of anthocyanins such as cyanidin and delphinidin may inhibit the expression of inflammatory mediators. Anthocyanins included in a group of polyphenolic compounds, especially the type of flavonoid compounds. Some studies suggest that flavonoids have a tendency to scavenge free radicals, so it does not form excessive ROS. ROS can stimulate phosphorylation of κβ Inhibitor (Iκβ). Iκβ serves to bind NF-κβ, so then it remains inactive in the cytoplasm. If Iκβ is

ISSN. 2087-2852
E-ISSN. 2338-1655

phosphorylated, the bond of NF-κβ and Iκβ aparts, so that NF-κβ active and migrate to the nucleus. In the nucleus, NF-κβ will activate transcription by binding to DNA sequences on a target gene, thus triggering the release of inflammatory cytokines such as TNFα. Therefore, when ROS was inhibited, then the activation of NF-κβ can be inhibited. Inhibition of activation of NF-κβ will also inhibit the secretion of inflammatory cytokines such as TNFα.

TNFα is an important mediator in the inflammatory process, it plays a role in increasing the inflammatory response of endothelial cells [18]. This study proved that rosella flower extract may decrease the activation of NF-κβ, so that the expression of TNFα on endothelial decreased. The highest reduction is in mice fed a rosella flower extract 200 $m.kg^{-1}$. This study showed that with increasing the doses of extract of Rosella, there was a decline in the ability to reduce the expression of TNFα. This might be due to along with increasing dose, there was an increase on the formation of CML. When the number of CML which binds to RAGE increased, the activation of NF-κβ increased. The incerased activation of NF-κβ resulted in increasing the secretion of TNFα.

Relationship Levels of CML, Activation of NF-κβ, and TNF-α by Using Correlation Analysis

The results of testing the correlation between the levels of CML and the activation of NF-κβ was obtained correlation coefficient of 0598 with a p-value of 0.002. p<0.05 indicated that there was a significant relationship between the levels of CML and the activation of NF-κβ. The correlation coefficient was worth 0598 showed the quite strong level of the relationship. The correlation coefficient was positive indicated that there was a positive relationship between levels of CML and the activation of NF-κβ. The increasement levels of CML would also be followed by the increased activation of NF-κβ and vice versa.

The results of testing the correlation between the expression levels of CML and TNF-α was obtained correlation coefficient of 0687 with a p-value of 0.000. p<0.05 indicated that there was a significant relationship between levels of CML and TNF-α expression. The correlation coefficient was worth 0687 showed the strong level of relationship. The correlation coefficient was positive indicated that there was a positive relationship between levels of CML and TNF-α. The increasement levels of CML would also be followed by the increase levels of TNF-α and vice versa.

The results of testing the correlation between the activation of NF-κβ and the expression of TNF-α was obtained correlation coefficient of 0753 with a p-value of 0.000. p<0.05 indicated that there was a significant correlation between the activation of NF-κβ and the expression of TNF-α. The correlation coefficient was worth 0753 showed the strong level of relationship. The correlation coefficient was positive indicated that there was a positive relationship between the activation of NF-κβ and the expression of TNF-α. The increasement activation of NFkB, would also be followed by the increased expression of TNF-α and vice versa.

CONCLUSION

Rosella ethanol extract can reduce the levels of *N-Carboxymethyl-Lysine* in serum, activation of NF-κβ and expresion of TNF α in aorta Wistar rats fed heated significantly. There are close relationship on the decreased levels of CML, ekspression of NF-κβ, and expression of TNF α.

REFERENCES

[1] Henle, T. 2007. Dietary advanced glycation end products - a risk to human health? A call for an interdisciplinary debate. *Mol. Nutr. Food Res.* 51(9). 1075-1078.

[2] Uribarri, J., W. Cai, O. Sandu, M. Peppa, T. Goldberg, H. Vlassara. 2005. Diet derived advanced glycation end products are major contributors to the body's AGE pool and induce inflammation in healthy subjects. *Ann. N. Y. Acad. Sci.* 1043. 461-466.

[3] Uribarri, J., W. Cai, M. Peppa, Goodman S, Ferrucci L, Striker G, Vlassara H. 2007. Circulating glycotoxins and dietary advanced glycation endproducts: two links to inflammatory response, oxidative stress, and aging. *J. Gerontol. A Biol. Sci. Med. Sci.* 62(4). 427-433.

[4] Luevano-Contreras, C., K. Chapman-Novakofski. 2010. Dietary advanced glycation end products and aging. *Nutrients.* 2. 1247-1265.

[5] Goldberg, T., W. Cai, M. Peppa, V. Dardaine, B.S. Baliga, J. Uribarri, H. Vlassara. 2004. Advanced glycoxidation end products in commonly consumed foods. *J. Am. Diet. Assoc.* 104. 1287-1291.

[6] Ramasamy, R., S.J. Vannucci, S.S. Yan, K. Herold, S.F. Yan, A.M. Schmidt. 2005. Advanced glycation end products and RAGE: a common thread in aging, diabetes, neurodegeneration, and in fl ammation. *Glycobiology.* 15. 16R-28R.

ISSN. 2087-2852
E-ISSN. 2338-1655

[7] Ames, J.M. 2008. Determination of Nε-(carboxymethyl) lysine in foods and related systems. *Ann. N. Y. Acad. Sci.* 1126. 20-24.
[8] Bengmark, S. 2007. Advanced glycation end products and lipoxidation - amplifiers of inflammation: the role of food. *J. Parenter. Enteral. Nutr.* 31. 430-440.
[9] Semba, R.D., E.J. Nicklett, L. Ferrucci. 2010. Does accumulation of advanced glycation end products contribute to the aging phenotype. *J. Gerontol. A Biol. Sci. Med. Sci.* 65. 963-975.
[10] Eggensperger, H., M. Wilker. 1996. *Hibiscus*-Extrakt-Ein hautverträglicher wirkstoffkomplex aus AHA's und polysaccharinde Teil 1. *Parfümerie und Kosmetik.* 77. 540-543.
[11] Yawadio, R., S. Tanimori, N. Morita. 2007. Identification of phenolic compounds isolated from pigmented rices and their aldose reductase inhibitory activities. *Food Chem.* 101. 1616-1625.
[12] Vauzour, D., A. Rodriguez-Mateos, G. Corona, M.J. Oruna-Concha, J.P. Spencer. 2010. Polyphenols and human health: prevention of disease and mechanisms of action. *Nutrients.* 2. 1106-1131.
[13] Ali, B.H., N. Al Wabel, G. Blunden. 2005. Phytochemicals, pharmacological and toxicological aspects of *Hibiscus sabdariffa* L: a review. *Phytother. Res.* 19. 369-375.
[14] Matsuda, H., T. Wang, H. Managi, M. Yoshikawa. 2003. Structural requirements of flavonoids for inhibition of protein glycation and radical scavenging activities. *Bioorg. Med. Chem.* 11. 5317-5323.
[15] Nzikou, J.M., Bouanga-Kalou, G., Matos, L., Ganongo-Po, F. B., Mboungou-Mboussi, P. S., Moutoula, F. E., et al. 2011. Characteristics and nutritional evaluation of seed oil from Roselle (*Hibiscus sabdariffa* L.) in Congo-Brazzaville. *Curr. Res. J. Biol. Sci.* 3. 141-146.
[16] Karlsen, A., L. Retterstøl, P. Laake, I. Paur, S.K. Bøhn, L. Sandvik, R. Blomhoff. 2007. Anthocyanins inhibit nuclear factor-KB activation in monocytes and reduce plasma concentration of pro-inflammatory mediators in healthy adults. *J. Nutr.* 137. 1951-1954.
[17] Ranzio, B. 2002. Anti-inflammatory activities of polyphenol-review: polyphenol as anti-inflammatory agents. *J. Naturopathic Med.* 9. 44-50.
[18] Ali, B.H., H.M. Mousa, El Mougys. 2003. The effect of water extract and anthocyanins of *Hibiscus sabdariffa* linn on paracetamol-induced hepatotoxicity in rats. *Phytother. Res.* 17. 56-59.

ISSN. 2087-2852
E-ISSN. 2338-1655

Effect of Banana Homogenate on Shoot Regeneration of Ciplukan (*Physalis angulata* L.)

Varni Apensa, Retno Mastuti*

Department of Biology, Faculty of Mathematics and Natural Sciences, University of Brawijaya, Malang, Indonesia

In vitro culture techniques can be used as an alternative problem solving in an effort to provide Ciplukan plant as a raw material of herbal medicine in a sustainable manner. The purpose of this study was to observe the effect of banana homogenate (BH) added into culture medium on shoot regeneration of Ciplukan (*Physalis angulata* L.) and plantlet development until acclimatization stage. The experimental design used was a randomized factorial group. The first factor was the two varieties of banana fruit namely, Ambon and Raja. The second factor was concentration of BH with four levels, 0 (control), 2.5%, 5% and 7.5 % and each treatment combination was repeated five times. Explant used in this research was the third node of 2 weeks old in vitro shoot after subculture to MS0 medium. Data analysis used ANOVA test. Eight week after culture (WAC) medium containing BH induced higher number of shoot compare to medium without BH. The addition of 5% BH var. Ambon had significant effect on increasing shoot number. Well rooted plantlets produced in MS0 rooting medium also showed high survival rate (66.7%< - 100%) two weeks after transferred to greenhouse. Therefore, the addition of BH into in vitro medium can be an alternative method for micropropagation of Ciplukan.

Keywords: Banana homogenate, Ciplukan, micropropagation, nodal explants.

INTRODUCTION

Ciplukan (*Physalis angulata* L.) is a wild plant species that will be commonly found especially on the edge of the forest, yard, and corn fields. Ciplukan has been widely used as traditional medicine [1]. Clinically, this plant is proven to have a lot of bioactive content. Ciplukan can be used as antihyperglycemic, antibacterial, antiviral, immunostimulant and immunosuppressant (immunomodulator), antiinflamation, antioxidant, analgesic, and cytotoxic. Also as diuretic, neutralize toxins, relieve cough, and activate the function of the body glands and anti-tumor. Ciplukan fruit can also be used to cure bleeding gums [2]. Currently, Ciplukan already widely used by the industry as herbal medicine. Therefore, to meet the needs of the industry, the demand for Ciplukan supply is increasing [3].

The increasing demand for medicinal plants causes over extraction from the wild source. Even though, the medicinal plants that obtained from various locations will have varies in productivity. Some environmental factors may affect all phases of growth and development [4] including biosynthesis of secondary metabolites.

To prevent the supply of medicinal plants from natural source which has various characters it should be accompanied by the availability of standardized source. In vitro tissue culture techniques can be used as an alternative problem solving in an effort to provide the plant as a sustainable raw material for herbal medicine. Large-scale plant tissue or organ culture for the production of secondary metabolites is an attractive alternative approach to traditional methods of cultivation of medicinal plants [5]. The advantages of this method are many; it is independent of soil, climatic interference, geographical location, does not require a very wide area for produce large quantities of plants at relatively narrow space [6] and it can provide a continuous and reliable source of natural products. The success of tissue culture techniques is influenced by several factors, including the composition of plant growing media [7,8]. Culture media frequently used for tissue culture techniques is Murashige and Skoog (MS) basal medium (1962). MS medium is widely used for tissue culture of most plant tissues as its balanced composition over other media. This basal medium contains complete macro nutrients (N, P, K, Ca, Mg, and Na) and micro (B, Co, Mn, I, Fe, Zn, and Cu). MS medium also contains other energy sources such as sugar, vitamins, amino acids and myo inositol [9].

In vitro culture media can also be added by complex organic matter as a source of sugar, vitamins, plant growth regulators and amino acids.

* Correspondence address:
Retno Mastuti
Email : mastuti7@ub.ac.id
Address : Dept. Biology, Faculty of Mathematics and Natural Science, University of Brawijaya, Veteran Malang, Malang 65145.

ISSN. 2087-2852
E-ISSN. 2338-1655

Natural organic compounds that have been widely used include coconut water, yeast extract, malt extract, potato extract, papaya extract, banana porridge (banana homogenate), tomato juice and wotel juice. The use of such organic organic compounds as additives to media can provide better growth and morphogenesis [10].

Bananas are commonly added to in vitro media in the form of slurry or homogenate. Banana homogenate (BH) has been able to increase the number of shoots of various orchids [11-16]. Provision of BH can improve regeneration response, number of shoots per explant and complete plantlet on *Cymbidium pendulum* compared to without addition of banana pulp [15]. Addition of 150 g.L^{-1} banana var Ambon and NAA 20 ppm can produce the highest average number of shoots on black orchid plant (*Coelogyne pandurata*) [17]. Bananas contain carbohydrates, proteins, fats, Ca, P, Fe, vitamin A, vitamin B-1, and vitamin C so it can help the regeneration process in plants [18]. Some types of bananas, ie banana var. Kepok, Mas, Raja, Ambon Lumut and Ambon Putih can produce different in vitro growth response on Phalaenopsis orchid planlet [19]. Banana var. Raja and Ambon were able to increased shoot number, plantlet height, leaf length and number and root number of orchids [20,21]. Therefore, in this study the influence of two local varieties of banana, namely Ambon and Raja on shoot regeneration and plantlet development of Ciplukan nodes explant was observed.

MATERIAL AND METHOD

Preparation of source explant

The ripe yellow Ciplukan fruit was split and seeds were taken and dried for 2-3 days. Dry seeds were germinated on agar medium (12 g.L^{-1}) without addition of growth regulator under 500 lux light intensity at 23 $\pm$ 2 °C. Cotyledon and shoot apical were excised from two weeks old seedling then subcultured into hormone free MS (MS0) medium. The nodal explants were taken from the third node of growing shoots.

In vitro culture medium

Shoot induction medium (SIM) used in this study was MS basal salt medium + growth regulator (BAP 2 mg.L^{-1} + IAA 0.05 mg.L^{-1}) + banana homogenate (BH) supplemented with 30 g.L^{-1} commercial granulated sugar. The effect of two local banana varieties, Ambon and Raja were observed in this study. Four concentrations for each banana, var. Ambon (PA) and Raja (PR), were 0, 2.5%, 5.0% and 7.5% (w/v). Banana homogenate were derived from finely ground ripened fruit shortly prior to add into the medium. After stirring evenly the medium solution was adjusted to pH 5.8 and solidified by 12 g.L^{-1} agar. There were two types root induction medium (RIM), ie 1) MS0 without growth regulator, and 2) MS + auxin (NAA 2 mg.L^{-1}+ IBA 1 mg.L^{-1}). Culture medium was sterilized by autoclaving at 121°C, 1.5 atm for 15 minutes.

Shoot induction and multiplication

Three nodal explants were inoculated on each bottle of SIM without BH as control (P0) or with BH (PA and PR) with five replicates to observe their capability of shoot induction and multiplication. The cultures were incubated in culture room at 24 $\pm$ 2°C under 500 lux light intensity for 24 hours. The number and height of shoots and the leaf number were measured eight week after culture (WAC). The shoot height was measured from the base of the shoots on the surface of the culture medium to the shoot tip.

Root induction and plantlet regeneration

The eight-week-old shoots induced in P0, PA and PR mediums were subcultured on two types root medium, ie MS0 and MS + auxin. The cultures were incubated in culture room at 24 $\pm$ 2°C under 500 lux light intensity for 24 hours. The number and length of roots in each shoot, plantlet height, leaf number and fresh weight (FW) of plantlets on MS0 medium and MS + auxin medium were measured one and three WAC, respectively.

Acclimatization

Plantlets with well developed root were removed from rooting medium. The root part was thoroughly washed with running water to remove the agar medium. The plantlet was then grown on a plastic cup (240 ml in size) containing a mixture of soil, compost and husk (ratio 1: 1: 1) and enclosed with transparent plastic for two weeks. Subsequently, the plants were moved to pots (ϕ 17 cm) with the same medium composition and placed in the green house for two weeks.

Experimental Design and Data Analysis

The results are presented as mean $\pm$ SD (standard deviation). Data analysis using ANOVA (Analysis of Variance) test to determine whether there is difference of influence between type and concentration of banana var. Ambon and Raja for all parameters observed.

ISSN. 2087-2852
E-ISSN. 2338-1655

RESULT AND DISCUSSION

Shoot Regeneration

The occurrences of green spots were noticed on the surface of nodal tissues two or three days of culture. The formation of green spots is positively correlated with shoot regeneration [22,23]. One WAC green leaves were observed in the medium with (Fig. 1B-C) and without BH addition (Fig. 1A).

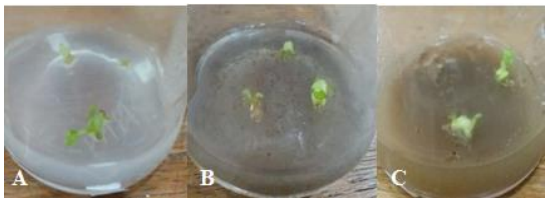

Figure 1. Shoot with green leaf 1 WAC. (A) P0 (control) medium, (B) PA medium, (C) PR medium.

Eight WAC shoot on P0 (control) medium (Figure 2A) had stems thicker and leaves smaller than in PA and PR medium. The PA medium produced more shoots and leaves number but had a shorter shoot height (Figure 2B) than the control and PR medium (Figure 2C). Banana has been frequently added as organic additive in in vitro culture because it is a good source of mineral, vitamin and natural plant growth regulators like IAA, gibberellin and zeatin [24,25]. Banana is also rich in carbohydrates that act as carbon source which supply energy to the heterotroph plant during the early stage in vitro culture [26,27].

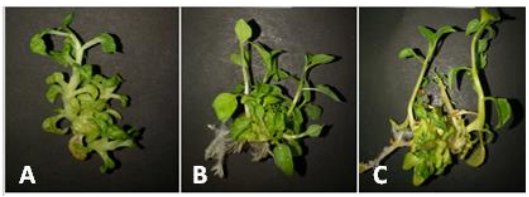

Figure 2. Shoot multiplication 8 WAC. (A) P0 (control) medium, (B) PA medium, (C) PR medium.

Medium containing either BH cultivars 'Ambon' (PA) or 'Raja' (PR) induced higher number of shoot (3.25 ± 1.29 or 3.33 ± 1.23) (Fig. 3A) than the medium without addition of BH (1.75 ± 0.5) eight WAC. Conversely, the height of shoots (Fig. 3B) and the number of leaves (Fig. 3C) produced in medium containing BH tends to decrease compared to those produced in control medium. High frequency of shoot number is a prerequisite for clonal propagation [8]. However, increase the number of shoot usually accompanied by decrease the shoot length [28].

Eight week after culture only 5% BH produced significantly high number of shoots while in other parameters were not significant effect (Fig. 4). The sucrose content in banana has a role in enhancing in vitro regeneration [14]. Medium containing 5% BH was also induced the highest regeneration frequency of *Cymbidium pendulum* [10]. The positive effect of 5% BH on enhancing shoot number is advantageous to provide the *P. angulata* plant as a raw material for herbal medicine.

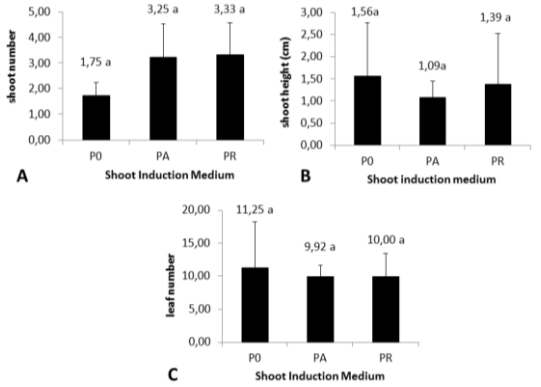

Figure 3. The effect of banana local variety to the shoot growth 8 WAC. (A) Shoot number, (B) Shoot length, (C) Leaf number. **Note**: the same letter on different shoot induction medium showed no significant difference in ANOVA test (α = 0.05).

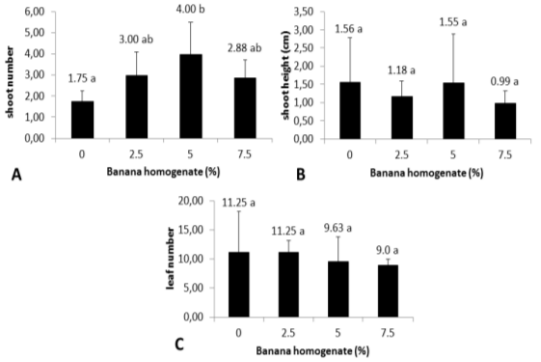

Figure 4. The effect of BH concentration in shoot induction medium to the shoot growth 8 weeks after culture. (A) Shoot number, (B) Shoot length, (C) Leaf number. **Note:** the same letter on different concentration of BH showed no significant difference in ANOVA test (α = 0.05).

Root Induction and Plantlet Regeneration

MS free hormone medium was able to induce roots one WAC. Meanwhile in MS + auxin medium the roots were induced three weeks after subculture. MS free hormone medium produced white, long and thick roots (Fig. 5A-C). While MS + auxin medium produced small fibers, short, thin and brownish white roots (Fig. 5D-F). This is consistent with the research of [29] which showed that roots produced in MS + auxin were short, thin and fragile. Auxin at low concentra-

ISSN. 2087-2852
E-ISSN. 2338-1655

tions increase root length while at high concentrations can inhibit root growth [30]. This results show that the auxin added to the root induction medium actually inhibits root growth. Thickened roots of *Carica papaya* L. with few lateral branches and no root hairs were making them difficult to acclimatize [31].

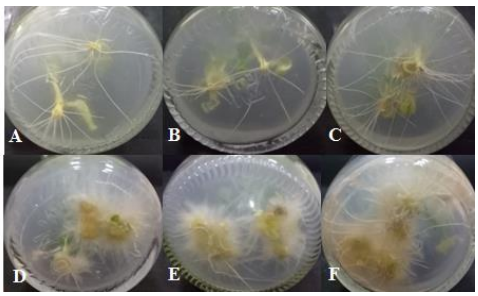

Figure 5. Roots formed from *P. angulata* shoots on MS0 medium (1 week old) and MS + auxin medium (3 weeks old). A & D. P0 (control) medium. B & E. PA Medium. C & F. PR Medium. A - C MS0 medium. D – F MS + auxin medium.

Plantlets with normal leaf was observed on MS0 medium (Fig. 6A) whereas the plantlet on MS + auxin medium showed curved leaf edge (Fig. 6B). Abnormal leaves in maize [32], bean and Arabidopsis [33] have been reported in medium with high concentration of auxin.

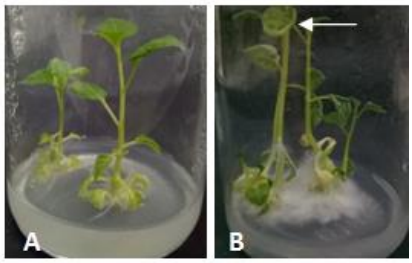

Figure 6. Planlet *P. angulata* on rooting medium. (A) planlet on MS0 medium (1 WAC), (B) planlet on MS + auxin medium (3 WAC).

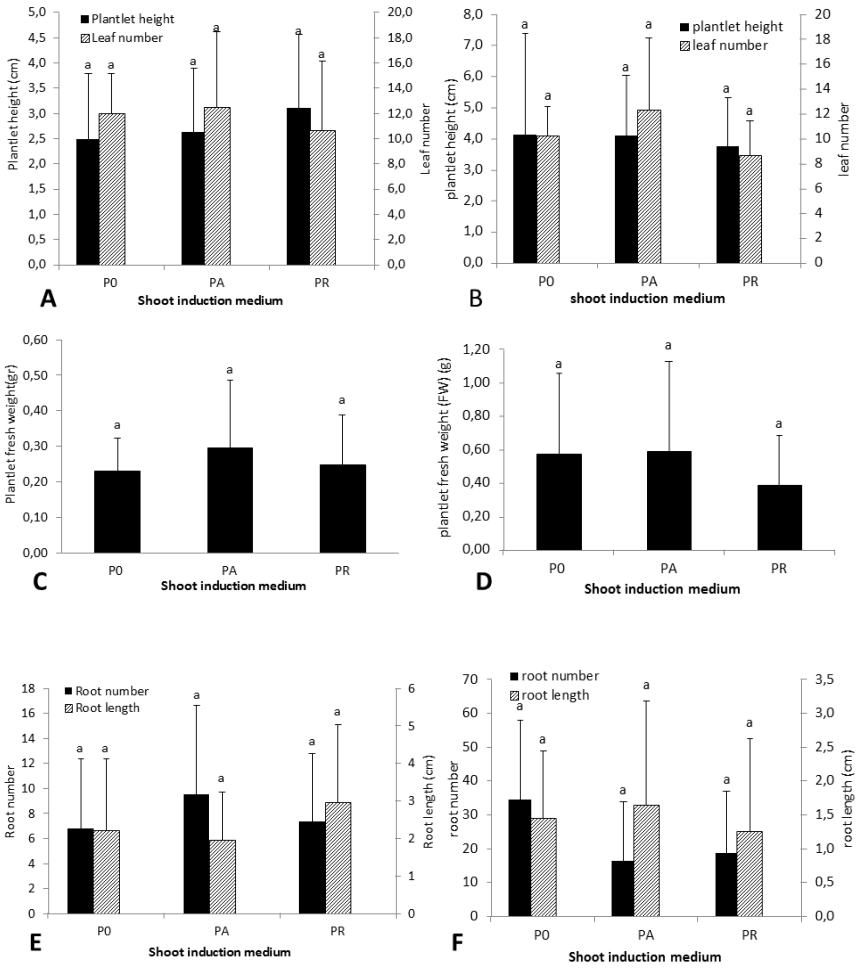

Figure 7. Effect of banana homogenate added in SIM on plantlet growth in MS0 and MS + auxin rooting medium. A. Plantlet height and leaf number in MS0 rooting medium, B. Plantlet height and leaf number in MS + auxin rooting medium, C. Plantlet FW in MS0 rooting medium, D. Plantlet FW in MS + auxin rooting medium, E. Root number and root length in MS0 rooting medium, F. Root number and root length in MS + auxin rooting medium.

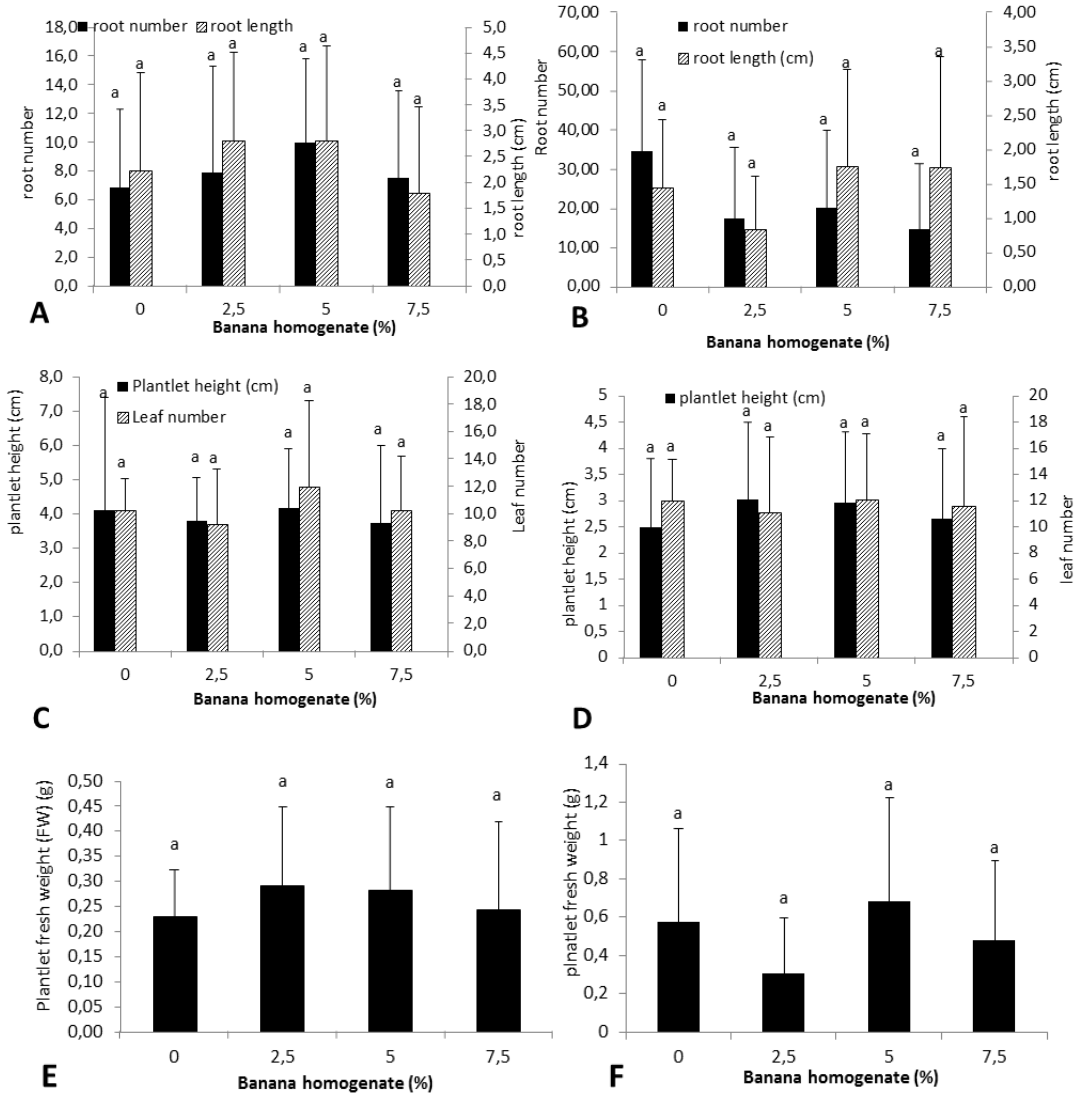

Figure 8. Effect of banana homogenate concentration added in SIM on plantlet growth in MS0 and MS + auxin rooting medium. A. Root number and root length in MS0 rooting medium, B. Root number and root length in MS + auxin rooting medium C. Plantlet height and leaf number in MS0 rooting medium, D. Plantlet height and leaf number in MS + auxin rooting medium Root number and root length in MS0 rooting medium E. Plantlet fresh weight in MS0 rooting medium, F. Plantlet fresh weight in MS + auxin rooting medium.

Shoot derived from PA medium showed better responses in almost all parameters studied (Fig. 7A-D) except for root number in MS0 medium (Fig. 7E) and root length in MS + auxin medium (Fig. 7F). As shown in Fig. 3A the shoot number induced in SIM medium containing BH especially PA medium (var. Ambon) was comparatively higher than P0 control medium. The addition of BH derived from var. Ambon can increase plantlet height, leaf number and root length of Dendrobium plantlet [34]. In this study high number of regenerated shoot in SIM produced high number of the sites of auxin synthesis. Consequently, the content of auxin endogenous hormone in plantlet increased. This results shows that BH supplements in SIM still influence plantlet growth in rooting medium.

In MS0 rooting medium shoot derived from SIM containing 2.5 and 5% BH tended to produce number and length of roots (Fig. 8A), height of plantlet (Fig. 8C) and fresh weight of plantlet (Fig. 8E) higher than shoots derived from 0% (control) and SIM containing 7.5% BH. However, in MS + auxin rooting medium the shoots derived from SIM medium containing 5% BH tended to produced higher root length (1.7 $\pm$ 1.4 cm) (Fig. 8B), plantlet height (4.2 $\pm$ 1.7 cm), number of leaves (12.0 $\pm$ 6.3) (Fig. 8D) and fresh weight of plantlet (0.7 $\pm$ 0.5 g) (Fig. 8F). The number and length of roots, number and length of leaves of new *D. lasianthera* will increase with the addition

ISSN. 2087-2852
E-ISSN. 2338-1655

of high concentration of BH, ie 150 g.L^{-1} (15%) [35]. This shows that regeneration of *P. angulata* plantlet could be induced with low concentrations of BH.

In this study banana var. Ambon and Raja added in SIM and all concentration tested did not significantly affect all parameters studied for ciplukan in both of MS0 and MS + auxin rooting medium. This is consistent with previous study [36] who stated that BH (2.5%, 5.0% and 7.5% v/v) did not significantly promote rooting of *Dimorphorchis lowii*. It was assumed that root formation required organic nitrogen compunds since the best performance of root regeneration was observed in culture media supplemented by coconut water, pepton and yeast [36].

In this study the difference in root number and morphology is more due to the presence or absence of growth hormone in culture medium (MS0 and MS +auxin). Auxin is an essential factor for induction of roots in plants. Adventitious roots produced in MS0 medium promoted by basipetal auxin transport from shoot tip toward the basal parts. Addition of exogenous auxin in rooting medium will increased its concentration in cellular level [37]. In this study high accumulation of auxin promoted more root number but might inhibited root elongation.

Acclimatization

Plantlets derived from SIM supplemented with BH can grow well in the early adaptation stage (Fig. 9). No significant different in all parameters was observed two weeks after transferred the plantlets to plastic glass.

Figure 9. Plant growth in acclimatization stage 2 weeks after planting. A, D. P0 medium (control), B, E. PA medium, CF. PR medium. A-C. medium MS0, and D-F. medium MS + auxin.

After being transferred to pot in greenhouse for 2 weeks the plantlets derived from MS0 rooting medium had better survival compared to the plantlets derived from MS + auxin rooting medium. The plant from P0 medium had the lowest survival rate (33.3%) compared to the plant from SIM containing BH (66.7 - 100%) (Table 1). Whereas, in MS + auxin rooting medium the plantlets with survival rate 100% was only obtained from 2.5% and 7.5% PR medium. Survival rate of plant from other SIM was only 50%.

Table 1. Survival rate of *P. angulata* plantlet after 2 weeks grown in the greenhouse

Shoot induction medium	Survival rate of plantlets (%)	
	MS0	MS + NAA 2 mg.L^{-1} + IBA 1 mg.L^{-1}
P0 (control)*)	33.30	50
PA 2.5	100	50
PA 5	100	50
PA 7.5	66.7	50
PR 2.5	100	100
PR 5	100	50
PR 7.5	83.3	100

Note: *): P0 (control)= without banana homogenate; PA: Banana var. "Ambon" ; PR: Banana var. "Raja"

After transferred to pot the plants derived from PA and PR medium for shoot induction and either MS0 or MS + auxin for rooting medium (Fig. 10B,E) remain had higher plant height and wider leaves than the plants derived from other mediums (Fig. 10A,D,C,F). While plants derived from P0 (control) medium and MS + auxin rooting medium have a narrower leaves than plants derived from MS0 rooting medium. Short thin root produced in MS + auxin rooting medium. The smooth and short roots appear to be less able to facilitate the absorption of water and minerals from the medium to support the growth of the vegetative organ.

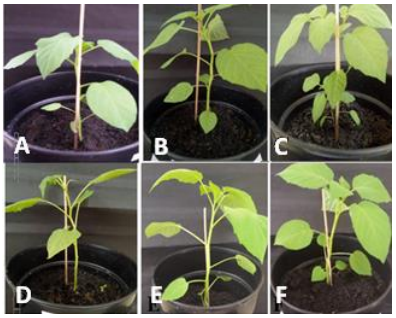

Figure 10. Acclimatization of in vitro micropropagation of *P. angulata* two weeks after transfer. A,D. P0 (control) medium; B,E. PA medium; C,F. PR medium; A,B,C. MS0 medium; D,E,F. MS + auxin medium.

Naturally, regeneration of adventitious organs depends on endogenous hormones [38]. Endogenous auxin is of primary importance initiating adventitious root formation [39]. This sug-

ISSN. 2087-2852
E-ISSN. 2338-1655

gests that the MS0 medium without hormones is capable for developing a functional root system. In vitro roots still functional and continue to grow during acclimatization [40). Therefore, formation of functional root system in in vitro plantlet is to be important step to survive after transplantation [41]. High survival of plants from MS0 rooting medium indicates that endogenous auxin of *P. angulata* plantlet has been able to produce good functional root system. Functional root system can absorb nutrients and water from acclimatization media in a good way thereby enhancing the growth of the plant.

CONCLUSION

Applications of 5% BH as supplement in tissue culture media should be considered due to positive response in shoot regeneration and multiplication of *P. angulata*. High survival rate (66.7%< - 100%) of plant in aclimatization stage after transferred to pot in greenhouse due to better rooting system in MS0 rooting medium. This condition support the sustainability of raw materials of herbal medicine.

REFERENCES

[1] Mahalakshmi, A.M., B. Ramesh, Nidavani. 2014. *Physalis angulata* L.: an Ethanopharmacological review. *J. Pharm. Res.* 4(3). 1479-1486.

[2] Santoso, H.B. 2008. Ragam dan khasiat tanaman obat. Agromedia Pustaka. Jakarta.

[3] Sukmadjaja, D., I. Mariska. 2003. Perbanyakan bibit Jati melalui kultur jaringan. Research Center of Biotechnology and Agriculture Genetic Resources. Bogor.

[4] Haferkamp, M.R. 1988. Environmental factors affecting plant productivity. In: White, R.S., R.E. Short (Eds). Fort Keogh Research Symposium. *Montana Agr. Exp. Sta.* Bozeman, Miles City. 27-36.

[5] Alamgir, A.N.M. 2017. Cultivation of herbal drugs, biotechnology, and In Vitro production of secondary metabolites, high-value medicinal plants, herbal wealth, and herbal trade. In: Therapeutic Use of Medicinal Plants and Their Extracts: Volume 1. Progress in Drug Research, Vol 73. Springer. Cham.

[6] Sharma, A., V. Agrawal. 2012. Tissue culture aspects of ornamental plants. *J. Biotechnol.* 1(1). 2319-3859.

[7] George, E.F., M.A. Hall, G.J.D. Klerk. 2008. Plant propagation by tissue culture, 3rd Ed. Springer. Netherland.

[8] Yildiz, M. 2012. The prerequisite of the success in plant tissue culture: high frequency shoot regeneration. In: Leva, A., L.M.R. Rinaldi (Eds). Recent Advances in plant In Vitro culture. *InTech.* DOI: 10.5772/51097.

[9] Sudipta, K.M., S.M. Kumara, M. Anuradha. 2013. Influence of various carbon sources and organic additives on in vitro growth and morphogenesis of *Leptadenia reticulata* (Wight & Arn), A valuable medicinal plant of India. *J. Pharm. Sci.* 21(2). 174-179.

[10] Molnar, Z., E. Virag, V. Ordog. 2011. Natural substances in tissue culture media of higher plants. *Article Acta Biologica Szegediensis.* 55(1). 123-127.

[11] Sudeep, R., P.K. Rajeevan, P.K. Valasalakumari, C. K. Geetha, 1997. Influence of organic supplements on shoot proliferation in Dendrobium. *J. Hortic.* 3. 38-44.

[12] Ngampanya B., W. Homlaaor. 2010. Simple media for *Dendrobium* orchid seed germination and protocorm development. *Acta hortic*. 878. 219-223.

[13] Lekha, R.C., C. Vidya, K. Rajmohan, S.T. Mercy. 2005. Protocorm differentiation and seedling growth in *Dendrobium* hybrid seed cultures as influenced by organic additives. *J. Orchid Soc. India.* 19. 67-70.

[14] Aktar, S., K.M. Nasiruddin, K. Hossain. 2008. Effects of different media and organic additives interaction on In Vitro regeneration of *Dendrobium* orchid. *J. Agr. Rural Dev.* 6. 69-74.

[15] Kaur, S., K.K. Bhutani, 2012. Organic growth supplement stimulants for in vitro multiplication of *Cymbidium pendulum* (Roxb.)sw. *J. Hortic. Sci.* (Prague). 39(1). 47-52.

[16] Islam, O., M.S. Islam, M.A. Saleh. 2016. Effect of banana extract on growth and development of protocorm like bodies in *Dendrobium* sp. orchid. *The Agriculturists.* 13(1). 101.

[17] Untari, R., M.P. Dwi. 2006. Pengaruh bahan organik dan NAA terhadap pertumbuhan Anggrek Hitam (*Coelogyne pandurata* Lindl.) dalam kultur In Vitro. *Jurnal Biodiversitas.* 7(3). 344-348.

[18] Mulyanti, S. 2005. Teknologi pangan. Trubus Agri Sarana. Surabaya.

[19] Widiastoety, D., R.W. Prasetio, Purbadi. 2004. Pengaruh bubur buah pisang terhadap pertumbuhan planlet Anggrek *Phalaenopsis* dalam media kultur. Research

ISSN. 2087-2852
E-ISSN. 2338-1655

and Development Center of Horticulture. Bogor.

[20] Djajanegara, I. 2010. Pemanfaatan limbah pisang dan air kelapa sebagai bahan media kultur jaringan Anggrek Bulan (*P. amabilis*) Tipe 229. *Jurnal Tenik Lingikungan.* 11(3).373-380.

[21] Agriani, E.B. 2010. Pengaruh penambahan berbagai ekstrak pisang pada media Vacin and Went (VW) terhadap pertumbuhan Anggrek *Cymbidium traceyanum* yang ditanam secara In Vitro. Bachelor Thesis. Faculty of Siences and Technology. Islamic State University of Alauddin. Makassar.

[22] Nabors, M.W., S.K. Catherine, D.M. McHugh. 1982. Green spots are predictors of high callus growth rates and shoot formation in normal and in salt stressed tissue cultures of Oat (*Avena sativa* L.). *Zeitschrift für Pflanzenphysiologie.* 105(4). 341-349.

[23] Ben Amer, I.M., A. Börner. 1997. Plant cell, tissue and organ culture. Available at: https://doi.org/10.1023/A:1005855912655.

[24] Khalifah, R.A. 1966. Indolyl-3-acetic acid from the developing banana. *Nature.* 212. 1471-1472.

[25] Arditti, J. 1968. Germination and growth of orchids on banana fruit tissue and some of its extracts. *Am. Orchid Soc. Bull.* 37. 112-116.

[26] Widiastoety, F.A. Bahar. 1995. Pengaruh berbagai sumber dan Kadar karbohidrat terhadap plantlet anggrek *Dendrobium*. *Jurnal Hortikultura.* 5(3). 76-80.

[27] Al-Khateeb, A.A. 2008. Regulation of In Vitro bud formation of date palm (*Phoenix dactylifera* L.) cv. Khanezi by different carbon sources. *Bioresour. Technol.* 99(14). 6550-6555.

[28] Praveena C., C. Veeresham. 2014. Multiple shoot regeneration and effect of sugars on growth and nitidine accumulation in shoot cultures of *Toddalia asiatica*. *Pharmacogn. Mag.* 10(Suppl 3). S480-S486.

[29] Sheeba, E., S. Palanivel, S. Parvathi. 2015. In vitro flowering and rapid propagation of *Physalis Minima* Linn. - a medicinal plant. Int. *J. Innov. Res. Sci. Eng. Technol.* 4(1). 18763-18768.

[30] Salisbury, F.B. & C.W. Ross. 1995. Perkembangan Tumbuhan dan Fisiologi Jilid III. ITB. ITB Press. Bandung.

[31] Kaity A., A.M. Parisi, S.E. Ashmore, R.A. Drew. 2009. Root initiation and acclimatization of papaya plants. *Acta Hortic.* 812. 387-394.

[32] Scanlon, M.J. 2003. The polar auxin transport inhibitor N-1-Naphthylphthalamic acid disrupts leaf initiation, KNOX protein regulation, and formation of leaf margins in Maize. *Plant Physiol.* 133(2). 597-605.

[33] Keller, C.P., R. Stahlberg, L.S. Barkawi, J.D. Cohen. 2004. Long-term inhibition by auxin of leaf blade expansion in bean and arabidopsis. *Plant Physiol.* 134(3). 1217-1226.

[34] Utami, P.K, B. Ginting, A. Santi. 2011. Pengaruh bahan organik terhadap pertumbuhan planlet Anggrek *Dendrobium* secara In Vitro. Proceeding of National Seminar on Floriculture. Research Center of Ornamental Plants. Cianjur.

[35] Utami, E.S.W., S. Hariyanto, Y.S.W. Manuhara. 2017. In Vitro propagation of the endangered medicinal orchid, *Dendrobium lasianthera* J.J.Sm through mature seed culture. *Asian Pac. J. Trop. Biomed.* 7(5). 406-410.

[36] Jainol, J.E., A.G. Jualang. 2015. In Vitro shoot multiplication and rooting of shoot tip explants of dimorphorchis lowii: an endemic orchid of Borneo. *J. Trop. Plant Physiol.* 7. 14-25.

[37] Overvoorde P., H. Fukaki, T. Beeckman. 2010. Auxin control of root development. *Cold Spring Harb. Perspect. Biol.* 2(6). a001537.

[38] Chen, X., Y. Qu, L. Sheng, J. Liu, H. Huang, L. Xu. 2014. A simple method suitable to study de novo root organogenesis. *Front Plant Sci.* 5. 208.

[39] Liu, J., L. Sheng, Y. Xu, J. Li, Z. Yang, H. Huang, L. Xu. 2014. WOX11 and 12 are involved in the first-step cell fate transition during de novo root organogenesis in Arabidopsis. *Plant Cell.* 26. 1081-1093.

[40] Nowak, J., K. Pruski. 2002. Priming tissue cultured propagulesin: Low cost options for tissue culture technology in developing countries. Proceedings of a Technical Meeting organized by the Joint FAO/IAEA Division of Nuclear Techniques in Food and Agriculture. Vienna. 68-81.

[41] da Silvaa, J.A.T., M.M. Hossain, M. Sharma, J. Dobránszki, J.C. Cardoso, Z. Songjun. 2017. Acclimatization of In Vitro-derived *Dendrobium*. *Hortic. Plant J.* 3(3). 110-124.

ISSN. 2087-2852
E-ISSN. 2338-1655

Microsatellite Marker for Cross-Species Amplification: Study Case for Indonesian Sundaland Python (Serpentes: Pythonidae)

Andri Maulidi[1], Fatchiyah Fatchiyah[1,2], Amir Hamidy[3], Nia Kurniawan[1*]

[1]Departement of Biology, Faculty of Mathematics and Natural Science, University of Brawijaya, Malang, Indonesia
[2]Research Center Smonagenes UB, Departement of Biology, Faculty of Mathematics and Natural Science, University of Brawijaya, Malang, Indonesia
[3]Laboratory of Herpetology, Museum Zoologicum Bogoriense, Research Center for Biology, Indonesian Institute of Sciences–LIPI, Cibinong, Indonesia

The python of Indonesian Sundaland has been traded for its distinct skin colour and patterns. The need for rapid method in cross-species amplification for Indonesian Sundaland python is useful to contribute in management of sustainability harvesting system. In this research, we screened 10 microsatellite primers which are previously used for Australian, New Guinean, Chinese and Burmese pythons and 7 potentially amplifiable primers for African and Asian reptiles. *Python breitensteini* showed a greater number of alleles (2-8 alleles) than *Python bivittatus* (1-3 alleles) and *Python brongersmai* (1-2 alleles). The observed and expected heterozygosity for all species were ranged from 0 to 1.00 and 0 to 0.79, respectively. According to the high cross-species amplification rates, 15 out of 17 primers were useful in assessing the genetic diversity and conservation genetic of Indonesian Sundaland python. Among the 15 primers, MS3 generated the highest number of allele for *P. breitensteini* (8 alleles), *P. bivittatus* (3 alleles), and *P. brongersmai* (2 alleles). We proposed MS3 locus as a suitable marker for Indonesian Sundaland python.

Keywords: microsatellite, Python, Sundaland.

INTRODUCTION

Python is a nonvenomous snake and famous for its large body size. Among five species of python distributed in Indonesian Sundaland (Java, Borneo, and Sumatera), two of them are categorized into long-tailed python, namely reticulated python (*Malayopython reticulatus*) and Burmese python (*Python bivittatus*) and three of them are categorized into short-tailed pythons, namely Sumatran short-tailed Python (*Python curtus*), Brongersma's short-tailed Python (*Python brongersmai*), and Bornean short-tailed Python (*Python breitensteini*). Currently, the availability of python in the wild has gathered a great attention from Indonesian wildlife authorities due to massive threats of hunting in nature, deforestation and land conversion for agriculture [1,2]. Moreover, the demand for Indonesian Sundaland python for its skin color and patterns in the international market urged many conservation agencies to assist the management of wildlife trade. The information on the sustainability of harvesting system of Indonesian reticulated python was already described [3,4]. Harvesting of reticulated python in Indonesia officially only included one subspecies, *P. reticulatus reticulatus* which was widely distributed in Sumatra, Kalimantan, Java, and Sulawesi. The trade of two other subspecies, *P. reticulatus saputrai* (Selayar Island and Southwest Sulawesi) and *P. reticulatus jampeanus* (Tanahjampe Island), were banned according to Indonesian annual quota system. Therefore, management support regarding the harvesting system, including the use of molecular data to detect the origin of the specimens will be very beneficial for its implementation.

The use of microsatellite markers has been widely developed to detect illegal trade in many species such as broad-headed snakes, *Hoplocephalus bungaroides* [5], Cape parrot, *Poicephalus robustus* [6], and the identification of ivory species origin traded in African black market [7]. Previous studies also revealed the use of microsatellite primers on python, such as those for Australian and New Guinean pythons [8], invasive Burmese python (*Python molurus bivittatus*) [9] and *Python bivittatus* in China [10]. Meanwhile, little is known about Indonesian Sundaland pythons, including their genetic diversity. However, the development of microsatellite primers may cost considerable price and time consuming, in order that the use of cross-species amplification becomes an alternative way to find a suitable marker for closely related species determination.

* Correspondence address:
Nia Kurniawan
Email : wawan@ub.ac.id
Address : Dept. Biology, Faculty of Mathematics and Natural Science, University of Brawijaya, Veteran Malang, Malang 65145.

ISSN. 2087-2852
E-ISSN. 2338-1655

MATERIALS AND METHODS

A total of 13 specimens collected directly from the wild consisted of *Python breitensteini* (n = 10) from Borneo, *P. bivittatus* (n = 2) from Java, and *P. brongersmai* (n = 1) from Sumatera in 2016. Distinct color patterns of the three Sundaland pythons is showed in Figure 1. Animal ethics was approved by the Ethical Committee of Brawijaya University with the letter of Ethical Clearance No: 68-KEP-UB. DNA was isolated from muscle tissue using Qiagen DNeasy kit following the manufacturer's instruction. Whole genomic DNA was analyzed qualitatively using 1% agarose gel and tested quantitatively using a spectrophotometer. We used 17 primers which have been designed for *Morelia spilota* [8] and *Python bivittatus* [9] and [11] (Supplementary 1).

Figure 1. Distinct color patterns of the three Sundaland Pythons along the body (a), dorsal part of the head (b), and lateral part of the head (c) for *Python breitensteini* (up), *Python bivittatus* (middle), *Python brongersmai* (bottom).

ISSN. 2087-2852
E-ISSN. 2338-1655

The PCR amplification was performed following the original authors for each primer, except that of [11] as followed: one cycle in 95°C for 5 minutes, 36 cycles in 94°C for 30 seconds, 55-62°C for 45 seconds, and 72°C for 40 seconds, and one cycle for final extension in 72°C for eight minutes. Annealing temperature for each primer and its amplification result can be seen in Supplementary 1. All PCR mixture was done in 40 µL of reaction volume containing 20 µL Go Taq® green (Promega Co., USA), 0.8 µM forward primer, 0.8 µM reverse primer, 14.4 µL nuclease-free water, and 4µL genomic DNA. The PCR products were visualized on 2% agarose gel with 100bp DNA Leader (Promega) as DNA marker. Calculation of the number of alleles (Na), observed heterozygosity (Ho), and expected heterozygosity (He) were performed using GenAlEx 6.501 [12].

RESULT AND DISCUSSION

Majority of loci were amplified among three different species of python except that of MS5 in *P. brongersmai* and MS27 for *P. bivittatus*. Fifteen out of 17 primers produced various number of alleles which ranged from 1 to 3 for *P. bivittatus*, 1 to 2 for *P. brongersmai*, and 2 to 8 for *P. breitensteini*. However, we found fewer alleles than those observed for MS9 and MS16 loci [9]; and for MS5, MS13, and MS16 loci [10]. Nevertheless, this discrepancy might due to differences in sample sizes between the three studies. Higher number of samples is beneficial for obtaining more genetic variety within the population. Limited number of samples can be caused by short duration of sampling in each region and the number of alleles and heterozygosity can be increased by adding more samples and loci, as well as selecting certain loci with multiple alleles. However, the potential primer for cross-species amplification can be determined by the multi-amplification ability. In this case, the co-occurrence of any alleles found in the three different species indicates the inferred potential primer.

Best markers were categorized by at least 50% of amplification success and those that were polymorphic with at least three alleles [13]. The observed heterozygosities (Ho) ranged from 0.00-0.60 for *P. breitensteini*, 0.00-1.00 for *P. bivittatus*, and 0.00 – 1.00 for *P. brongersmai*. The expected heterozygosity (He) ranged from 0.20-0.79 for *P. breitensteini*, 0.00-0.63 for *P. bivittatus*, and 0.00-0.50 for *P. brongersmai*. Heterozygosity reflects allele variation within different loci which is an appropriate parameter for measuring genetic variation in a population [14]. The differences in genetic variability is likely due to differences in geographical and ecological conditions by which all three studied species were found in different islands. *Python breitensteini* is found only in Borneo, meanwhile *P. brongersmai* in Sumatera and *P. bivittatus* in Java Island [15].

The highest number of alleles was generated by MS3 for *P. breitensteini* (8 alleles), followed by MS1 (5 alleles), MS27 (5 alleles), MS13 (4 alleles), Pmb N14 (4 alleles) and KE961431.1 (4 alleles). However, MS3 was also amplified in *P. bivittatus* (3 alleles) and *P. brongersmai* (2 alleles) with higher number of alleles and samples than the other primers. The co-occurence of alleles found in this study and those observed in 13 python species [8] and in *P. m. bivittatus* of Florida [9] indicates the potensial use of these studied primers as forensic molecular markers. The success of cross-species amplification can occur due to the taxonomic proximity of the samples [16]. In addition, the high rate of amplification success in *P. breitensteini* provides the possibility for these markers, especially MS3 locus, in an untested species of Sumatran short-tailed python (*Python curtus*). Therefore, microsatellite loci described in our study would be useful for future identification of genetic diversity and population structure among Indonesian Sundaland python as well as providing effective information for wildlife management of python in Indonesia.

CONCLUSION

Cross-species amplification was successful in all three python species in Indonesia except in MS5 in *P. brongersmai* and MS27 for *P. bivittatus*. From these results it is found that MS3 is a marker with the highest number of alleles (8 alleles) for *P. breitensteini*.

ACKNOWLEDGEMENT

We would like to thank NK Research members, especially A.M. Kadafi and Agung Sih K., for helping the samples collection in Java and Sumatera and also to Wolly Candramila and Fitra Arya D.N. for constructive critique for improving this manuscript. This research was funded by LPDP Scholarship from the Ministry of Finance of Indonesia (PRJ-4409/LPDP.3/ 2016).

REFERENCES

[1] Myers, N., R.A. Mittermeier, C.G. Mittermeier, G.A.B. da Fonseca, J. Kent.

ISSN. 2087-2852
E-ISSN. 2338-1655

2000. Biodiversity hotspots for conservation priorities. *Nature*. 403. 853-858.

[2] Sodhi, N.S., L.P. Koh, B.W. Brook, K.L.N. Peter. 2004. Southeast Asian biodiversity: an impending disaster. *Trends Ecol. Evol*. 19(12). 654-660.

[3] Shine, R., Ambariyanto, P.S. Harlow, Mumpuni. 1999. Reticulated pythons in Sumatra: biology, harvesting and sustainability. *Biol. Conserv*. 87(3). 349-357.

[4] Natusch, D.J.D., J.A. Lyons, Mumpuni, A. Riyanto, R. Shine. 2016. Jungle giants: assessing sustainable harvesting in a difficult-to-survey species (*Python reticulatus*). *PLoS ONE*. 11(7). e0158397.

[5] Frankham, G.J., M.C. Hinds, R.N. Johnson. 2015. Development of 16 forensically informative microsatellite loci to detect the illegal trade of broad headed snakes (*Hoplocephalus bungaroides*). *Conserv. Genet. Resour.* 7. 533.

[6] Pillay, K., D.A. Dawson, G.J. Horsburgh, M.R. Perrin, T. Burke, T.D. Taylor. 2010. Twenty-two polymorphic microsatellite loci aimed at detecting illegal trade in the Cape parrot, *Poicephalus robustus* (Psittacidae, AVES). *Mol. Ecol. Resour*. 10. 142-149.

[7] Wasser, S.K., A.M. Shedlock, K. Comstock, E.A. Ostrander, B. Mutayoba, S.M. Stephen. 2004. Assigning African elephant DNA to geographic region of origin: applications to the ivory trade. Proceedings of the National Academy of Sciences of the United States of America. 101. 14847-14852.

[8] Jordan, P.W., A.E. Goodman, S. Donnellan. 2002. Microsatellite primers for Australian and New Guinean pythons isolated with an efficient marker development method for related species. *Mol. Ecol. Notes.* 2. 78-82.

[9] Hunter, E.M., K.M. Hart. 2013. Rapid microsatellite marker development using next generation pyrosequencing to inform invasive Burmese Python-*Python molurus bivittatus*-management. *Int. J. Mol. Sci*. 14. 4793-4804.

[10] Duan, Y., Y. Wang, S. Bai, X. Tian, K. Rong, J. Ma, 2016. Genetic diversity and population genetic structure of *Python bivittatus* in China. *J. For. Res.* 1-8.

[11] Shaney, K.J., R.H. Adams, N. Kurniawan, A. Hamidy, E.N. Smith, T.A. Castoe. 2016. A suite of potentially amplifiable microsatellite loci for reptiles of conservation concern from Africa and Asia. *Conserv. Genet Resour*. 8(3). 307-311.

[12] Peakall, R., O. Smouse. 2012. GenAlEx 6.5: Genetic analysis in Excel. Population genetic software for teaching and research – an update. *J. Bioinf*. 28(19). 2537-2539.

[13] Engelhardt, A., L. Muniz, D.P. Farajallah, A. Widdig. 2017. Highly polymorphic microsatellite markers for the assessment of male reproductive skew and genetic variation in critically endangered Crested Macaques (*Macaca nigra*). *Int. J. Primatol*. 38. 672-691.

[14] Frankham, R., J.D. Ballou, D.A. Briscoe. 2002. Introduction to conservation genetics. Cambridge University. Oxford. 78-83.

[15] Keogh, J.K., D.G. Barker, R. Shine. 2001. Heavily exploited but poorly know: systematics and biogeography of commercially harvested Pythons (*Python curtus* group) in Southeast Asia. *Biol. J. Linnean Soc*. 73. 113-129.

[16] Barbara, T., C. Palma-Silva, G.M. Paggi, F. Bered, M.F. Fay, C. Lexer. 2007. Cross-species transfer of nuclear microsatellite markers: potential and limitations. *Mol. Ecol*. 16. 3759-3767.

ISSN. 2087-2852
E-ISSN. 2338-1655

Suplementary 1. Amplification results for 17 microsatellite loci of three Sundaland Pythons

Loci	Primer Sequence (5'-3')	Repeat Motif	Ta (°C)	*P. breitensteini* (n=10) (Least Concern)					*P. bivittatus* (n=2) (Vulnerable)					*P. brongersmai* (n=1) (Least Concern)				
				Success	Range (bp)	Na	Ho	He	Success	Range (bp)	Na	Ho	He	Success	Range (bp)	Na	Ho	He
*MS1**	F:CACCATCCCCATCCTGAG R:GAGAAGGATAATGCTGGATG	$(AAAG)_{18}$	58	10/10	480-550	5	0.10	0.67	1/2	600	1	0.00	0.00	1/1	300	1	0.00	0.00
*MS3**	F: CCACAACCTAACCCAATC R: ATCTGGAGCCTGAAGTCC	$(AAAG)_{15}$	54	10/10	194-236	8	0.60	0.79	2/2	202-238	3	0.50	0.63	1/1	237	2	1.00	0.50
*MS4**	F: TATTTCATTTTCCCTATCTTCG R: CAACTCAGTAGGGTGTCAG	$(AAAG)_{18}$	58	10/10	312-359	3	0,00	0.58	2/2	359	1	0.00	0.00	1/1	359	1	0.00	0.00
*MS5**	F: TAGGGTGTCAGTCATTGCTC R: TGGCATCCAGCAGTCATAG	$(TTTC)_{17}$	59	9/10	273-313	3	0.00	0.57	2/2	313	1	0.00	0.00	0/1	-	-	-	-
*MS9**	F: CAGTGGGCTTGAGATTGAC R: CATTCCTTAAAACACTCTCAC	$(AAAG)_{18}$	58	9/10	198-218	3	0.00	0.59	2/2	198-207	2	0.00	0.50	1/1	207	1	0.00	0.00
*MS13**	F: AACAGAGAAGCACAATCACC R: TGGCTCTCACTTGATATATTAG	$(TTTC)_{16}$	59	10/10	201-230	4	0.00	0.70	2/2	201	1	0.00	0.00	1/1	201	1	0.00	0.00
*MS16**	F: GAGTTCTGGTCTTGCTTTCG R: CAGGTACAACTTTCTCCAAC	$(AAAG)_{12}$	59	8/10	284-326	3	0.00	0.59	1/2	303	1	0.00	0.00	1/1	284	1	0.00	0.00
*MS27**	F: TTACACAACAACCGCCATAG R: CTTCTTATCCTGTTTACTCTG	$(TCTC)_{7}$	58	10/10	233-279	5	0.30	0.72	0/2	-	-	-	-	1/1	262	1	0.00	0.00
*Pmb-K11***	F: TTTGCTGCCCAGAGTTGTC R: AGCAGTTTGACCTCATTCCAG	$(AGAT)_{14}$	57	10/10	226-235	2	0.00	0.48	2/2	226	1	0.00	0.00	1/1	226	1	0.00	0.00
*Pmb-N14***	F: TTGGTAGTGGTGGTGGTGG R: GGCTGGCTGCTACTGAAAC	$(GAT)_{13}$	62	10/10	205-221	4	0.00	0.66	2/2	231	1	0.00	0.00	1/1	221	1	0.00	0.00
KE966557.1***	F: GCCTCCTACTCAAAGGGTGG R: CATGGGAGGCAAGGTAAAGG	$(AC)_{15}$	58	9/10	348-378	2	0.00	0.20	2/2	378	1	0.00	0.00	1/1	348	1	0.00	0.00
KE961431.1***	F: GAAGGGAGGCCCAAATATCC R: GAGAGACCTGGTGCAAACCC	$(TC)_{10}$	58	9/10	374-601	4	0.11	0.50	2/2	414	1	0.00	0.00	1/1	414	1	0,00	0,00
KE955519.1***	F: AATTTTAGCTGCAGGCTGTGG R: TCTGCTAGGGCAAAACTGGG	$(AC)_{90}$	59	10/10	218-248	3	0.00	0.64	2/2	248	1	0.00	0.00	1/1	248	1	0.00	0.00
KE961310.1***	F: AGGGTCAGGATTGAGGAGGG R: TAGAGGCTGAAGGAGCCTGG	$(TCC)_{11}$	59	10/10	305-336	2	0.00	0.42	2/2	336	1	0.00	0.00	1/1	336	1	0.00	0.00
KE955203.1***	F: TGCATTTTCTCTTCCACAGGG R: ATCTTCTGGGGAACCAACCC	$(TTC)_{35}$	57	7/10	450-521	2	0.00	0.24	2/2	521	1	0.00	0.00	1/1	450	1	0.00	0.00
KE959105.1***	F: CACTGTTTTGGGCCATCTCC R:GGGTTTAGGATGTGTTCTGATTCC	$(AATC)_{8}$	55	8/10	514-527	3	0,25	0.53	1/2	514-523	2	1.00	0.50	1/1	526	1	0.00	0.00
KE961083.1***	F: AGTCCCAAACATCCAGAGGG R: GGATCAAACCTGGACAAGCC	$(TTCC)_{13}$	59	10/10	309-344	3	0.00	0.54	2/2	344	1	0.00	0.00	1/1	344	1	0.00	0.00

Success, indicated the number of successful amplification over total number of individuals tested; Na, total number of different alleles; Ne, total number of effective alleles; Ho, observed heterozygosity; He, expected heterozygosity. *Primers designed by [8]; **Primers designed by [9]; ***Primers designed by [11].

ISSN. 2087-2852
E-ISSN. 2338-1655

Numerical Solution of a Fractional-Order Predator-Prey Model with Prey Refuge and Additional Food for Predator

Rio Satriyantara, Agus Suryanto*, Noor Hidayat

Department of Mathematics, Faculty of Mathematics and Natural Sciences, University of Brawijaya, Malang, Indonesia

Abstract

In this paper, a fractional-order predator-prey model with prey refuge and additional food for predator is solved numerically. For that aim, the model is discretized using a piecewise constant arguments. The equilibrium points of the discrete fractional-order model are investigated. Numerical simulations are conducted to see the stability of each equilibrium point. The numerical simulations show that stability of the equilibrium points is dependent on the time step.

Keywords: Additional Food, Fractional-Order, Predator-Prey, Prey Refuge.

INTRODUCTION

In ecology, understanding the dynamical relationship between prey and predator are center of goal [1]. Relationship between prey and predator plays important role for universal existence [2]. In 1928, Lotka [3] and Volterra [4] studied the relationship between prey and predator then introduced a predator-prey model. Recently, Ghosh et al. introduced the following prey-predator model with prey refuge and additional food for predator [5].

$$\begin{aligned}\frac{dx}{dt} &= x\left(1-\frac{x}{\gamma}\right)-\frac{(1-c')xy}{1+\alpha\xi+x},\\ \frac{dy}{dt} &= \frac{\beta((1-c')x+\xi)y}{1+\alpha\xi+x}-\delta y,\end{aligned} \qquad (1)$$

where x and y denote the density of prey and predator with all parameters are positive. Model (1) explain that prey population grows logistically with environmental carrying capacity γ. In the second part of right-hand-side the prey population, parameter xy characterize as predation rate on prey by modified functional respon *Holling-type* II. The refuge on prey is exhibit in order to avoid the extinction of prey population caused by predation. In present, It is found that refuge shown by barnacle *Balanus glandula* (prey) in the higher intertidal stabilizes its interaction with snails *Thais* (the predator) [6]. Term c' be the prey refuge where $c' \in (0,1)$. Considering the limited resources caused by prey refuge, the predators need alternative food to prolong their survivability or it is known as additional food. For example in real life, in the Channel Island (archipelago off the French coast), golden eagle *Aquila chrysaetos* is reduced three resident fox populations by over 95%. The review reported that the *A. chrysaetos* are primarily sustained by hyper abundant alternative food species, the fox itself [7]. In model (1), the additional food is characterized as $\alpha\xi$ with both are quality and quantity of additional food, respectively. Parameter β represent the effect of predation, while δ be the death rate of predator. Solutions of model (1) has to satisfy the positivity condition that is $x > 0$ and $y > 0$ for all $t > 0$, due to biological nature.

Ghosh et al. showed that model (1) has three equilibrium points [5]: trivial equilibrium point $(0,0)$, axial equilibrium point $(\gamma,0)$ and co-existing equilibrium point (x^*,y^*) with $x^* = \frac{\delta+\alpha\delta\xi-\beta\xi}{\beta(1-c')-\delta}$ and $y^* = \left(1-\frac{x^*}{\gamma}\right)\left(\frac{1+\alpha\xi+x^*}{1-c'}\right)$.

Systematically, predator-prey model forms a system of first-order differential equations. In recent years, differential equation model with fractional-order atrracted researchers because of its applications in a lot of science areas [8]. Fractional-order differential equation provides excellent instrument for the description of memory and heredity of various materials and processes [9]. As a generalization of integer-order differential equation, the fractional-order exhibit dynamic behaviors, such as period-2^n-orbits [10]. Thus, fractional-order model gives interpretation of real phenomena realistically. Furthermore, the fractional-order model are naturally related to models with memory which exists in most biological models [11,12,13].

The fractional derivatives have several definitions. One of the most common definitions is the Caputo fractional derivatives which is often used in real applications.

* Correspondence address:
Agus Suryanto
Email : suryanto@ub.ac.id
Address : Dept. Mathematics, Faculty of Mathematics and Natural Science, University of Brawijaya, Veteran Malang, Malang 65145.

ISSN. 2087-2852
E-ISSN. 2338-1655

$$ {}_{a}^{C}D_{t}^{n}u(t) = \frac{1}{\Gamma(m-n)}\int_{a}^{t}\frac{u^{m}(\tau)}{(t-\tau)^{n-m+1}}d\tau \qquad (2) $$

where $(m-1) < n < m$ [14].

Population dynamics model becomes more appropriate and realistic when it is modeled by difference equations. A discretization of fractional-order models is needed because nonlinear fractional-order models generally have no analytical solution expressible in terms of a finite representation of elementary functions [15]. A discrete fractional-order is a something new for scientist. Miller and Ross pioneering this work [16]. The discrete memory effect of the model indicates that the momentum x_p depend on the past information $x_0, \dots, x_{p-1}$ [17].

In this paper, a fractional-order predator-prey model is discussed. Model (1) is then modificated by forming it into a discrete fractional-order with piecewise constant arguments. The aim of this study is to give an overview of population densities based on numerical simulations of the discrete fractional-order model.

MATERIAL AND METHOD

Discrete Model

Model (1) is modified into a fractional-order by replacing the first order derivative $\frac{dx}{dt}$ and $\frac{dy}{dt}$ into fractional order derivative $D_t^n x$ and $D_t^n y$. The modified model (1) is of the form

$$ \begin{aligned} D_t^n x &= x(t)\left(1-\frac{x(t)}{\gamma}\right)-\frac{(1-c')x(t)y(t)}{1+\alpha\xi+x(t)}, \\ D_t^n y &= \frac{\beta\left((1-c')x(t)+\xi\right)y(t)}{1+\alpha\xi+x(t)}-\delta y(t), \end{aligned} \qquad (3) $$

where $0 < n < 1$. Following Elsadany and Matouk [11], and El-Sayed and Salman [18], the discretization process of model (3) can be performed to obtain

$$ \begin{aligned} x_{m+1} &= x_m + \frac{s^n}{n\Gamma(n)}\left(x_m\left(1-\frac{x_m}{\gamma}\right)\right) - \\ &\frac{s^n}{n\Gamma(n)}\left(\frac{(1-c')x_m y_m}{1+\alpha\xi+x_m}\right), \\ y_{m+1} &= y_m - \frac{s^n}{n\Gamma(n)}(\delta y_m) + \\ &+\frac{s^n}{n\Gamma(n)}\left(\frac{\beta\left((1-c')x_m+\xi\right)y_m}{1+\alpha\xi+x_m}\right). \end{aligned} \qquad (4) $$

Notice that if $n \to 1$ then model (4) becomes the Euler discretization of model (1).

Determination of the Equilibrium Point

The equilibrium point of the model is obtained when the population growth rate are zero. The equilibrium point illustrates a constant solution of the model.

Numerical Simulation

Numerical simulations will be performed to study the behavior of model (4). Furthemore, the interpretation of the resulted numerical simulations is then discussed.

RESULT AND DISCUSSION

Equilibrium Points

Point x^* and y^* is called the equilibrium point (zero solution) of model (4) if $x_m = x^*$ and $y_m = y^*$ for all m [19]. Therefore, x^* and y^* is the equilibrium point of model (4) if it satisfies

$$ \begin{aligned} x^* &= x^* + \frac{s^n}{n\Gamma(n)}\left(x^*\left(1-\frac{x^*}{\gamma}\right)\right) - \\ &\frac{s^n}{n\Gamma(n)}\left(\frac{(1-c')x^*y^*}{1+\alpha\xi+x^*}\right), \\ y^* &= y^* - \frac{s^n}{n\Gamma(n)}(\delta y^*) \\ &+\frac{s^n}{n\Gamma(n)}\left(\frac{\beta\left((1-c')x^*+\xi\right)y^*}{1+\alpha\xi+x^*}\right). \end{aligned} \qquad (5) $$

Obviously, model (4) has three equilibrium points:

1. The trivial equilibrium point $E_0 = (0,0)$,
2. The axial equilibrium point $E_1 = (\gamma, 0)$, and
3. The co-existing equilibrium point $E_2 = (x^*, y^*)$ with $x^* = \frac{\delta+\alpha\delta\xi-\beta\xi}{\beta(1-c')-\delta}$ and $y^* = \left(1-\frac{x^*}{\gamma}\right)\left(\frac{1+\alpha\xi+x^*}{1-c'}\right)$.

Numerical Method and Simulations

To illustrate the model (4), some results of our numerical simulations are provided. The numerical simulations are performed using parameter values as in Table 1.

Table 1. Parameters Value

Parameters	α	γ	c'	ξ	δ	β	n
Value	0.6	2.6	0.6	0.2	0.08	0.21	0.9

Using parameter values on Table 1, it can be shown that both of equilibrium point $E_0 = (0,0)$ and $E_1 = (2.6, 0)$ exist, but equilibrium point E_2 does not exist.

In Figure 1 to Figure 3, we plot numerical solutions using $s = 0.5, 2.0,$ and 2.1. Equilibrium point E_1 is asymptotically stable while others are unstable. In Figure 1 and Figure 2, a relatively small value of time step (s) is chosen. The solution of prey population is convergent to a constant value, i.e. $x = 2.6$, while the predator

population directly goes to extinct. This shows that $E_1 = (2.6, 0)$ is asymptotically stable. For a larger s (that is $s = 2.1$), the numerical solution of prey population is unstable (Fig. 3). Figure 3 show that the prey population oscillates around $x = 2.6$. In more detail, period-2^{nd}-orbits appears in prey population.

For next simulation, we still use parameters as in Table 1, except $\gamma = 4$, $c' = 0.21$, $\beta = 0.15$, and $\delta = 0.09$. Using those parameters, equilibrium point $E_0 = (0,0)$, $E_1 = (4,0)$, and $E_2 = (2.4842, 1.7288)$ exist.

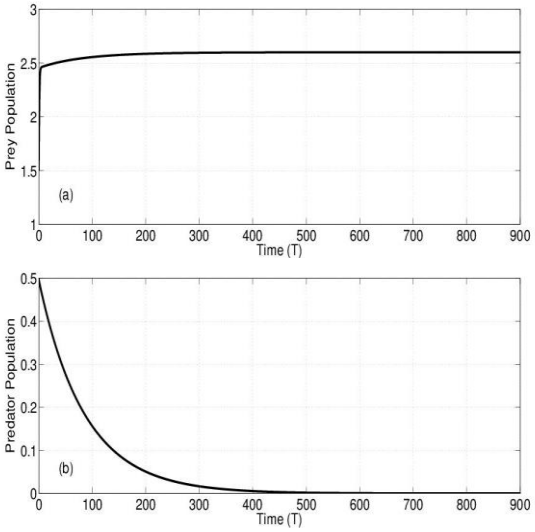

Figure 1. Numerical solution using $\alpha = 0.6, \gamma = 2.6, c' = 0.6, \xi = 0.2, \delta = 0.08, \beta = 0.21,$ and $n = 0.9$ for $s = 0.5$ on both (a) prey and (b) predator population.

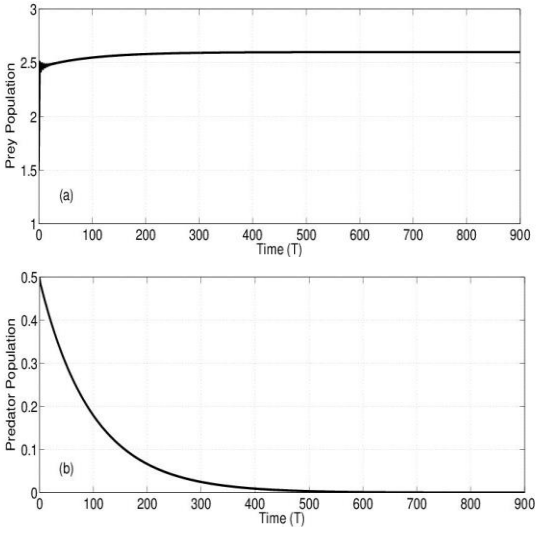

Figure 2. Numerical solution using $\alpha = 0.6, \gamma = 2.6, c' = 0.6, \xi = 0.2, \delta = 0.08, \beta = 0.21,$ and $n = 0.9$ for $s = 2$ on both (a) prey and (b) predator population.

In Figure 4 and Figure 5, using a relatively small value of s, the numerical solutions of each population are seem to be asymptotically stable and converge to equilibrium point $E_2 = (2.4842, 1.7288)$. In Figure 6, a larger value of s is chosen. In this case, the solution blows up and is not convergent to any point. This indicates that E_2 is unstable with a larger s value.

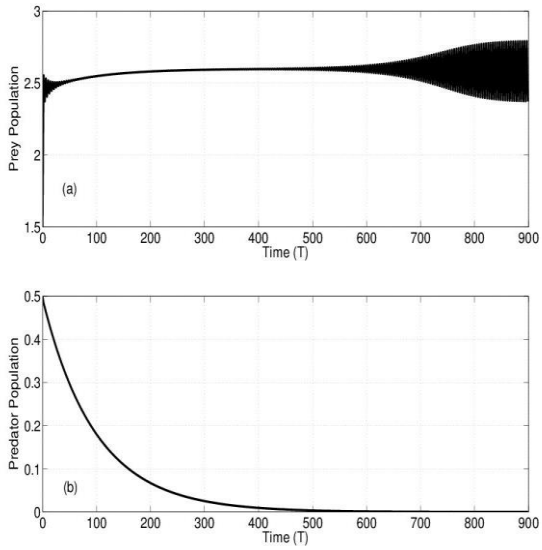

Figure 3. Numerical solution using $\alpha = 0.6, \gamma = 2.6, c' = 0.6, \xi = 0.2, \delta = 0.08, \beta = 0.21,$ and $n = 0.9$ for $s = 2.1$ on both (a) prey and (b) predator population.

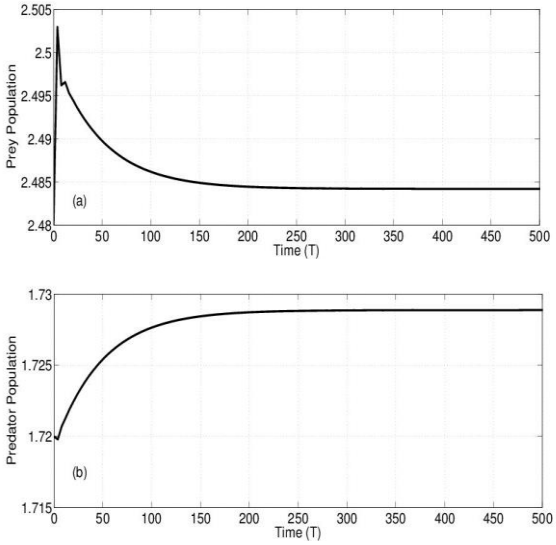

Figure 4. Numerical solution using $\alpha = 0.6, \gamma = 4, c' = 0.21, \xi = 0.2, \delta = 0.09, \beta = 0.15,$ and $n = 0.9$ for $s = 4$ on both (a) prey and (b) predator population.

ISSN. 2087-2852
E-ISSN. 2338-1655

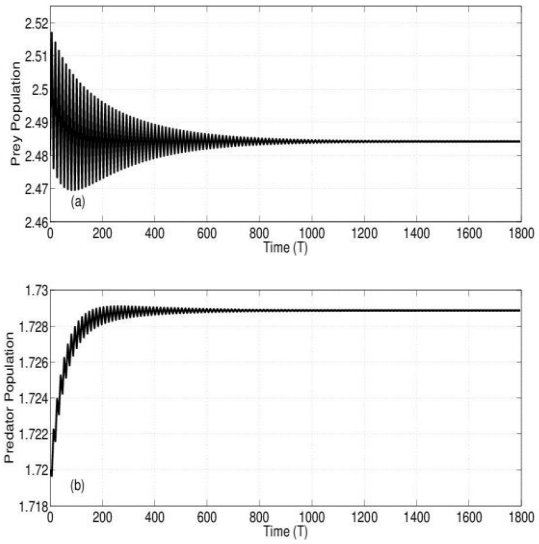

Figure 5. Numerical solution using $\alpha = 0.6$, $\gamma = 4$, $c' = 0.21$, $\xi = 0.2$, $\delta = 0.09$, $\beta = 0.15$, and $n = 0.9$ for $s = 6.8$ on both (a) prey and (b) predator population.

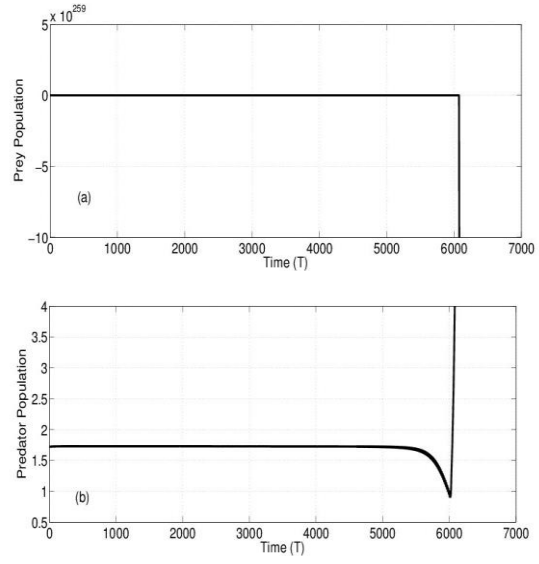

Figure 6. Numerical solution using $\alpha = 0.6$, $\gamma = 4$, $c' = 0.21$, $\xi = 0.2$, $\delta = 0.09$, $\beta = 0.15$, and $n = 0.9$ for $s = 6.91$ on both (a) prey and (b) predator population.

CONCLUSION

In this paper, a discrete fractional-order predator-prey model has been investigated. The discrete model has three equilibrium points, namely the trivial (E_0), the axial (E_1), and the co-existing (E_2) equilibrium point. The numerical simulations show that equilibrium point of discrete model may be stable only for relatively small time step (s). If higher value of s is selected, then complex dynamical behavior such as a period-2^{nd}-orbits appeares. In the future, we will explore the dynamics of the model analytically.

REFERENCES

[1] Ghorai, S., S. Poria. 2016. Pattern formation and control of spatiotemporal chaos in a reaction diffusion prey-predator model supplying additional food. *J. Chaos Solitons Fractals*. 85. 57-67.

[2] Pal, D., P. Santra, G.S. Mahaputra. 2017. Dynamical behavior of three species predator-prey model with mutual support between non refuge prey. *Ecol. Genet. Genomics*. 3(5). 1-6.

[3] Lotka, A.J. 1925. Elements of physical biology. William and Winlkins. Baltimore.

[4] Volterra, V. 1931. Lecons sur la theorie mathematique de la lutte pour la vie. Gauthier-Villars. Paris.

[5] Ghosh, J., B. Sahoo, S. Poria. 2017. Prey-predator dynamics with prey refuge providing additional food to predator. *Chaos Solitons Fractals*. 96. 110-119.

[6] Chakraborty, S., P.K. Tiwari, S.K. Sasmal, S. Biswas, S. Bhattacharya, J. Chattopadhyay. 2017. Interactive effects of prey refuge and additional food for predator in a diffusive predator-prey system. *Appl. Math. Model*. 47. 128-140.

[7] Gibson, L. 2006. The role of lethal control in managing the effects of apparent competition on endangered prey species. *Wildl. Soc. Bull*. 34. 1220–1224.

[8] El Raheem, Z.F., S.M. Salman. 2014. On a discretization process of fractional-order Logistic differential equation. *J. Egypt. Math. Soc*. 22. 407-412.

[9] Chen, F., X. Luo, Y. Zhou. 2011. Existence results for nonlinear fractional difference equation. *Advances in Difference Equations*. ID: 713201.

[10] Ji, Y.D., L. Lai, S.C. Zhong, L. Zhang. 2018. Bifurcation and chaos of a new discrete fractional-order logistic map. *Commun. Nonlinear Sci. Numer. Simulat*. 57. 352-358.

[11] Elsadany, A.A., A.E. Matouk. 2015. Dynamical Behaviors of fractional-order Lotka-Volterra predator-prey model and its discretization. *J. Appl. Math. Comput*. 49. 269-283.

[12] Nugraheni, K., A. Suryanto, and Trisilowati. 2017. Dynamics of a fractional order eco-epidemiological model. *J. Trop. Life Sci*. 7. 243-250.

[13] Huda, M.N., Trisilowati, A. Suryanto. 2017. Dynamical analysis of fractional-order Hastings-Powell food chain model with alternative food. *J. Exp. Life Sci*. 7(1). 39-44.
[14] Petras, I. 2011. Fractional order nonlinear models. Higher Education Press, Beijing, and Springer-Verlag. Berlin Heidelberg.
[15] Matouk, A.E., A.A. Elsadany, E. Ahmed, H.N. Agiza. 2015. Dynamical behavior of fractional order Hastings-Powell food chain model and its discretization. *Commun. Nonlinear Sci. Numer. Simulat*. 27. 153-167.
[16] Miller, K.S., B. Ross. 1988. Fractional difference calculus. In: Proceedings of the International Symposium on Univalent Functions, Fractional Calculus and Their Applications. Nihon University, Koriyama, Japan. *Journal Ellis Horwood Ser. Math. Appl.* Horwood, Chichester 139-152.
[17] Liu, Z., T. Xia. 2017. Novel two dimensional fractional-order discrete chaotic map and its application to image encryption. *Appl. Comput. Informatics*. 10.1016/j.aci.2017.07.002.
[18] El-Sayed, A.M.A., S.M. Salman. 2013. On a discretization process of fractional order Riccati Differential Equation. *J. Fract. Calc. Appl*. 4(2). 251-259.
[19] Elaydi, S. 2005. An introduction to difference equations, 3rd Ed. Springer. United States of America.

ISSN. 2087-2852
E-ISSN. 2338-1655

MANUSCRIPT SUBMISSION

FOCUS AND SCOPE

Journal of Experimental Life Science (JELS) is scientific journal published by Graduate Program of Brawijaya University as distribution media of Indonesian researcher's results in life science to wider community. JELS is published in every four months. JELS published scientific papers in review, short report, and life sciences especially nanobiology, molecular biology and cellular biology. JELS is scientific journal that published compatible qualified articles to academic standard, scientific and all articles reviewed by expert in their field.

Journal of Experimental Life Science (JELS) have vision to become qualified reference media to publish the best and original research results, and become the foundation of science development through invention and innovation on cellular, molecular, and nanobiology rapidly to community.

Journal of Experimental Life Science (JELS) have objectives to published qualified articles on research's results of Indonesian researchers in life science scope. JELS encompasses articles which discuss basic principles on nature phenomenon with cellular, molecular, and nanobiology approach.

PEER REVIEW PROCESS

Publication of articles by JITODE is dependent primarily on their validity and coherence, as judged by peer reviewers, who are also asked whether the writing is comprehensible and how interesting they consider the article to be. All submitted manuscripts are read by the editorial staff and only those articles that seem most likely to meet our editorial criteria are sent for formal review. All forms of published correction may also be peer-reviewed at the discretion of the editors. Reviewer selection is critical to the publication process, and we base our choice on many factors, including expertise, reputation, and specific recommendations. The editors then make a decision based on the reviewers' advice, from among several possibilities:

Accepted, with or without editorial revisions
Invite the authors to revise their manuscript to address specific concerns before a final decision

Rejected, but indicate to the authors that further work might justify a resubmission

Rejected outright, typically on grounds of specialist interest, lack of novelty, insufficient conceptual advance or major technical and/or interpretational problems

PUBLICATION FREQUENCY

JELS publish 2 Issues per year until 2017. JELS started to publish 3 Issues per year since 2018.

OPEN ACCESS POLICY

This journal provides immediate open access to its content on the principle that making research freely available to the public supports a greater global exchange of knowledge.

COPYRIGHT NOTICE

Authors who publish with this journal agree to the following terms:

Authors retain copyright and grant the journal right of first publication with the work simultaneously licensed under a Creative Commons Attribution License that allows others to share the work with an acknowledgement of the work's authorship and initial publication in this journal.

Authors are able to enter into separate, additional contractual arrangements for the non-exclusive distribution of the journal's published version of the work (e.g., post it to an institutional repository or publish it in a book), with an acknowledgement of its initial publication in this journal.

Authors are permitted and encouraged to post their work online (e.g., in institutional repositories or on their website) prior to and during the submission process, as it can lead to productive exchanges, as well as earlier and greater citation of published work (The Effect of Open Access).

PRIVACY STATEMENT

The names and email addresses entered in this journal site will be used exclusively for the stated purposes of this journal and will not be made available for any other purpose or to any other party.

ETHICS PUBLICATION

Research that using animal, human, and clinical testing is should already have ethical clearance certificate from authorized institution.

Title Typed in Bold, Capitalize each First Letter of Each Word, Except Conjunctive, *Scientific name* should not be Abbreviated (Calibri 14 Bold Center, should not exceed 12 words, except conjuctive)

First Author[1]*, Second Author[2], Third Author[3] (Calibri 12 Center, without title)

[1]First Author Affiliation, Correspondence author should be indicated by * symbol (Calibri 9 Center)
[2]Department of Biology, Faculty of Mathematics and Natural Sciences, University of Brawijaya, Malang, Indonesia
[3]Laboratorium of Physiology, Faculty of Medicine, University of Brawijaya, Malang, Indonesia

Abstract (Calibri 9 Bold Center)

This article illustrates preparation of your paper using MS-WORD (.doc or .rtf). Manuscript was numbered consecutively. Main text typed in two columns (67 characters), except title and abstract in one column. The manuscript should be written in English. The length of manuscript should not exceed 10 pages including table and figure in this format using A4 paper single space. The text should be in the margin of 3 cm up, down and left side, 2.5 cm on right side. Abstract includes the research purposes, research method and research results in one paragraph of *essay,* not *enumerative*. No citation in abstract. Abstract should not exceed 200 words. Keywords typed after abstract. (Calibri 9 Justify).

Keywords: manuscript, English, format, 5 words maximum (Calibri 9 Left)

INTRODUCTION* (Calibri 10 Bold, Left, Capslock)

All submitted manuscripts should contain original research which not previously published and not under consideration for publication elsewhere. Articles must be written in ENGLISH and manuscripts may be submitted for consideration as research report articles, short reports or reviews.

The introduction explains the background of the problem, the study of literature and research purposes. Some initial introduction paragraphs explain the problem and background to these problems [1]. The next few paragraphs explain the study of literature that contains recent knowledge development which is directly related to the issues. The last paragraph of the introductory section contains a description of the purposes of the study. (Calibri 10 Justify)

MATERIAL AND METHOD (Calibri 10 Bold, Left, Capslock)

This section describes the types of methods (qualitative, quantitative or mixed-method) with details of methods of data collection and data analysis [2]. This section also describes the perspective that underlying the selection of a particular method. (Calibri 10 Justify)

Correspondence address: (Calibri 8 Bold, Left)
Full name of correspondence author
Email : sapto@jurnal.ub.ac.id
Address : afiliation address include post code

Data Collection (Calibri 10 Bold, Left)

Explain the data collection methods, i.e. surveys, observations or archive, accompanied by details of the use of such methods. This section also describes the population, sampling and sample selection methods. (Calibri 10 Justify)

The use of English language should followed proper grammar and terms. Name of organism shoul be followed by its full scientific name in the first mention, in *italic* [3]. Author of the scientific name and the word of "var." typed regular. Example: *Stellaria saxatillis* Buch. Ham. First abbreviation typed in colon after the abbreviated phrase.

Author must use International Standard Unit (SI). Negative exponent used to show the denominator unit. Example: g l^{-1}, instead of g/l. The unit spaced after the numbers, except percentage [4]. Example: 25 g l^{-1}, instead of 25gl^{-1}; 35% instead of 35 %. Decimal typed in dot (not coma). All tables and figures should be mentioned in the text.

RESULT AND DISCUSSION (Calibri 10 Bold, Left, Capslock)

This section contains the results of the analysis and interpretation or discussion of the results of the analysis. Describe a structured, detailed, complete and concise explanation, so that the reader can follow the flow of analysis and thinking of researchers [5]. Part of the results study should be integrated with the results of the

analysis and the results and discussion are not separated.

Table

Table should be submitted within the manuscript and in separated file of *Microsoft Excel* (xls.). Table whould not exceed 8 cm (one column) and 17 cm (two columns). Table should be embedded in different page after references.

Table should be numbered in sequence. Table title should be brief and clear above the table, with uppercase in initial sentence. Vertical line should not be used. Footnote use number with colon and superscripted. Symbol of (*) or (**) was used to show difference in confidence interval of 95 and 99%.

Table 1. Example of the Table (Calibri 8.5 Left)

No	Point (Calibri 8.5 Justify)	Description
1		
2		
3		
4		
5		

Sources: Journal of PPSUB (Calibri 8.5 Left)

Figures

Figures should be in high resolution and well contrast in JPEG or PDF with the following conditions:

- Monochrome image (line art), figures of black and white diagram (solid/no shades of gray), resolution 1000-1200 dpi (dot per inch).
- Combination Halftone, combine figure and text (image containing text) and coloured graphic or in grayscale format. Resolution 600-900 dpi.
- Halftone, coloured figure or grayscale format without text. Resolution 300 dpi.
- Black and white figure should be in the grayscale mode, while coloured figures should be in RGB mode.
- Figure should not exceed the width of 8 cm (one column), 12.5 cm (1.5 columns) or 17 cm (two columns).
- Figures title typed clearly below the figure.
- Figure with pointing arrow should be grouped (grouping).
- Figures were recommended in black and white.
- Legend or figure description should be clear and complete. If compressed, the figure should be readable.
- Statistic graphic should be supplemented with data sources.
- If the figures come from the third party, it should have the copyright transfer from the sources.

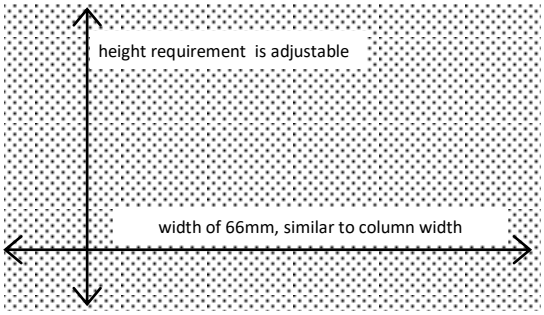

Figure 1. Illustration of Dimensional Figure of one column width. Figure dimension adjusted to the width of one column. Name the figure (diagram) written below the image. (Calibri 8.5 Justify)

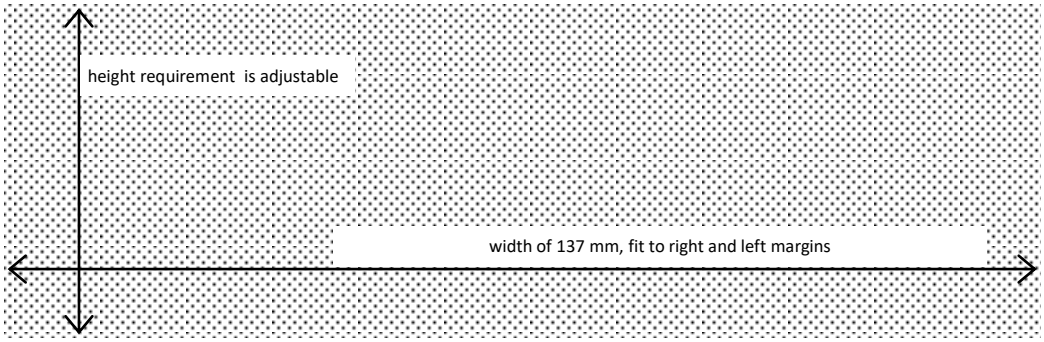

Figure 2. . Illustration of Dimensional Figure of two column width. Figure dimension adjusted to the width of two columns (137 mm). Figure were align top or bottom of the page. (Calibri 8.5 Justify)

References

1. Primary references include journal, patent, dissertation, thesis, paper in proceeding and text book.
2. Avoid self citation.
3. Author should avoid reference in reference, popular book, and internet reference except journal and private ana state institution.
4. Author was not allowed to use abstract as references.
5. References should been published (book, research journal or proceeding). Unpublished references or not displayed data can not be used as references.
6. References typed in numbering list (format number 1,2,3,…), ordered sequentially as they appear in the text (system of Vancouver or author-number style).
7. Citation in the manuscript typed only the references number (not the author and year), example: Obesity is an accumulation of fat in large quantities which would cause excessive body weight (overweight) [1]. Obesity is a risk factor of diabetic, hypertension dan atherosclerosis [2].

CONCLUSION (Calibri 10 Bold, Left, Capslock)

Conclusion of the study's findings are written in brief, concise and solid, without more additional new interpretation. This section can also be written on research novelty, advantages and disadvantages of the research, as well as recommendations for future research.(Calibri 10 Justify)

ACKNOWLEDGEMENT (Calibri 10 Bold, Left, Capslock)

This section describes gratitude to those who have helped in substance as well as financially. (Calibri 10 Justify)

REFERENCES (Calibri 10 Bold, Left, Capslock)

[1]. (Calibri 10 Justify, citation labelling by references numbering)
[2]. Vander, A., J. Sherman., D. Luciano. 2001. Human Physiology: The Mecanisms of Body Function. McGraw-Hill Higher Education. New York. (Book)
[3]. Shi, Z., M. Rifa'i, Y. Lee, K. Isobe, H. Suzuki. 2007. Importance of CD80/CD86-CD28 interaction in the recognation of target cells by $CD8^{+}CD122^{+}$ regulatory T cells. *Journal Immunology.* 124. 1:121-128. (Article in Journal)
[4]. Syafi'i, M., Hakim, L., dan Yanuwiyadi, B. 2010. Potential Analysis of Indigenous Knowledge (IK) in Ngadas Village as Tourism Attraction. pp. 217-234. In: Widodo, Y. Noviantari (eds.) Proceed-ing *Basic Science National Seminar 7* Vol.4. Universitas Brawijaya, Malang. (Article within conference proceeding)
[5]. Dean, R.G. 1990. Freak waves: A possible explanation. p. 1-65. *In* Torum, A., O.T. Gudmestad (eds). Water wave kinetics. CRC Press. New York. (Chapter in a Book)
[6]. Astuti, A.M. 2008. The Effect of Water Fraction of *Stellaria* sp. on the Content of TNF-α in Mice (*Mus musculus* BALB-C). Thesis. Department of Biology. University of Brawijaya. Malang. (Thesis)

Cover Images:

3D Structure of EGCG (*Epigallocatechin-3-Gallate*)
Green Tea Component

Created by:
Widodo, S.Si.,M.Si.,Ph.D MED Sc.

Address:

Building E, 2nd Floor, Graduate Program, University of Brawijaya
Jl. Mayor Jenderal Haryono 169, Malang, 65145
Telp: (0341) 571260 ; Fax: (0341) 580801
Email: jels@ub.ac.id
Web: jels.ub.ac.id

9 772087 285007